University of Pretoria etd – Brennan, NF (2006)

Structural studies of thallium(I)-thiourea complexes

by

Nicholas Frederick Brennan

Submitted in partial fulfillment of the requirements for the degree

Magister Scientiae

In the Faculty of Natural and Agricultural Sciences,
University of Pretoria

December 2005

University of Pretoria etd – Brennan, NF (2006)

TABLE OF CONTENTS

University of Pretoria etd – Brennan, NF (2006)

ACKNOWLEDGEMENTS

I would whole heartedly like to thank my supervisor Prof. van Rooyen for all his help and guidance throughout this project and for always assuring me that there was light at the end of the tunnel.

To my co-supervisor Prof. Boeyens I would like to extend my gratitude for much valued input.

The following people's help and assistance was very much appreciated:
Dave Liles
Linda Prinsloo
Eric Palmer
Yvette Naude
Leonore Smit

To my parents, Anne and John, without whose love and financial help this would not have been possible.

And finally to my fiancée, Cas, for always believing in me.

University of Pretoria etd – Brennan, NF (2006)

SUMMARY

Structural Studies of Thallium(1)-Thiourea Complexes

by

Nicholas Frederick Brennan

Supervisor: Prof. P. H. van Rooyen

Co-supervisor: Prof. J. C. A. Boeyens

Submitted in partial fulfilment of the requirements for the degree Magister Scientiae

Department of Chemistry, University of Pretoria

It is known that from research carried out in 1968 by L.H.W. Verhoef and J.C.A. Boeyens that the combination of thallium(1) salts, thiourea and benzoic acid results in the formation of ($Tl^{+}.4TU$)$_n$ coordination columns (TU = Thiourea) with the benzoate ions also positioning themselves in linear stacks or columns [1].

Various complexes were synthesised from Tl_2CO_3 with different benzoic acid derivatives and thiourea in order to observe the effects this may have on the Tl(1)-thiourea complexes. It was also possible to confirm the formation of the intermediate product [Tl $(OC(O)C_6H_4)R$], R = 4-NH_2, by single crystal analysis.

The benzoic acid derivatives incorporated a wide range of both electron withdrawing and electron donating substituent groups at the ortho, meta and para positions. Also included for completeness were bulky group substituents.

[NH_2, NO_2, CH_3, Cl, F, Br]$_{ortho,\ meta\ and\ para}$, 4-methoxy, and 2-hydroxy benzoic acid derivatives were the specific substituents included in this study. The only benzoic acid derivative complexes which yielded diffraction quality crystals suitable for single crystal studies were the 2-fluoro, 3-fluoro, 3-amino and benzoate complexes. The crystal structures for the complexes with PF_6^- and BF_4^- as anions were also determined as well as that of 2Tl(I), 2(TU) 2(Tph) $2H_2O$ (Tph = terephthalate benzene-1,4-dicarboxylate) complex.

All benzoic acid derivative complexes were analysed using x-ray powder diffraction. The powder diffraction data of all benzoate complexes could be split into five different groupings of complexes with similar patterns. One such group contained

the four isostructural complexes. Another group had eight complexes with only 2- and 4-substituted benzoates present.

The results of the x-ray powder and single crystal diffraction studies prove beyond doubt that the four benzoic acid derivative complexes are isostructural. Thus changing the substituent on the aromatic ring in the anion plays little or no role in the size or shape of the cavity/channel that forms with in the complex.

Spectroscopic studies (IR, Raman, UV, NMR) as well as thermal and mass spectroscopy studies were carried out on all the complexes as a means of identification and proof of complexation, as well as to study the molecular interactions in the solid state.

As a result of this and the similarity of the IR/Raman, UV and thermal studies of these four complexes to the other synthesised complexes, one can say that all the complexes that were prepared have indeed very similar solid state interactions.

The thermal studies reflected the effects of changing the electronic character of the substituent on the benzoate. Also, the thermal behaviour of the thiourea molecules in the the complexes was analysed.

Reference: [1] L. H. W. Verhoef and J. C. A. Boeyens, Acta Cryst. 1969. **B25**, 607

CHAPTER 1
BACKGROUND AND SYNTHESIS

1.1 INTRODUCTION

The origins of crystal engineering are rooted in the understanding and control of intermolecular interactions, which include in general weak and strong hydrogen bonds, halogen-halogen interactions, π-π interactions and van der Waals forces. Although originally applied to organic solids, the field has grown to include materials that contain both organic and inorganic species [1].

In the presence of alkali halides, many thallium(I) salts and two lead(II) salts, thiourea self-assembles into molecular cages around the positive cations, which in turn is connected to each other to form highly stable, 1-d macromolecular coordination columns, with fourfold symmetry. In these columns the cations form a linear array, each in a position of eightfold coordination, with respect to sulphur atoms at the corners of a cubically distorted Archimedean antiprism. Together with the anions involved, these columns represent the basic building units of unique stoichiometric complexes.

Madelung interactions between the permanent dipole moment of thiourea, in the polarizing crystal fields of the complexes, and the positive cations have been calculated by numerical methods. The calculations show that the cohesion in the complexes is almost exclusively due to electrostatic interactions and complexing only occurs, for energetic reasons, with ionic salts, which have lattice energies less than ~160kcal/mole [2].

Space group and molar volume similarities subdivide the family into a number of groups. The largest group is complexes with formula MX.4TU (M=metal, TU=thiourea). Thallium salt complexes are easily obtainable from most thallous salts, while complexes of alkali metal salts containing doubly or triply charged anions have so far been impossible to prepare. Other non-thallium MX.4TU that have been prepared include CsBr.4TU, CsCl.4TU and RbI.4TU, to name but a few [3].

The polarizable thiourea ligand in these ionic complexes act as bridges between the separated anions and cations. Vibrational spectra of the thiourea ligand

are sensitive to structural changes and have been used extensively to obtain more information about covalent metal-thiourea coordination compounds and thiourea inclusion compounds. The appearance of an additional band would indicate the formation of a covalent metal-thiourea bond.

Interest in the chemical and physical properties of a number of Tl(I) + Thiourea complexes, L. H. W. Verhoef and J. C. A. Boeyens in 1968 [4] stimulated this study.

The main concept of their research was that ionic thiourea complexes could be synthesized that allowed cations and anions to pack into linear stacks or columns in the solid state. What they discovered was that the structure of an ionic thiourea complex is in fact determined by the anion in the complex as it is the anion that plays a vital role in the formation of the coordination columns and not the close packing of tetragonal $(M^{+}.4TU)_{n}$ columns [4]. Their reasoning in synthesizing a thallium based thiourea complex with benzoate as the anion was that the benzoate is large enough to perturb the column but not symmetrical enough to have the same effect on all sides of the column. Thallium was the metal of choice as it is known that thallous salts of the benzoate form well defined complexes with in thiourea [4].

From an extensive search of the Cambridge Database Version 5.26, also included 2005 updates during Feb., May, Aug. [5] numerous complexes involving thallium (I) and organic salts were found. However, very few were found that had complexations between organic thallium(I) salts and thiourea. The presence of thiourea constitutes an essential part of the structural framework to be investigated.

In fact only five complexes were found and all had a very noticeable similarity, all the salts possessed an $R\text{-}O^{-}$ functional group, where R represents Cl, P, C and N. This in itself was a strong indication that sulphides (R-S), nitriles (C-N) and imines (C=N) were not known to complex with thallium(I) and thiourea.

With all the above background as an initial basis to this current study, the direction and motivation of this project was to synthesize ionic thallium-thiourea complexes but with different substituted benzoates as the anions. The motivation behind this was to try and determine the role that both steric and electronic changes on the anion might have on the packing of the complex in the solid state, if any. Also the electron charge distribution of the benzene ring when bonded to various substituents could also be examined using spectroscopic techniques in the solid state, should this

result in observable and more than just subtle changes in the solid state conformations [6]. The substituents chosen, were decided upon due to their varying degrees of electron donating and withdrawing effects. Also included were anions with large bulky groups to see what effect that might have on structure, bonding and packing. While still other anions had similar but not identical properties to the benzoate ion.

All in all the anions encompass an extremely wide range of possible effects the ions might have on the properties of the complexes.

With in this study various analytical techniques will be used. Infrared and Raman spectroscopy will be made use of in order to ensure the complexes have indeed been synthesised by the presence and absence of specific bands. These techniques will also be used to investigate the possibility of hydrogen bonding with in the complexes which will be indicated by any shifting of the bands. It is expected that hydrogen bonding will be observed between the organic acid functional group and possibly the thiourea molecules.

UV spectroscopy will also be used. It will confirm the presence of the benzoic acid derivatives which should all be distinguishable by different shifting of the aromatic bands resulting from the different electronic effects caused by the various substituents. UV spectroscopy will also indicate if charge transfer reactions are taking place with in the complexes. This will be seen by the presence of an extra band.

The main intention behind using solution NMR spectroscopy will be to determine the stiochiometric ratio of the complexes as well as prove the presence of both the benzoic acid derivatives and the thiourea with in the complexes. It is also hoped that shifting of the peaks will be seen as this will indicate hydrogen bonding in solution, although this does not imply hydrogen bonding in the solid state.

The use of thermal analysis will be to identify the complexes, as it will be hoped that the various substituents of the complexes will decompose with in different temperature ranges mainly as a result of stronger or weaker inter and intramolecular forces as a result of changing the ionic character. Mass spectroscopy will be incorporated into the thermal work as analysis will be done on the complexes with in temperature ranges that correspond to the thermal events. It was expected that the identity of the leaving groups could be determined using this accurate mass facility.

Finally, all the complexes will undergo x-ray analysis. It is hoped to obtain single crystals of any complexes in order to investigate and correlate the structural

data of each. However, powder diffraction may also have to be used in the event of not all the complexes producing single crystals, mainly to study the powder patterns as an indicator of categories of similar and different crystal structures. This could assist in analysing any other data collected for comparable categories of groups of effects.

Note: The main nomenclature used throughout the thesis to describe the thallium-benzoate-thiourea complexes is the substituent of the particular complex plus the word 'complex', e.g. 2-fluoro complex.

1.2 ORGANIC SALTS FROM WHICH IONS WERE DERIVED

2-aminobenzoic acid	electron donating
3-aminobenzoic acid	
4-aminobenzoic acid	
2-nitrobenzoic acid	electron withdrawing
3-nitrobenzoic acid	
4-nitrobenzoic acid	
2-fluorobenzoic acid	weaker electron withdrawing
3-fluorobenzoic acid	
4-fluorobenzoic acid	
2-chlorobenzoic acid	
3-chlorobenzoic acid	
4-chlorobenzoic acid	
2-bromobenzoic acid	
3-bromobenzoic acid	
4-bromobenzoic acid	
2-methylbenzoic acid	similar to benzoic acid
3-methylbenzoic acid	
4-methylbenzoic acid	
4-methoxybenzoic acid	bulky group
2-hydroxybenzoic acid	
NH_4 PF_6	could accommodate 4-fold symmetry
BF_4	similar to NH_4PF_6

1.3 SYNTHESIS OF ORGANIC SALTS

The organic benzoic acid derivatives which are to be investigated can all be purchased direct from chemical distributors as was the case for this particular study. The chemical distributor was Fluka. However, it is also possible to synthesise the salts in a laboratory using basic organic chemistry techniques.

A few examples are given below :

4-aminobenzoic acid and 4-nitrobenzoic acid can be synthesized by using toluene as a starting material [7].

2-aminobenzoic acid and 2-nitrobenzoic acid are formed using the same procedure as above. This is due to the fact that direct introduction of one nitro group into toluene yields a separable mixture of the liquid 2-nitrotoluene and 4-nitrotoluene [7].

2-aminobenzoic acid can also be synthesized by the hydrolysis of phthalimide to give phthalamidic acid which then undergoes the Hoffmann reaction with the addition of NaOCl to give 2-Aminobenzoic acid [8].

3-aminobenzoic acid and 3-nitrobenzoic acid both stem from toluene. The 3-aminobenzoic acid is formed by the reduction of 3-nitrobenzoic acid [7].

The halogenated benzoic acids can be prepared relatively easily [9, 10].

1.4 EXPERIMENTAL

1.4.1 SYNTHESIS OF COMPLEXES

The same method of synthesis was used for all the complexes. However, the final method took a relatively large amount of trial and error to obtain the best possible results, i.e. ensuring optimum amounts of solvent, optimum temperatures, etc.

Before detailing the methodology, a general overview of how the complexes were to be synthesized is given :

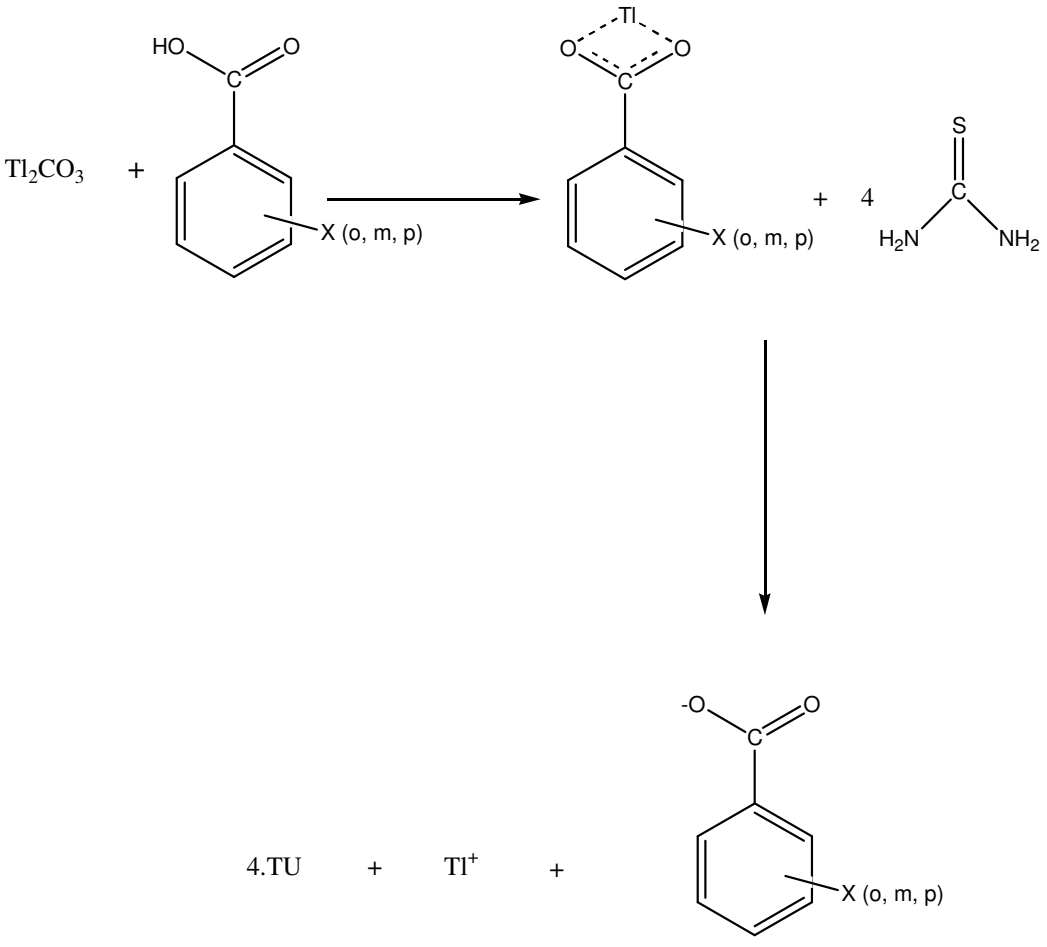

Fig. 1.1 General synthesis of complexes : X refers to the substituents listed in 1.2.

The most likely structure for the thallium benzoate intermediate would show the thallium bonded to both oxygens of the carboxylic acid with the charge being equally distributed [11]. This arrangement was also proved by the structure determination of one of the thallium benzoates isolated in this study (Chapter 2) to prove the general method and also the existence of this intermediate.

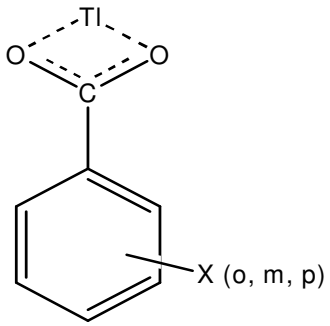

Fig. 1.2 Thallium benzoate intermediate

Before commencing this initial experiment a risk assessment of the starting materials along with the necessary safety precautions had to be taken into consideration.

Thallium, in the form of thallium nitrate ($TlNO_3$) used initially to prepare the complexes, or thallium carbonate (Tl_2CO_3) can have serious side effects. These include abdominal pain, nausea and negative effects on both the cardiovascular and nervous systems. Another notable problem is thallium's toxicity to the aquatic environment [12].

In the case of thiourea and the derivatives of benzoic acid is limited to causing irritation to skin, eyes, etc [12]. Therefore, the necessary safety precautions include wearing protective gloves and clothing, appropriate eye protection (safety glasses) and carrying out all synthesis in a fumecupboard [12].

1.4.2 EXPERIMENTAL METHOD

The standard published method of preparing the thallium benzoate complex was followed and a crystal structure of the thallium-4-aminobenzoate was determined to confirm that the method was used successfully. A total of nine different Tl (I) benzoate complexes prepared by this method from Tl_2CO_3, including *catena*-[(3,4-dimethoxybenzoato)thallium(I)] and *catena*-[(3,5-dimethoxybenzoato)thallium(I)] were recorded in the Cambridge Database [5, 11, 17].

The method involved stoichiometric amounts (1:1) of Tl_2CO_3 and the respective benzoic acid derivatives added to 60 ml of distilled water. The solutions were then allowed to boil while stirring for two hours which resulted in clear solutions. These solutions were left to recrystallise, however, as stated above, the thallium-4-aminobenzoate was the only benzoate to yield single diffraction quality crystals. The other benzoates gave precipitates. At this stage no further effort was made to attempt to recrystallise all the intermediate benzoates as this was not the focus of the study, and this literature method is well proven.

The precipitates were then redissolved in 60 ml of distilled water. The thiourea (4:1) was added, once the solutions were clear various recrystallisation methods were used in an attempt to gain single diffraction quality crystals.

1.4.3 RECRYSTALLISATION

In terms of optimum dimensions for single crystal x-ray analysis, a crystal should preferably have dimensions of approximately 0.1 mm [13].

As was stated in the experimental methodology, the crystals formed would be best described as long, thin, needle-like, white crystals whose dimensions are too small for use, and hence the reason why a great deal of time and effort was put into the challenge of obtaining larger crystals.

The initial technique that was tried was that of simply combining the dissolved starting materials then heating and stirring the precipitate along with the addition of 5ml of distilled water until all the precipitate had dissolved [4]. The temperature of the dissolved solution at this stage was 50˚C. It was then placed in a fume cupboard at

room temperature and left to recrystallise. This technique of slow cooling produced poor quality crystals in terms of size. However, the theory of slow cooling is sound as the slower a crystal grows, the lower the levels of entropy induced defects to its perfection [14]. Therefore adjustments to the slow cooling technique along with completely different methods needed to be considered.

The slow cooling variations involved allowing the dissolved mixture of starting materials to cool down at a much slower rate with the hope that larger crystals would form. Instead of dissolving the precipitate formed when the starting materials were added together at a temperature of 50˚C and leaving it to recrystallise, the dissolved precipitate was heated to 70˚C and placed in a water bath whose temperature was 65˚C. This process allowed recrystallisation to occur over a longer period of time as the solution took a relatively long time to cool.

This method turned out to be the method of choice, however, other techniques needed to be investigated in the search for bigger crystals.

Although not a new technique in itself, the above slow cooling method was repeated but with changes in both the temperatures of solution and water bath.

TEMPERATURE OF DISSOLVED SOLUTION / ˚C	TEMPERATURE OF WATER BATH / ˚C
80	80
100	90
75	70
60	50
40	30

Table 1.1 Temperatures of solution and water bath

It was found that there was no change in the crystal size whether the two temperatures were the same, varied by a few degrees, or varied by 10 degrees or more.

The next method to be tried was that of using different solvents. This entailed redissolving the formed crystals in a variety of solvents. Solvents were chosen in accordance to their dielectric constants, i.e. those with values similar to ethanol. These

included methanol, propanol and acetone. However, a variety of other solvents were also used so that a wide spectrum was covered and larger crystals had every chance of forming.

As with ethanol, these solvents required a small amount of water to be added in order for the crystals to redissolve. The ratio of water to solvent was also varied as can be seen below, all leading to the same low quality crystal.

SOLVENT	WATER : SOLVENT RATIOS
Methanol	1:1, 2:1, 5:1
DMSO	1:1, 2:1, 5:1
Acetic acid	1:1, 2:1, 5:1
Propan-2-ol	1:1, 2:1, 5:1
Acetone	1:1, 2:1, 5:1
Chloroform	1:1, 2:1, 5:1
Amyl acetate	1:1, 2:1, 5:1

Table 1.2 Ratios of water to solvent

The temperature that all the dissolved complexes were heated to was 50˚C. Once the solutions had cooled to room temperature they were then placed in the fridge for period of 2-3 hours in an unsuccessful attempt to aid recrystallisation.

As with the slow cooling technique, slight variations to the different solvent method were also tried. The main variation was repeating the synthesis of the complexes from scratch and using the various solvents in the place of ethanol each time. However, as with the other techniques this proved unfruitful.

Vapour diffusion otherwise known as isothermal distillation [15] was the next technique to be tried. The principles of this technique center around polarity. The sample is dissolved in a suitable solvent and placed in a test tube. A less polar solvent than that used for dissolving the sample is placed in a beaker. The test tube is then placed in the beaker and the beaker is sealed. The theory is that the less polar solvent

diffuses through the vapour phase into a solution of a compound in the more polar solvent and hence reducing the solubility. This slow diffusion should cause crystals to form.

The first complex to be investigated using this technique was the complex containing the 2-fluorobenzoic acid, i.e. Tl_2CO_3, TU, 2-fluorobenzoic acid. A mass of 0.005g of the complex was dissolved in a warm (60˚C) 2:1 ethanol mixture in a test tube and then placed in a beaker containing diethyl ether. The diethyl ether was not warmed as it has a boiling point of 35˚C. The beaker was then left at room temperature to se if crystals would form. Some crystals did begin to form after a period of a few hours, however, they were of poor quality.

This process was repeated several times using crystals of the 2-fluoro, thallium, thiourea complex but the solvents used were varied along with temperatures.

COMPLEX	DISSOLVING SOLVENT	LESS POLAR SOLVENT
Tl_2CO_3, TU, 2-fluorobenzoic acid	Ethanol/Water (60˚C)	Diethyl ether (RT)
	Ethanol/Water (60˚C)	Hexane (RT)
	Ethanol/Water (60˚C)	Hexane (60˚C)
	Ethanol/Water (60˚C)	THF (RT)
	Ethanol/Water (60˚C)	THF (50˚C)
	Ethanol/Water (60˚C)	Chloroform (RT)
	Ethanol/Water (60˚C)	Chloroform (50˚C)
	Ethanol/Water	CCl_4 (RT)

	(60˚C)	
	Ethanol/Water (60˚C)	CCl_4 (50˚C)

Table 1.3 Variation of solvent

As seen from the results this method did produce crystals, unfortunately initially though not of diffraction quality for single crystal diffraction. At a later stage this compound was again recrystallised and then produced usable single crystals from the mother liquor.

A variant of the vapour diffusion method is a process known as the Hanging Drop Method, this too was tried. This is normally a technique reserved for the crystallisation of macromolecules, such as proteins [16].

The principle is the same as for vapour diffusion. In this case, a drop of complex dissolved in solvent is placed in vapour equilibrium with a liquid reservoir of solvent. For equilibrium to be achieved vapour begins to leave the drop and eventually reaches the reservoir. Hence the sample increases in supersaturation. The concentration of both the complex and solvent increases as solvent leaves the drop for the reservoir. Therefore when both the drop and the reservoir have an equal concentration, equilibrium is reached [16].

The complex used in this technique was the 2-methyl complex.
Six different solvents were tested, each in a 1:1 ratio with water apart from DMSO which had a ratio of 1:5. The solvents included ethanol, DMSO, methanol, 2-propanol, DMF, amyl acetate. Saturated solutions of the complex and the various solvents were prepared. A drop of each solution was then placed on individual glass cover slides. Six different wells were then filled with the respective solvent and water ratios. Carefully the slides were placed above the relative wells and left in the hope that crystals would form.

Over a period of 2-3 days some crystals did begin to form, however, their quality was not what was hoped for. The crystals that did form were those with the DMSO/water,

ethanol/water and methanol/water. As with the other techniques the crystals were long and needle-like and much to thin for single crystal x-ray diffraction.

As has already been mentioned previously the best technique was that of slow cooling using a water bath set a few degrees below the temperature of the dissolved solution. Even though these were the best quality crystals, they were still not of sufficiently good quality for single crystal x-ray analysis to be carried out.

As another concluding note to this recrystallisation research, it must be noted that when dissolving the precipitate or crystallized material (formed when starting materials were combined) and redissolving crystals of the complexes, water is always needed for the dissolving process to occur. The only solvent that did not require water was DMSO, however, the resulting crystals were of no better quality. Water may in some way influence the growth of crystals and hence the reason why all crystals produced by all different recrystallisation methods were of such poor quality.

A total of 20 different benzoic acid derivatives, complexed with Tl^{+}.4TU, were prepared. A further two complexes with PF_6^- and BF_4^- as anions were also prepared. These complexes were subjected to the instrumental analysis described earlier. These results are described in the following chapters.

1.5 REFERENCES

CHAPTER 1

1. A. M. Beatty, CrysEngComm, 2001, **51**, 1-13
2. J. C. A. Boeyens and G. Gafner, The Journal of Chemical Physics, 1968, **49(5)**, 2435-2438
3. F. H. Herbstein and J. C. A. Boeyens, Inorg. Chem. 1967, **6(7)**, 1408-1425
4. L. H. W. Verhoef and J. C. A. Boeyens, Acta Cryst. 1969, **B25**, 607
5. The Cambridge Structural Database: a quarter of a million crystal structures and rising, F. H. Allen, Acta Crystallogr., **B58**, 380-388, 2002, Version 5.26, also included 2005 updates during Feb., May, Aug.
6. W. Lewandowski, L. Fuks, M. Kalinowska and P. Koczon, Spectrochimica Acta Part A, 2003, **59**, 3411
7. Allinger, Cava, De Jongh, Johnson, Lebel, Stevens, Organic Chemistry, 2nd ed., Worth Publishing Inc., 1976, 623-624
8. L. F. Fieser and M. Fieser, Organic Chemistry, 3rd ed., Reinhold Publishing Corporation, New York, 1956, 661
9. I. L. Finar, Organic Chemistry, The Fundamental Principles, Vol. 1, 1967, Longmans, Green and Co. Ltd, 724
10. www.orgsyn.org/orgsyn/prep.asp?prep=cv2p0299
11. Olof Kristiansson, Eur. J. Inorg. Chem., 2002, 2355-2361
12. International Chemical Safety Cards, ICSC : 0077, 0680
13. D. Boyle, www.xray.ncsu.edu/GrowXtal
14. www.oci.unizh.ch/service/cx/Crystal_Growth.pdf, page 4
15. www.ccp14.ac.uk/ccp/webmirrors/blake/~pczajb2/growcrys.htm.orig#Vapour_diffusion
16. www.hamptonresearch.com/support/pdf101/CG101HDC.pdf page 1
17. F. Wiesbrock and H. Schmidbaur, J. Am. Chem. Soc., Vol. 125, NO. 12, 2003, 3624

CHAPTER 2
CRYSTALLOGRAPHIC ANALYSIS

2.1 INTRODUCTION

The only benzoic acid derivative complexes which yielded diffraction quality crystals suitable for single crystal studies were the 2-fluoro, 3-fluoro, 3-amino benzoate and unsubstituted benzoate complexes. Note that the crystal structure for the benzoate complex had already been solved by photographic methods [1], however, the results obtained from the diffractometer for the complex in this thesis were of a much higher quality.

All the remaining benzoic acid derivative complexes had a generic look when viewed under the microscope. The crystals were very thin, hair-like in nature. However, powder diffraction studies of these complexes showed that they were not all identical.

In an attempt to obtain more diffraction quality single crystals, complexes were synthesised that contained BF_4^- and PF_6^- as the anions. This proved fruitful and two further crystal structures were obtained. However, it must be noted that the PF_6^- complex was prepared from $TlNO_3$ and not Tl_2CO_3 and therefore there is a possibility of NO_3^- contamination in the complex.

Another diffraction quality single crystal was prepared using the 4-aminobenzoic acid as the anion, the precursor (without thiourea) isolated to prove that the synthesis route applied included the formation of this species. This was also in accordance with at least nine examples in the literature [2, 9].

Another crystal structure that could be determined resulted from the synthesis, in the same manner as the other benzoic acid derivative complexes, in this case the 2-aminobenzoic acid as the anion. However, the structure obtained was most different to the other structures
And its space group was $P2_1/c$ (monoclinic). The other four benzoates all crystallised in Cmcm (orthorhombic). The structure's results are given in this chapter, however, it was suspected that the formation of this product resulted from some irreproducible change in reaction conditions. Unfortunately no spectroscopic data was obtained to help clarify the structure as there was insufficient material available.

The BF_4^- and PF_6^- complexes were not fully analysed with all the spectroscopic methods used for the analysis of the benzoate complexes as these two products were obtained using $TlNO_3$ as starting material. As there was some uncertainty about a possible NO_3^- contamination of these crystals, the PF_6-complex was subjected to analysis using a nitrate-specific electrode, showing that there was no NO_3^- present. At this stage the BF_4^-complex was not analysed by other spectroscopic methods, as the structure was solved and refined correctly without any disorder.
The PF_6^-complex was refined in the space group P4cc and could not be solved and refined with success in P4/mcc (the space group suggested for the NO_3^- complex). The 4-aminobenzoate non-thiourea complex was analysed in both the IR/Raman and thermal analysis chapters in order to confirm the bands/peaks which related specifically to thiourea.

2.2 SINGLE CRYSTAL STUDY

The resulting molecular structures produced from the single crystal analysis of the 2-fluoro, 3-fluoro, 3-amino and benzoate complexes are very similar to those reported for the benzoate [1]/ NO_3^-/ ClO_4^-/ ClO_3^-/ $P(OH)_2O^-$ complex [3]. Note that the non-thiourea 4-aminobenzoate complex has a different structure and will be discussed later.

Thallium - Thiourea Complexes - Crystal Structures with various anions

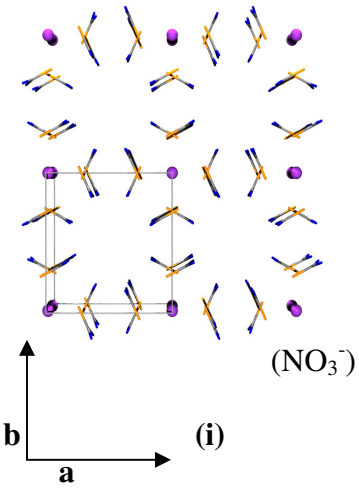

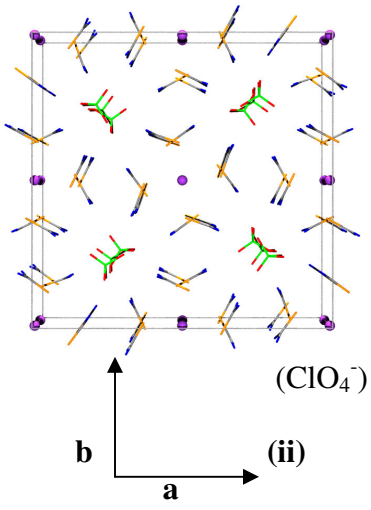

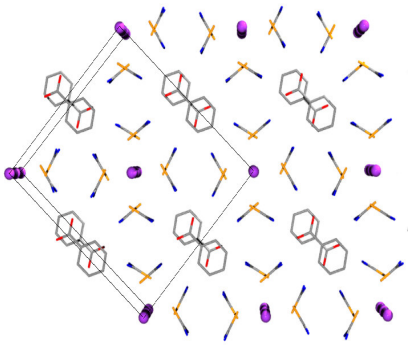

($C_6H_5COO^-$)

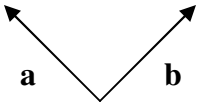

(iii)

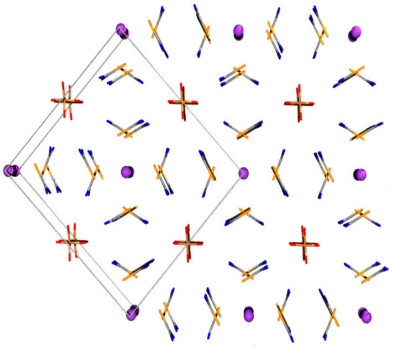

($P(OH)_2O_2^-$)

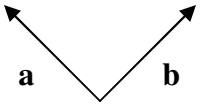

(iv)

(i)NO_3^- Tetragonal, P4/mcc
a = b = 10.34Å, c = 8.29Å
Viewed along the c axis

(ii)ClO_4^- Tetragonal, P4/mnc
a = b = 21.07Å, c = 8.28Å
Viewed along the c axis

(iii)$C_6H_5COO^-$ Orthorhombic, Cmcm
a = 15.64Å, b = 17.09Å, c = 8.15Å
Viewed along the c axis

(iv)$P(OH)_2O_2^-$ Orthorhombic, Cccm
a = 15.40Å, b = 14.64Å, c = 8.27Å
Viewed along the c axis

(v)ClO_3^- Monoclinic, B2/m
a = 22.037Å, b = 9.869Å, c = 8.201Å
γ = 103.95°
Viewed along the c axis

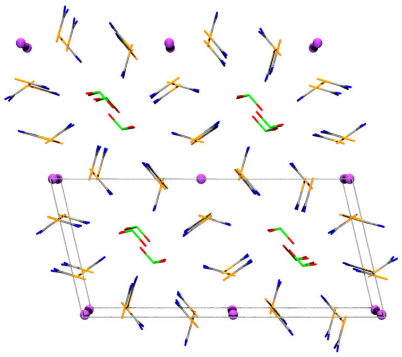

(ClO_3^-)

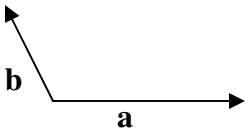

(v)

Fig. 2.1 **Projection of Thallium – Thiourea complexes generated from the Cambridge database (version 5.26, as well as the 2005 updates during February, May, August) (i) to (v) viewed along the c-axis.**

The above structures were generated from the Cambridge Database (version 5.26, as well as the 2005 updates during February, May, August) [4] and clearly show that in all cases the thallium and thiourea molecules arrange themselves in such a way as to form an open channel in the centre of the complex. This cavity is filled by the various anionic moieties that are added to the

thallium and thiourea in the synthesis, i.e. in terms of this thesis it is the benzoic acid derivatives, the BF_4^- and PF_6^- anions.

2.2.1 EXPERIMENTAL

The crystal data and processing parameters are given in Tables 2.1 – 2.12, 2.19 – 2.30 and 2.33 – 2.56. Data collection, cell refinement and data reduction was executed using the SMART software [5].

Programs used to determine and refine the structures :
SHELXS 97 and SHELXL 97 [6]
Molecular graphics : Ortep – 3 [7]
POV-Ray. [8]

The structures were in general determined using Patterson methods and a series of difference maps yielded the remaining atom positions, after subsequent refinement. The hydrogen atoms were experimentally located and refined without any restrictions, apart from those hydrogen atoms in the PF_6^- and 4-aminobenzoate complexes which were placed in theoretical positions and included in the refinements. The improved structural data for the benzoate complex did not reveal any additional structural detail not already indicated by the original report [1].

2.2.2 CRYSTALLOGRAPHIC LABELLING SYSTEM

The labelling system used for the crystallographic tables that follow is seen below in Fig. 2.2, taking the symmetry operators of the space group Cmcm into consideration:

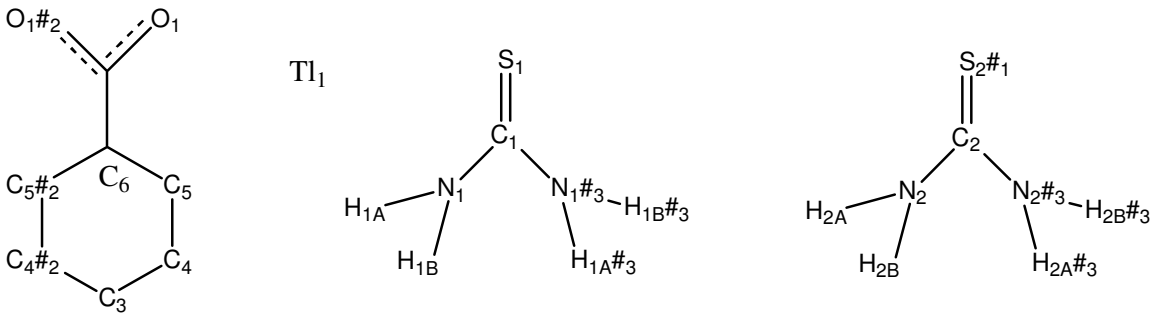

Various Substituents: F_1

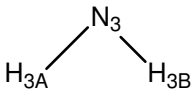

The hydrogen atoms on the benzoate rings were labelled according to the parent carbon atom.

Note: Symmetry transformations used to generate equivalent atoms:

#1	x, y-1, z	only for Cmcm
#2	-x, y, -z + ½	
#3	x, y, -z + ½	

Fig. 2.2 Crystallographic labelling system for the complexes

2. 3 CRYSTALLOGRAPHIC RESULTS FOR THE FOUR BENZOATE COMPLEXES

2.3.1 RESULTS FOR THE 2-FLUORO COMPLEX CRYSTAL ANALYSIS

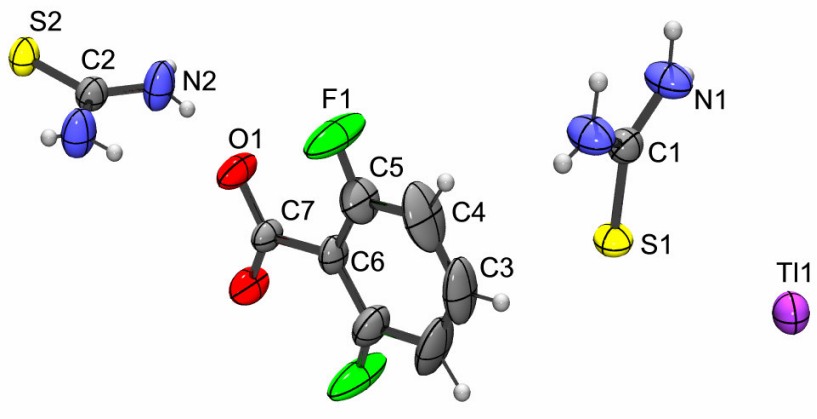

Fig. 2.3 **Molecular structure of the components involved in the 2-Fluoro complex, with displacement ellipsoids drawn at the 50% probability level. H-atoms are shown.**

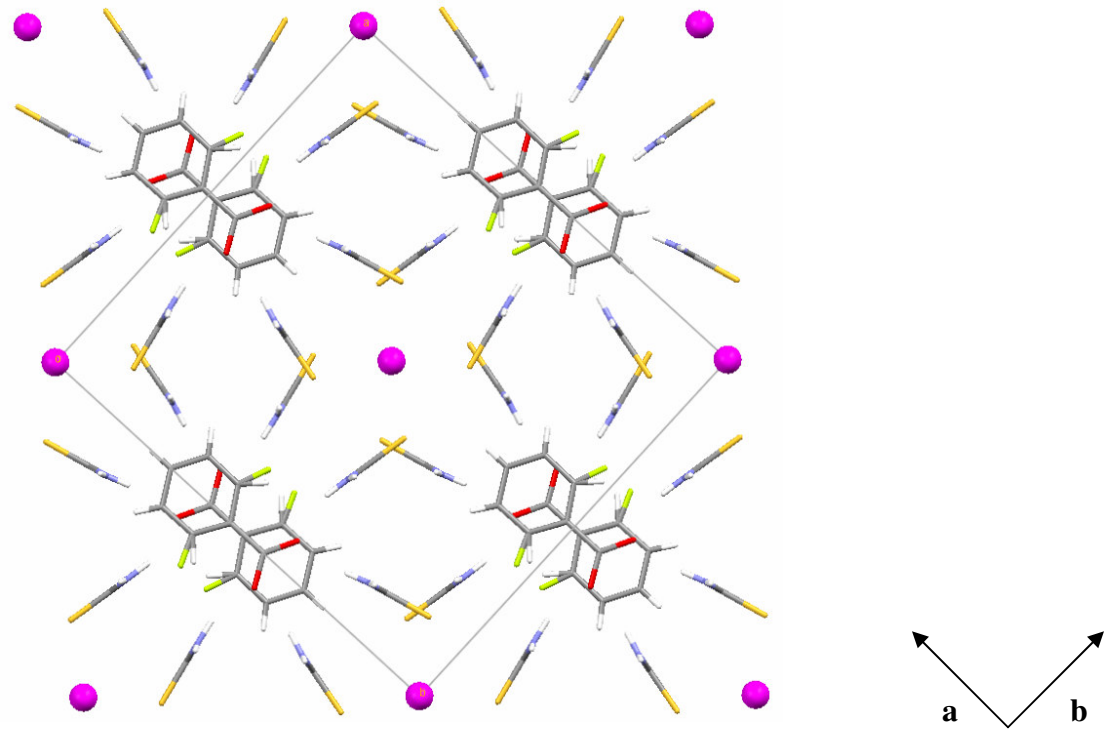

Fig. 2.4 **Molecular packing of the 2-Fluoro complex viewed along the direction of the c axis. The direction of the a and b axes are shown above.**

CRYSTAL STRUCTURE TABLES FOR 2-FLUORO COMPLEX

Identification code	nb11_abs	
Empirical formula	C_{11} H_{20} F N_8 O_2 S_4 Tl	
Formula weight	647.96	
Temperature	293(2) K	
Wavelength	0.71073 Å	
Crystal system	Orthorhombic	
Space group	C m c m	
Unit cell dimensions	a = 15.7317(10) Å	α= 90º.
	b = 17.0319(11) Å	β= 90º.
	c = 8.0881(5) Å	γ = 90º.
Volume	2167.1(2) $Å^3$	
Z	4	
Density (calculated)	1.986 Mg/m^3	
Absorption coefficient	7.870 mm^{-1}	
F(000)	1248	
Crystal size	0.30 x 0.25 x 0.20 mm^3	
Theta range for data collection	2.59 to 26.45º.	
Index ranges	-18<=h<=16, -20<=k<=21, -10<=l<=3	
Reflections collected	5739	
Independent reflections	1177 [R(int) = 0.0309]	
Completeness to theta = 25.00º	99.5 %	
Absorption correction	Semi-empirical from equivalents	
Max. and min. transmission	0.207 and 0.125	
Refinement method	Full-matrix least-squares on F^2	
Data / restraints / parameters	1177 / 0 / 105	
Goodness-of-fit on F^2	1.230	
Final R indices [I>2σ(I)]	R1 = 0.0373, wR2 = 0.0745	
R indices (all data)	R1 = 0.0384, wR2 = 0.0757	

Extinction coefficient	0.0068(4)
Largest diff. peak and hole	1.313 and -3.027 e.Å^{-3}

* $w = 1/ [\sigma^2 (F_0^2) + (0.0707P)^2 + 0.0977P]$ where $P = (F_0^2 + 2Fc^2)/ 3$

$\Delta\rho$ max = 1.2 e.Å^{-3} (0.5Å from C1)

$\Delta\rho$ min = -1.69e.Å^{-3}

Table 2.1 Crystal data and structure refinement for Tl^{+1} 4(TU) 2-Fluorobenzoate.

Tl(1)-S(1)	3.3792(7)		
Tl(1)-S(2)#1	3.4235(8)	S(1)-Tl(1)-S(2)#1	67.539(16)
S(1)-C(1)	1.708(4)	C(1)-S(1)-Tl(1)	111.28(8)
C(1)-N(1)	1.319(3)	N(1)#3-C(1)-N(1)	117.6(3)
N(1)-H(1A)	0.89(4)	N(1)-C(1)-S(1)	121.18(17)
N(1)-H(1B)	0.70(5)	C(1)-N(1)-H(1A)	118.4(15)
S(2)-C(2)	1.710(3)	C(1)-N(1)-H(1B)	129(4)
C(2)-N(2)	1.313(3)	H(1A)-N(1)-H(1B)	112(4)
N(2)-H(2A)	0.78(4)	N(2)-C(2)-N(2)#3	117.0(4)
N(2)-H(2B)	0.62(5)	N(2)-C(2)-S(2)	121.48(19)
O(1)-C(7)	1.234(4)	C(2)-N(2)-H(2A)	114(2)
C(3)-C(4)#2	1.361(8)	C(2)-N(2)-H(2B)	126(5)
C(3)-C(4)	1.361(8)	H(2A)-N(2)-H(2B)	120(5)
C(3)-H(3)	0.89(10)	C(4)#2-C(3)-C(4)	121.0(6)
C(4)-C(5)	1.412(6)	C(4)#2-C(3)-H(3)	119.5(3)
C(4)-H(4)	0.92(6)	C(4)-C(3)-H(3)	119.5(3)
C(5)-F(1)	1.159(7)	C(3)-C(4)-C(5)	118.9(6)
C(5)-C(6)	1.372(5)	C(3)-C(4)-H(4)	114(4)
C(6)-C(5)#2	1.372(5)	C(5)-C(4)-H(4)	127(4)
C(6)-C(7)	1.537(7)	F(1)-C(5)-C(6)	126.9(5)
C(7)-O(1)#2	1.234(4)	F(1)-C(5)-C(4)	110.9(5)

C(6)-C(5)-C(4)	122.2(5)	C(5)#2-C(6)-C(7)	121.5(3)
C(5)-C(6)-C(5)#2	116.9(6)	O(1)#2-C(7)-O(1)	124.8(5)
C(5)-C(6)-C(7)	121.5(3)	O(1)#2-C(7)-C(6)	117.6(2)
O(1)-C(7)-C(6)	117.6(2)		

Symmetry transformations used to generate equivalent atoms:

#1 x,y-1,z #2 -x,y,-z+1/2 #3 x,y,-z+1/2

Table 2.2 Bond lengths [Å] and angles [º] for Tl^{+1} 4(TU) 2-Fluorobenzoate

D-H...A	d(D-H)	d(H...A)	d(D...A)	<(DHA)
N(1)-H(1A)...O(1)#4	0.89(4)	2.19(4)	2.974(4)	147(2)
N(2)-H(2A)...O(1)	0.78(4)	2.30(4)	3.044(4)	160(3)

Symmetry transformations used to generate equivalent atoms:

#1 x,y-1,z #2 -x,y,-z+1/2 #3 x,y,-z+1/2 #4 -x+1/2,y-1/2,-z+1/2

Table 2.3 Hydrogen bonds for Tl^{+1} 4(TU) 2-Fluorobenzoate [Å and º].

2.3.2 RESULTS FOR THE 3-FLUORO COMPLEX CRYSTAL ANALYSIS

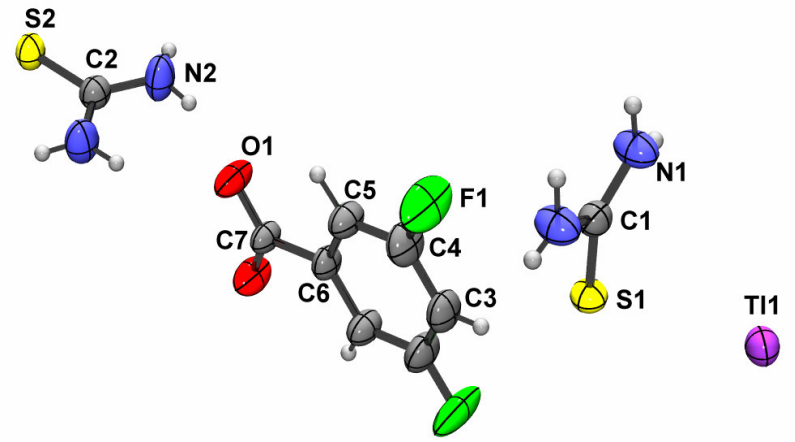

Fig. 2.5 **Molecular structure of the components involved in the 3-Fluoro complex, with displacement ellipsoids drawn at the 50% probability level. H-atoms are shown.**

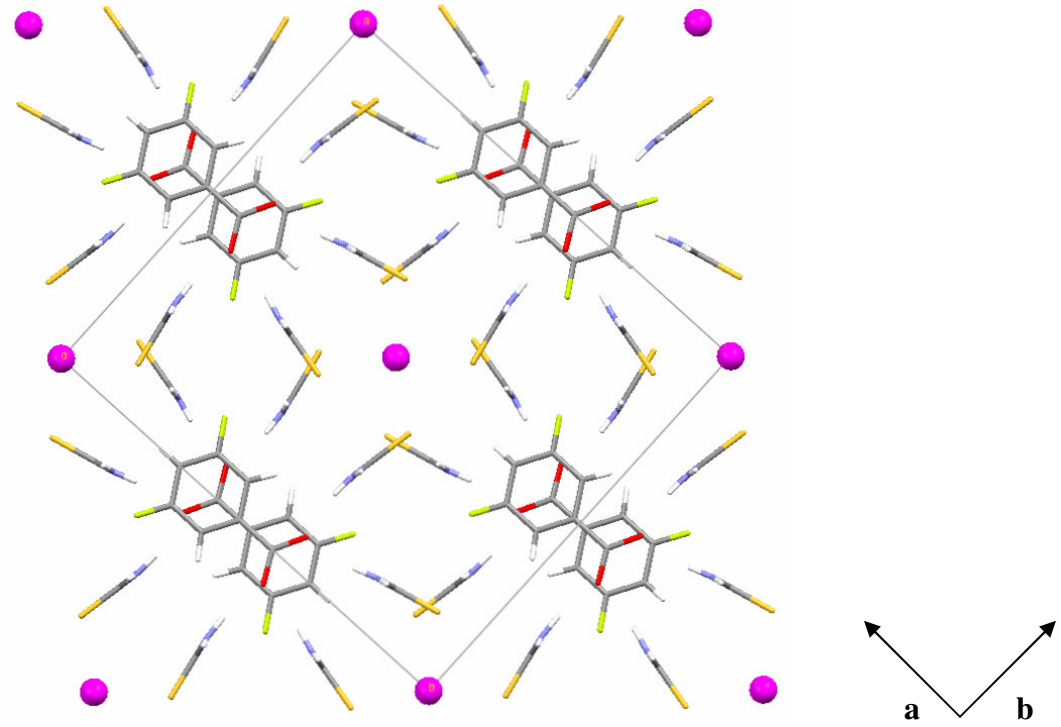

Fig. 2.6 **Molecular packing of the 3-Fluoro complex viewed along the direction of the c axis. The direction of the a and b axes are shown above**

CRYSTAL STRUCTURE TABLES FOR 3-FLUORO COMPLEX

Identification code	nb18_abs	
Empirical formula	C_{11} H_{20} F N_8 O_2 S_4 Tl	
Formula weight	647.96	
Temperature	293(2) K	
Wavelength	0.71073 Å	
Crystal system	Orthorhombic	
Space group	C m c m	
Unit cell dimensions	a = 15.6079(8) Å	α= 90º.
	b = 17.1485(9) Å	β= 90º.
	c = 8.0752(4) Å	γ = 90º.
Volume	2161.34(19) Å^3	
Z	4	
Density (calculated)	1.991 Mg/m^3	
Absorption coefficient	7.891 mm^{-1}	
F(000)	1248	
Crystal size	0.31 x 0.25 x 0.24 mm^3	
Theta range for data collection	2.38 to 26.57º.	
Index ranges	-17<=h<=19, -21<=k<=19, -3<=l<=10	
Reflections collected	5754	
Independent reflections	1183 [R(int) = 0.0249]	
Completeness to theta = 25.00º	99.9 %	
Absorption correction	Semi-empirical from equivalents	
Max. and min. transmission	0.150 and 0.118	
Refinement method	Full-matrix least-squares on F^2	
Data / restraints / parameters	1183 / 0 / 105	
Goodness-of-fit on F^2	1.061	
Final R indices [I>2σ(I)]	R1 = 0.0226, wR2 = 0.0594	
R indices (all data)	R1 = 0.0237, wR2 = 0.0605	

Extinction coefficient	0.00075(14)
Largest diff. peak and hole	0.561 and -0.563 e.Å^{-3}

* $w = 1/ [\sigma^2 (F_0^2) + (0.0707P)^2 + 0.0977P]$ where $P = (F_0^2 + 2Fc^2)/ 3$

$\Delta\rho$ max = 1.2 e.Å^{-3} (0.5Å from C1)

$\Delta\rho$ min = -1.69e.Å^{-3}

Table 2.4 Crystal data and structure refinement for Tl^{+1} 4(TU) 3-Fluorobenzoate.

Tl(1)-S(1)	3.3537(7)		
Tl(1)-S(2)#1	3.4142(8)	S(1)-Tl(1)-S(2)#1	67.231(16)
S(1)-C(1)	1.707(3)	C(1)-S(1)-Tl(1)	111.74(8)
C(1)-N(1)	1.319(3)	N(1)#3-C(1)-N(1)	117.4(3)
N(1)-H(1A)	0.89(3)	N(1)-C(1)-S(1)	121.32(17)
N(1)-H(1B)	0.70(4)	C(1)-N(1)-H(1A)	118.2(17)
S(2)-C(2)	1.711(3)	C(1)-N(1)-H(1B)	125(4)
C(2)-N(2)	1.315(3)	H(1A)-N(1)-H(1B)	116(4)
N(2)-H(2A)	0.83(4)	N(2)#3-C(2)-N(2)	117.5(4)
N(2)-H(2B)	0.80(4)	N(2)-C(2)-S(2)	121.27(18)
C(3)-C(4)#2	1.382(5)	C(2)-N(2)-H(2A)	116(2)
C(3)-C(4)	1.382(5)	C(2)-N(2)-H(2B)	120(3)
C(3)-H(6)	0.85(7)	H(2A)-N(2)-H(2B)	123(4)
C(4)-F(1)	1.258(6)	C(4)#2-C(3)-C(4)	118.9(5)
C(4)-C(5)	1.392(5)	C(4)#2-C(3)-H(6)	120.5(2)
C(5)-C(6)	1.382(4)	C(4)-C(3)-H(6)	120.5(2)
C(5)-H(4)	0.95(5)	F(1)-C(4)-C(3)	118.1(4)
C(6)-C(5)#2	1.382(4)	F(1)-C(4)-C(5)	121.3(5)
C(6)-C(7)	1.522(6)	C(3)-C(4)-C(5)	120.6(4)
C(7)-O(1)#2	1.242(3)	C(6)-C(5)-C(4)	120.4(4)
C(7)-O(1)	1.242(3)	C(6)-C(5)-H(4)	116(3)

C(4)-C(5)-H(4)	124(3)	O(1)#2-C(7)-O(1)	124.5(5)
C(5)#2-C(6)-C(5)	119.2(5)	O(1)#2-C(7)-C(6)	117.8(2)
C(5)#2-C(6)-C(7)	120.4(2)	O(1)-C(7)-C(6)	117.8(2)
C(5)-C(6)-C(7)	120.4(2)		

Symmetry transformations used to generate equivalent atoms:

#1 x,y-1,z #2 -x,y,-z+1/2 #3 x,y,-z+1/2

Table 2.5 Bond lengths [Å] and angles [º] for Tl^{+1} 4(TU) 3-Fluorobenzoate.

D-H...A	d(D-H)	d(H...A)	d(D...A)	<(DHA)
N(1)-H(1A)...O(1)#4	0.89(3)	2.12(3)	2.922(4)	150(2)
N(1)-H(1B)...S(2)#5	0.70(4)	2.74(4)	3.413(3)	165(5)
N(2)-H(2A)...O(1)#2	0.83(4)	2.28(4)	3.057(4)	156(3)
N(2)-H(2B)...S(1)#6	0.80(4)	2.66(4)	3.449(3)	171(5)

Symmetry transformations used to generate equivalent atoms:

#1 x,y-1,z #2 -x,y,-z+1/2 #3 x,y,-z+1/2 #4 x+1/2,y-1/2,z

#5 x,-y+1,z+1/2 #6 x,-y+1,z-1/2

Table 2.6 Hydrogen bonds for Tl^{+1} 4(TU) 3-Fluorobenzoate [Å and º].

2.3.3 RESULTS FOR THE 3-AMINO COMPLEX CRYSTAL ANALYSIS

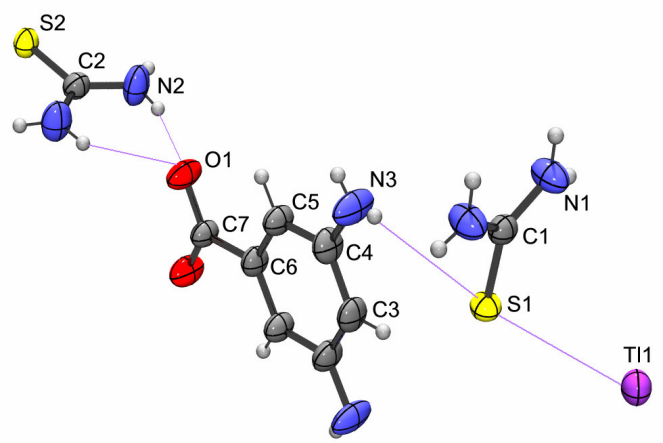

Fig. 2.7 **Molecular structure of the components involved in the 3-Amino complex, with displacement ellipsoids drawn at the 50% probability level. H-atoms are shown. Close contacts are also indicated**

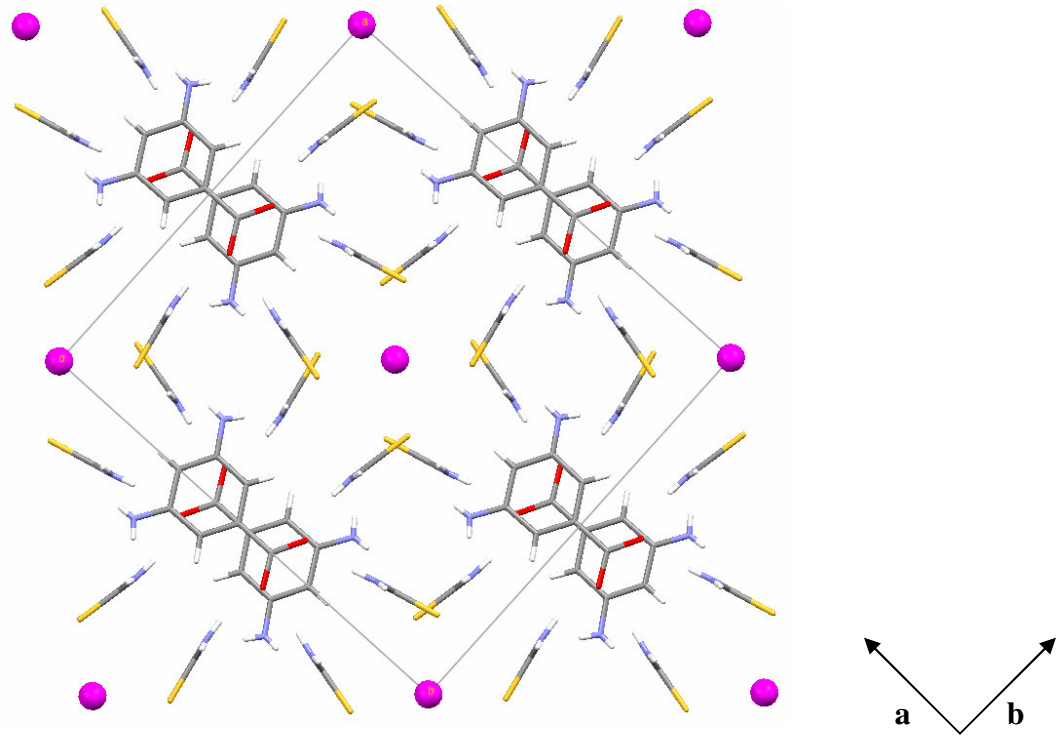

Fig. 2.8 **Molecular packing of the 3-Amino complex viewed along the direction of the c axis. The direction of the a and b axes are shown above.**

CRYSTAL STRUCTURE TABLES FOR 3-AMINO COMPLEX

Identification code	nb09_abs	
Empirical formula	C_{11} H_{22} N_9 O_2 S_4 Tl	
Formula weight	645.05	
Temperature	293(2) K	
Wavelength	0.71073 Å	
Crystal system	Orthorhombic	
Space group	C m c m	
Unit cell dimensions	a = 15.5683(11) Å	α= 90º.
	b = 17.1150(12) Å	β= 90º.
	c = 8.1352(5) Å	γ = 90º.
Volume	2167.6(3) $Å^3$	
Z	4	
Density (calculated)	1.977 Mg/m^3	
Absorption coefficient	7.848 mm^{-1}	
F(000)	1136	
Crystal size	0.34 x 0.26 x 0.26 mm^3	
Theta range for data collection	2.62 to 26.54º.	
Index ranges	-18<=h<=19, -21<=k<=20, -3<=l<=10	
Reflections collected	5782	
Independent reflections	1172 [R(int) = 0.0248]	
Completeness to theta = 25.00º	99.4 %	
Absorption correction	Semi-empirical from equivalents	
Max. and min. transmission	0.130 and 0.102	
Refinement method	Full-matrix least-squares on F^2	
Data / restraints / parameters	1172 / 0 / 111	
Goodness-of-fit on F^2	1.098	
Final R indices [I>2σ(I)]	R1 = 0.0247, wR2 = 0.0627	
R indices (all data)	R1 = 0.0255, wR2 = 0.0637	

Extinction coefficient	0.0128(5)
Largest diff. peak and hole	1.171 and -0.985 e.Å^{-3}

* $w = 1/ [\sigma^2 (F_0^2) + (0.0707P)^2 + 0.0977P]$ where $P = (F_0^2 + 2Fc^2)/ 3$

$\Delta\rho$ max = 1.2 e.Å^{-3} (0.5Å from C1)

$\Delta\rho$ min = -1.69e.Å^{-3}

Table 2.7 Crystal data and structure refinement for Tl^{+1} 4(TU) 3-Aminobenzoate.

Tl(1)-S(1)	3.3588(6)	N(3)-H(3A)	0.56(7)
Tl(1)-S(2)#1	3.4209(7)	N(3)-H(3B)	0.66(8)
S(1)-C(1)	1.715(3)		
S(2)-C(2)	1.713(3)	S(1)-Tl(1)-S(2)#1	66.867(15)
O(1)-C(7)	1.248(3)	C(1)-S(1)-Tl(1)	111.56(8)
C(1)-N(1)	1.316(3)	N(1)-C(1)-N(1)#3	118.2(3)
C(3)-C(4)	1.386(5)	N(1)-C(1)-S(1)	120.91(16)
C(3)-C(4)#2	1.386(5)	C(4)-C(3)-C(4)#2	121.3(4)
C(3)-H(3)	0.85(6)	C(4)-C(3)-H(3)	119.3(2)
N(1)-H(1A)	0.82(3)	C(4)#2-C(3)-H(3)	119.3(2)
N(1)-H(1B)	0.72(4)	C(1)-N(1)-H(1A)	121.0(16)
C(5)-C(6)	1.380(4)	C(1)-N(1)-H(1B)	124(3)
C(5)-C(4)	1.402(5)	H(1A)-N(1)-H(1B)	114(4)
C(5)-H(5)	0.89(5)	C(6)-C(5)-C(4)	121.4(4)
C(7)-O(1)#2	1.248(3)	C(6)-C(5)-H(5)	117(3)
C(7)-C(6)	1.514(6)	C(4)-C(5)-H(5)	122(3)
C(6)-C(5)#2	1.380(4)	O(1)#2-C(7)-O(1)	123.3(4)
N(2)-C(2)	1.317(3)	O(1)#2-C(7)-C(6)	118.3(2)
N(2)-H(2A)	0.81(3)	O(1)-C(7)-C(6)	118.3(2)
N(2)-H(2B)	0.79(4)	C(5)#2-C(6)-C(5)	118.8(5)
C(4)-N(3)	1.285(8)	C(5)#2-C(6)-C(7)	120.6(2)

C(5)-C(6)-C(7)	120.6(2)	C(3)-C(4)-C(5)	118.5(4)
C(2)-N(2)-H(2A)	116(2)	N(2)#3-C(2)-N(2)	117.4(3)
C(2)-N(2)-H(2B)	120(3)	N(2)-C(2)-S(2)	121.28(17)
H(2A)-N(2)-H(2B)	123(4)	C(4)-N(3)-H(3A)	125(8)
N(3)-C(4)-C(3)	118.4(5)	C(4)-N(3)-H(3B)	108(6)
N(3)-C(4)-C(5)	123.1(5)	H(3A)-N(3)-H(3B)	127(10)

Symmetry transformations used to generate equivalent atoms:

#1 x,y-1,z #2 -x,y,-z+1/2 #3 x,y,-z+1/2

Table 2.8 Bond lengths [Å] and angles [º] for Tl^{+1} 4(TU) 3-Aminobenzoate.

D-H...A	d(D-H)	d(H...A)	d(D...A)	<(DHA)
N(1)-H(1A)...O(1)#4	0.82(3)	2.20(3)	2.908(4)	145(2)
N(2)-H(2A)...O(1)	0.81(3)	2.27(3)	3.022(4)	156(3)

Symmetry transformations used to generate equivalent atoms:

#1 x,y-1,z #2 -x,y,-z+1/2 #3 x,y,-z+1/2 #4 -x+1/2,y-1/2,-z+1/2

Table 2.9 Hydrogen bonds for Tl^{+1} 4(TU) 3-Aminobenzoate [Å and º].

2.3.4 RESULTS FOR THE BENZOATE COMPLEX CRYSTAL ANALYSIS

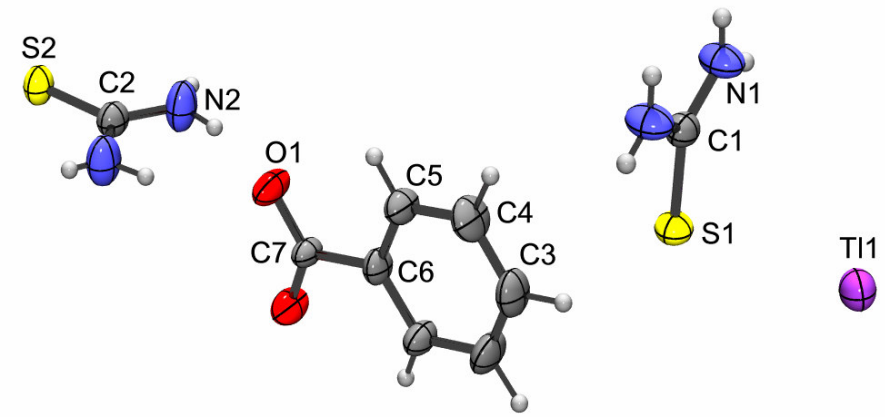

Fig. 2.9 **Molecular structure of the components involved in the Benzoate complex, with displacement ellipsoids drawn at the 50% probability level. H-atoms are shown.**

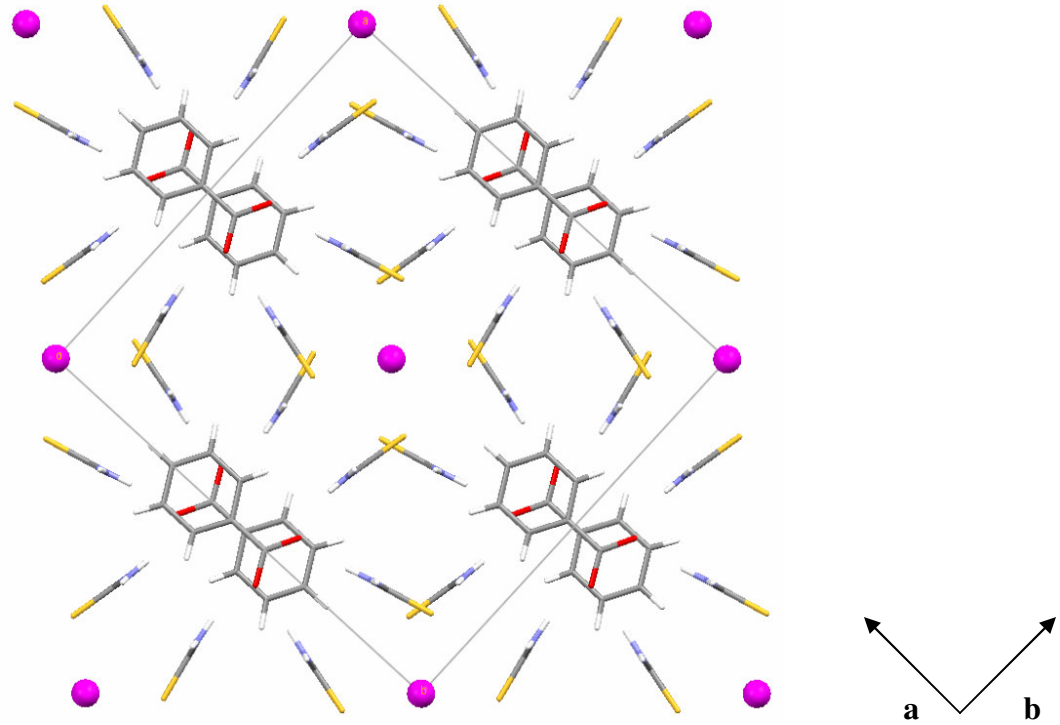

Fig. 2.10 **Molecular packing of the Benzoate complex viewed along the direction of the c axis. The direction of the a and b axes are shown above.**

CRYSTAL STRUCTURE TABLES FOR BENZOATE COMPLEX

Identification code	nb10_abs	
Empirical formula	C_{11} H_{21} N_8 O_2 S_4 Tl	
Formula weight	629.97	
Temperature	293(2) K	
Wavelength	0.71073 Å	
Crystal system	Orthorhombic	
Space group	C m c m	
Unit cell dimensions	a = 15.5482(11) Å	α= 90º.
	b = 17.0021(12) Å	β= 90º.
	c = 8.0954(6) Å	γ = 90º.
Volume	2140.0(3) $Å^3$	
Z	4	
Density (calculated)	1.955 Mg/m^3	
Absorption coefficient	7.961 mm^{-1}	
F(000)	1216	
Crystal size	0.40 x 0.18 x 0.16 mm^3	
Theta range for data collection	2.62 to 26.43º.	
Index ranges	-18<=h<=19, -7<=k<=21, -10<=l<=9	
Reflections collected	5719	
Independent reflections	1157 [R(int) = 0.0285]	
Completeness to theta = 25.00º	99.8 %	
Absorption correction	Semi-empirical from equivalents	
Max. and min. transmission	0.280 and 0.146	
Refinement method	Full-matrix least-squares on F^2	
Data / restraints / parameters	1157 / 0 / 102	
Goodness-of-fit on F^2	1.105	
Final R indices [I>2σ(I)]	R1 = 0.0327, wR2 = 0.0789	
R indices (all data)	R1 = 0.0340, wR2 = 0.0808	

Extinction coefficient	0.0046(4)
Largest diff. peak and hole	1.574 and -1.865 e.Å^{-3}

* $w = 1/ [\sigma^2 (F_0^2) + (0.0707P)^2 + 0.0977P]$ where $P = (F_0^2 + 2Fc^2)/ 3$

$\Delta\rho$ max = 1.2 e.Å^{-3} (0.5Å from C1)

$\Delta\rho$ min = -1.69e.Å^{-3}

Table 2.10 Crystal data and structure refinement for Tl^{+1} 4(TU) Benzoate.

Tl(1)-S(1)	3.3642(7)		
Tl(1)-S(2)#1	3.4345(9)	S(1)-Tl(1)-S(2)#1	67.103(15)
S(1)-C(1)	1.718(4)	C(1)-S(1)-Tl(1)	111.10(8)
C(1)-N(1)	1.316(3)	N(1)#3-C(1)-N(1)	119.0(4)
N(1)-H(1A)	0.73(3)	N(1)-C(1)-S(1)	120.52(19)
N(1)-H(1B)	0.81(4)	C(1)-N(1)-H(1A)	117.1(18)
S(2)-C(2)	1.710(3)	C(1)-N(1)-H(1B)	125(4)
C(2)-N(2)	1.315(3)	H(1A)-N(1)-H(1B)	118(4)
N(2)-H(2A)	0.86(4)	N(2)#3-C(2)-N(2)	117.5(4)
N(2)-H(2B)	0.68(4)	N(2)-C(2)-S(2)	121.27(18)
O(1)-C(7)	1.243(4)	C(2)-N(2)-H(2A)	113(2)
C(3)-C(4)#2	1.373(5)	C(2)-N(2)-H(2B)	126(4)
C(3)-C(4)	1.373(5)	H(2A)-N(2)-H(2B)	121(4)
C(3)-H(3)	1.01(8)	C(4)#2-C(3)-C(4)	121.3(5)
C(4)-C(5)	1.407(5)	C(4)#2-C(3)-H(3)	119.4(2)
C(4)-H(4)	0.98(5)	C(4)-C(3)-H(3)	119.4(2)
C(5)-C(6)	1.381(5)	C(3)-C(4)-C(5)	119.1(4)
C(5)-H(5)	0.92(5)	C(3)-C(4)-H(4)	118(3)
C(6)-C(5)#2	1.381(5)	C(5)-C(4)-H(4)	122(3)
C(6)-C(7)	1.523(6)	C(6)-C(5)-C(4)	120.7(4)
C(7)-O(1)#2	1.243(4)	C(6)-C(5)-H(5)	122(3)

C(4)-C(5)-H(5)	117(3)	O(1)-C(7)-O(1)#2	124.6(5)
C(5)#2-C(6)-C(5)	119.0(6)	O(1)-C(7)-C(6)	117.7(2)
C(5)#2-C(6)-C(7)	120.5(3)	O(1)#2-C(7)-C(6)	117.7(2)
C(5)-C(6)-C(7)	120.5(3)		

Symmetry transformations used to generate equivalent atoms:

#1 x,y-1,z #2 -x,y,-z+1/2 #3 x,y,-z+1/2

Table 2.11 Bond lengths [Å] and angles [º] for Tl^{+1} 4(TU) Benzoate.

D-H...A	d(D-H)	d(H...A)	d(D...A)	<(DHA)
N(1)-H(1A)...O(1)#4	0.73(3)	2.25(3)	2.900(4)	150(2)
N(2)-H(2A)...O(1)	0.86(4)	2.22(4)	3.038(4)	161(3)

Symmetry transformations used to generate equivalent atoms:

#1 x,y-1,z #2 -x,y,-z+1/2 #3 x,y,-z+1/2 #4 -x+1/2,y-1/2,-z+1/2

Table 2.12 Hydrogen bonds for Tl^{+1} 4(TU) Benzoate [Å and º].

2.4 STRUCTURAL ANALYSIS OF THE FOUR BENZOIC ACID DERIVATIVE COMPLEXES

2.4.1 CELL DIMENSIONS AND VOLUMES

What is most evident in the four benzoic acid derivative structures obtained in this study, is that they are all isostructural, space group Cmcm. In fact their unit cell dimensions and volumes are almost identical which would indicate that the channel/cavity is of a fixed size and that varying the substituents on the aromatic ring makes little to no difference to the channel size.

COMPLEX	UNIT CELL DIMENSIONS (Å) AND VOLUMES (Å^3)			
	a	b	c	VOLUME
2-Fluoro	15.7317(10)	17.0319(11)	8.0881(5)	2167.1(2)
3-Fluoro	15.6079(8)	17.1485(9)	8.0752(4)	2161.34(19)
3-Amino	15.5683(11)	17.1150(12)	8.1352(5)	2167.6(3)
Benzoate	15.5482(11)	17.0021(12)	8.0954(6)	2140.0(3)

Table 2.13 **Table showing how similar the unit cell dimensions and volumes are for the four benzoic acid derivative complexes.**

This is most clearly illustrated by an overlay of the molecular packing of all four structures, Shown in Fig 2.11.

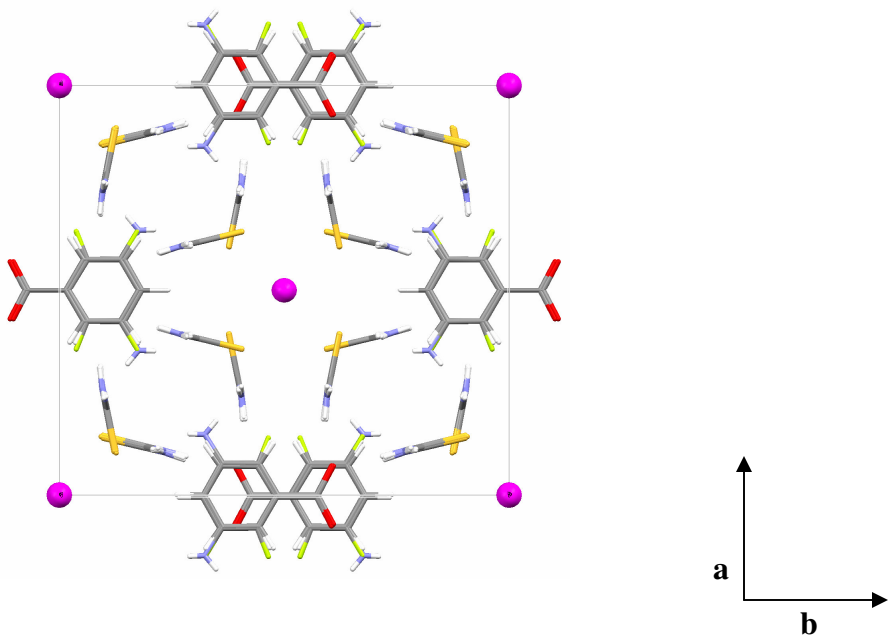

Fig.2.11 **An overlay of the molecular packing of all four benzoic acid derivative complexes viewed along the direction of the c axis. The direction of the a and b axes are shown above.**

2.4.2 CHANNEL SIZES

The channel sizes of the four complexes were in fact measured and the results confirmed that they are of very similar sizes. The two channels of each complex that were measured were the thallium cation channel and the benzoate derivative anion channel.

As was reported for the original benzoate complex [1], the thallium channel size was found by measuring the distances between the following:

- The sulphur atoms of the thiourea molecules involved in the Tl-S close approaches – referred to in Table 2.14 as S1 distances.
- The sulphur atoms of the thiourea molecules involved in van der Waal contacts – referred to Table 2.14 as S2 distances.
- The sulphur atoms belonging to thiourea molecules of unlike type – referred to in Table 2.14 as S3 distances.

Table 2.14 gives the values found for the four complexes prepared in this study as well as those reported for the original benzoate structure. Note how similar all the distances are to each other. The largest differences with in the S1, S2 and S3 values of the four complexes are 0.032 Å, 0.078 Å and 0.045 Å respectively. This suggests that the size of the substituents do not have any significant effect on the packing in the solid state. From Fig. 2.11 it is also clear that there is sufficient space between the 2 different amino groups of the thiourea molecules to accommodate the different substituents on the benzoate moiety. Thus, it seems that the lattice described by Tl^+ and the four thiourea molecules do not require much adjusting to accommodate a variety of substituent groups (with in reason). The meta substituents show similar distances from the two closest (TU)NH_2 groups. This suggests that other meta substituted benzoates may also crystallise in this space group (see Table 2.15).

COMPLEX	**S1 DISTANCES (Å)**	**S2 DISTANCES (Å)**	**S3 DISTANCES (Å)**
2-Fluoro	3.366	4.476	3.781
3-Fluoro	3.334	4.470	3.747
3-Amino	3.345	4.462	3.736
Benzoate	3.352	4.517	3.758
Benzoate #	3.360	4.540	3.770

Note: Benzoate # [1]

Table 2.14 **Table showing the similar sulphur distances used to indicate the size of the cation channels in the four complexes.**

ATOMS ANALYSED	INTERATOMIC DISTANCES (Å)
(TU)NH_2……2F	3.173
(TU)NH_2……2H	3.273
(TU)NH_2……3F	3.210 3.332
(TU)NH_2……3H	3.201 3.434
(TU)NH_2……3N(H_2)	3.236 3.355

Note: (TU)NH_2 refers to the hydrogens associated with the thiourea molecule

2F refers to the fluorine atom in the 2-fluoro complex

2H refers to the ortho hydrogen atom in the benzoate complex

3H refers to the meta hydrogen atom in the benzoate complex

3F refers to the fluorine atom in the 3-fluoro complex

3N refers to the nitrogen atom at the meta position in the 3-amino complex

Table 2.15 Interatomic distances between the hydrogens of the thiourea molecule and the ortho-fluorine atom, ortho-hydrogen of benzoate, meta-fluorine atom, meta-hydrogen atom and meta-nitrogen of amino the substituent.

The anionic channel containing the benzoate derivatives was not measured for the original benzoate structure [1]. For the four complexes, three different measurements as an approximation of the size of each channel were taken. Firstly the width of the channel was measured by the distance between two H1 hydrogens from similar thiourea molecules on either side of the width of the cavity (referred to as distance 1 in Table 2.16). The second measurement was the length of the channel which was measured by the distance between two H2 hydrogens from similar thiourea molecules on either side of the length of the cavity (referred to as distance 2 in Table 2.16). The final measurement was taken from the para hydrogen on a benzoate anion to the para hydrogen of the second benzoate anion with in the same cavity (referred to as distance 3 in Table 2.16).

It should be noted that distances 1 and 3 are measured from atoms which are not in the same plane as each other, however, the same atoms were measured in all four complexes, therefore, these distances used to indicate the relative sizes of the anionic channels for all four complexes.

As with the thallium cation channel, the Table 2.16 indicates the similarity of the sizes of the channels in all four complexes. The largest differences with in the distance 1, 2 and 3 values

are 0.289 Å, 0.204 Å and 0.370 Å respectively. These distances may appear significantly larger than for the cation channel differences, but these values are for channels containing bulky ligands as compared to those around a single Tl^+ atom.

COMPLEX	DISTANCE 1 (Å)	DISTANCE 2 (Å)	DISTANCE 3 (Å)
2-Fluoro	5.947	8.666	8.967
3-Fluoro	5.806	8.709	8.770
3-Amino	5.916	8.710	8.740
Benzoate	6.095	8.506	9.110

Table 2. 16 **Table showing the similar distances used to indicate the size of the anion channels in the four complexes.**

2.4.3 ATOMIC INTERACTIONS

As was reported for the original benzoic acid complex [1], the four complexes also show two distinct Tl – S interactions within each of the complexes.

COMPLEX	Tl(1) – S(1) Å	Tl(1) – S(2)#1 Å
2-Fluoro	3.3792(7)	3.4235(8)
3-Fluoro	3.3537(7)	3.4142(8)
3-Amino	3.3588(6)	3.4209(7)
Benzoate	3.3642(7)	3.4345(9)

Table 2.17 **Table showing the two different Tl – S interatomic distances**

In terms of hydrogen bond interactions the four benzoic acid derivative complexes once again correspond to the results of the initial benzoate complex where by each benzoate ion is hydrogen bonded to the surrounding amino groups of the thiourea molecules and that there are two different NH…O approaches. Those ranging between 2.90 – 2.97 Å which indicate powerful hydrogen bonds and those ranging from 3.02 – 3.06 Å which are within the range of O-H-N hydrogen bonds given by Pimentel and Mc Clellan [1]. The exact values are given in the

respective tables for each complex. There is also a certain amount of hydrogen bonding within the other complexes of this chapter and as with the benzoic acid derivative complexes, the hydrogen bond values are given in the relevant tables.

COMPLEX	**N(1)……O(1) (Å)**	**N(2)……O(1) (Å)**
2-Fluoro	2.974(4)	3.044(4)
3-Fluoro	2.922(4)	3.057(4)
3-Amino	2.908(4)	3.022(4)
Benzoate	2.900(4)	3.038(4)

Table 2.18 Common N…O distances between the four complexes and the two thiourea molecules involved in hydrogen bonding.

Table 2.18 indicates that the two distances associated with the 3-fluoro and 3-amino benzoate complexes differ for both complexes. Also in terms of the 3-substituted complexes (3-benzoate, 3-fluoro and 3-amino benzoates) the 3-amino benzoate has the shorter N……O distance, and the 3-fluoro benzoate has the longer N……O distance. This is in accordance with the electron donating character of the 3-amino group, that results in a higher concentration of electron density on the oxygen atoms. The more electronegative fluorine substituent causes the opposite effect, as could be expected. The N……O distances for the benzoate complex and the 2-fluoro benzoate complex are such that the hydrogen bonding for the benzoic acid complex is stronger than that for the 2-fluoro complex, again as a result of the electronegativity of the fluorine atom.

2.5 CRYSTALLOGRAPHIC RESULTS FOR THE REMAINING COMPLEXES

2.5.1 RESULTS FOR THE PF_6^- COMPLEX CRYSTAL ANALYSIS

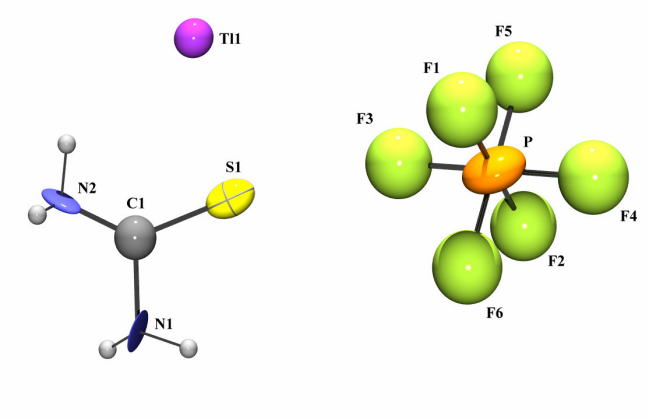

Fig. 2.12 **Molecular structure of the components involved in the PF_6^- complex, with displacement ellipsoids drawn at the 50% probability level. H-atoms are shown.**

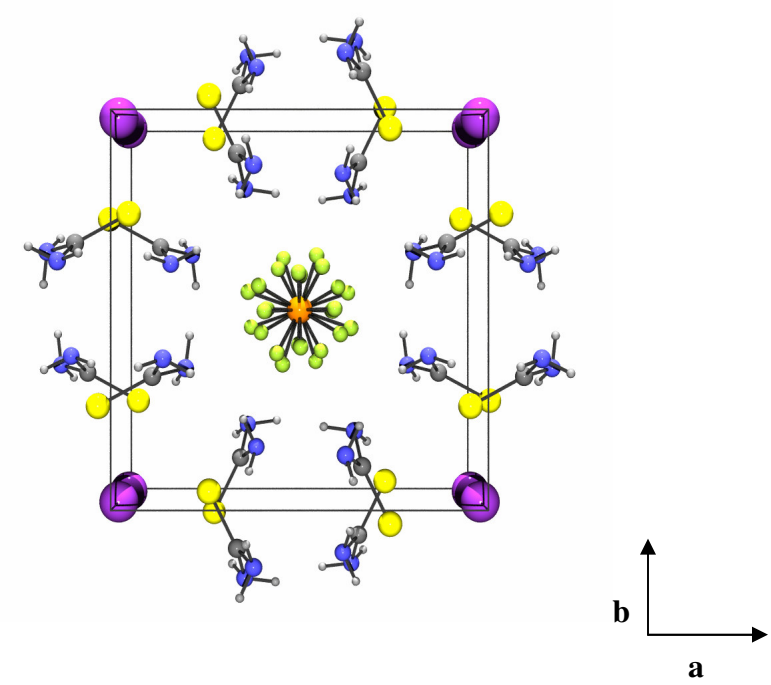

Fig. 2.13 **Molecular packing of the PF_6^- complex viewed along the direction of the c axis. The direction of the a and b axes are shown above.**

CRYSTAL STRUCTURE TABLES FOR PF_6^- COMPLEX

Identification code	nb01	
Empirical formula	$C_4 H_{16} F_6 N_8 P S_4 Tl$	
Formula weight	653.83	
Temperature	293(2) K	
Wavelength	0.71073 Å	
Crystal system	Tetragonal	
Space group	P4cc	
Unit cell dimensions	a = 10.4608(3) Å	α= 90º.
	b = 10.4608(3) Å	β= 90º.
	c = 8.2304(5) Å	γ = 90º.
Volume	900.64(7) $Å^3$	
Z	2	
Density (calculated)	2.411 Mg/m^3	
Absorption coefficient	9.584 mm^{-1}	
F(000)	620	
Crystal size, colour	0.32 x 0.17 x 0.15 mm, (cream needles)	
Theta range for data collection	2.75 to 26.54º.	
Index ranges	-13<=h<=12, -12<=k<=13, -3<=l<=10	
Reflections collected	4318	
Independent reflections	555 [R(int) = 0.0309]	
Completeness to theta = 25.00θ	99.5 %	
Absorption correction	Multi scan (SADABS, Buker 2001)	
Max. and min. transmission	1.0 and 0.813205	
Refinement method	Full-matrix least-squares on F^2	
Data / restraints / parameters	555 / 1 / 49	
Goodness-of-fit on F^2	1.082	
Final R indices [I>2sigma(I)]	R1 = 0.0671, wR2 = 0.1848 *	
R indices (all data)	R1 = 0.0683, wR2 = 0.1856	

Absolute structure parameter	0.10(7)
Largest diff. peak and hole	1.203 and -1.689 e.Å^{-3}

* $w = 1/ [\sigma^2 (F_0^2) + (0.0707P)^2 + 0.0977P]$ where $P = (F_0^2 + 2Fc^2)/ 3$

$\Delta\rho$ max = 1.2 e.Å^{-3} (0.5Å from C1)

$\Delta\rho$ min = -1.69e.Å^{-3}

Table 2.19 Crystal data and structure refinement for Tl^{+1} 4(TU) PF_6^-

---

S(1)-C(1)	1.71(2)		
C(1)-N(2)	1.34(4)		
C(1)-N(1)	1.45(5)		
P-F(1)	1.56	P-F(2)	1.57
P-F(4)	1.56	P-F(3)	1.57
P-F(6)	1.57	P-F(5)	1.57

N(2)-C(1)-N(1)	116(2)				
N(2)-C(1)-S(1)	134(3)				
N(1)-C(1)-S(1)	109(3)				
F(1)-P-F(4)	90.5	F(1)-P-F(2)	1.79.6	F(3)-P-F(4)	179.4
F(1)-P-F(6)	90.4	F(1)-P-F(3)	89.8	F(5)-P-F(6)	179.3
F(4)-P-F(6)	90.2	F(1)-P-F(5)	90.3		

Symmetry transformations used to generate equivalent atoms:

Table 2.20 Bond lengths [Å] and angles [º] for Tl^{+1} 4(TU) PF_6^-.

D-H...A	d(D-H)	d(H...A)	d(D...A)	<(DHA)
N(1)-H(1A)...F(6)#1	0.86	1.94	2.70(7)	147.1
N(1)-H(1A)...F(4)#2	0.86	1.96	2.8(2)	153.6
N(1)-H(1A)...F(5)#3	0.86	1.97	2.78(19)	156.3

Symmetry transformations used to generate equivalent atoms:

#1 -x+1,-y,z #2 x,y-1,z #3 y,-x,z

Table 2.21 Hydrogen bonds for Tl^{+1} 4(TU) PF_6^{-1} [Å and º].

2.5.2 RESULTS FOR THE BF_4^- COMPLEX CRYSTAL ANALYSIS

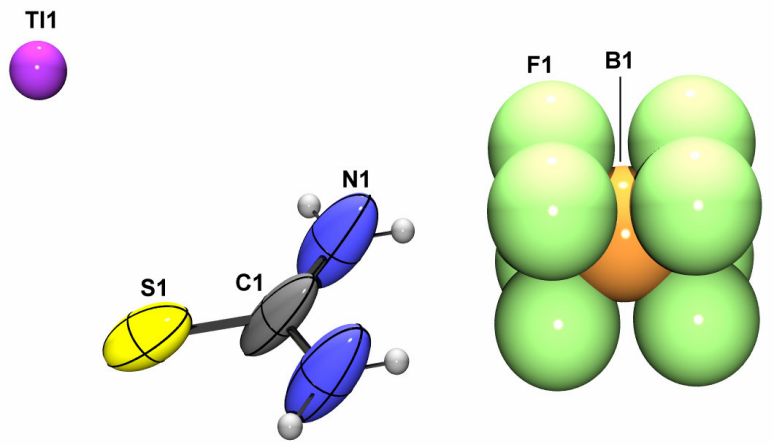

Fig. 2.14 **Molecular structure of the components involved in the BF_4^- complex, with displacement ellipsoids drawn at the 50% probability level. H-atoms are shown.**

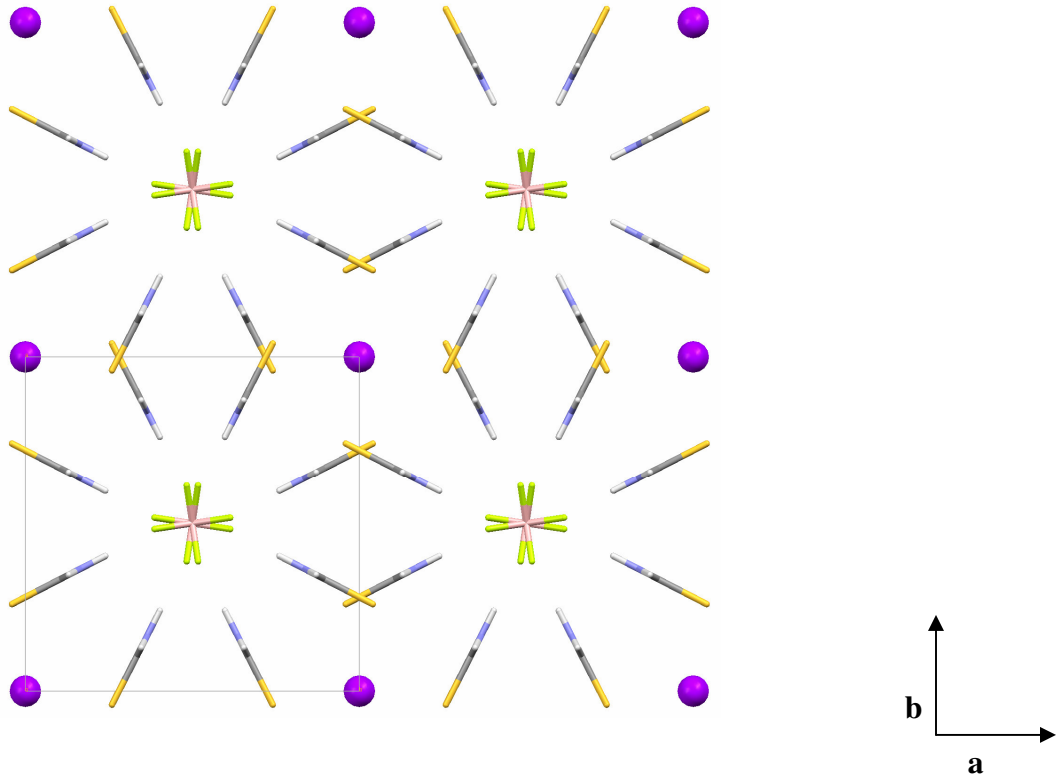

Fig. 2.15 **Molecular packing of BF_4^- complex viewed along the direction of the c axis. The direction of the a and b axes are shown above.**

CRYSTAL SRUCTURE TABLES FOR BF_4^- COMPLEX

Identification code	nb05_abs	
Empirical formula	$C_4 H_{16} B F_4 N_8 S_4 Tl$	
Formula weight	595.67	
Temperature	293(2) K	
Wavelength	0.71073 Å	
Crystal system	Tetragonal	
Space group	P 4/m c c	
Unit cell dimensions	a = 10.3640(4) Å	α = 90º.
	b = 10.3640(4) Å	β = 90º.
	c = 8.2340(7) Å	γ = 90º.
Volume	884.43(9) $Å^3$	
Z	2	
Density (calculated)	2.237 Mg/m^3	
Absorption coefficient	9.645 mm^{-1}	
F(000)	564	
Crystal size	0.24 x 0.10 x 0.10 mm^3	
Theta range for data collection	2.78 to 26.50º.	
Index ranges	-7<=h<=12, -12<=k<=12, -10<=l<=6	
Reflections collected	4272	
Independent reflections	475 [R(int) = 0.0244]	
Completeness to theta = 25.00º	99.5 %	
Absorption correction	Semi-empirical from equivalents	
Max. and min. transmission	0.381 and 0.240	
Refinement method	Full-matrix least-squares on F^2	
Data / restraints / parameters	475 / 2 / 29	
Goodness-of-fit on F^2	1.410	
Final R indices [I>2σ(I)]	R1 = 0.0269, wR2 = 0.0713	
R indices (all data)	R1 = 0.0318, wR2 = 0.0761	

Extinction coefficient	0
Largest diff. peak and hole	1.232 and -0.488 e.Å^{-3}

* $w = 1/ [\sigma^2 (F_0^2) + (0.0707P)^2 + 0.0977P]$ where $P = (F_0^2 + 2Fc^2)/ 3$

$\Delta\rho$ max = 1.2 e.Å^{-3} (0.5Å from C1)

$\Delta\rho$ min = -1.69e.Å^{-3}

Table 2.22 Crystal data and structure refinement for Tl^{+1} 4(TU) BF_4^-.

Tl(1)-S(1)	3.4103(19)
S(1)-C(1)	1.709(12)
C(1)-N(1)#1	1.330(8)
C(1)-N(1)	1.330(8)
N(1)-H(1)	0.8600
N(1)-H(2)	0.8600
B(1)-F(1)	1.307(13)

C(1)-S(1)-Tl(1)	104.6(3)
N(1)#1-C(1)-N(1)	117.8(10)
N(1)#1-C(1)-S(1)	121.1(5)
N(1)-C(1)-S(1)	121.1(5)
C(1)-N(1)-H(1)	120.0
C(1)-N(1)-H(2)	120.0
H(1)-N(1)-H(2)	120.0
F(1)-B(1)-F(1)#2	99.9(7)

Symmetry transformations used to generate equivalent atoms:

#1 x,y,-z #2 y,-x+1,-z

Table 2.23 Bond lengths [Å] and angles [º] for Tl^{+1} 4(TU) BF_4^-.

D-H...A	d(D-H)	d(H...A)	d(D...A)	<(DHA)
N(1)-H(1)...F(1)#3	0.86	2.02	2.84(2)	161.1

Symmetry transformations used to generate equivalent atoms:

#1 x,y,-z #2 y,-x+1,-z #3 -y+1,x,-z

Table 2.24 Hydrogen bonds for Tl^{+1} 4(TU) BF_4^- [Å and º].

2.5.3 RESULTS FOR THE THALLIUM – 4-AMINOBENZOATE CRYSTAL ANALYSIS

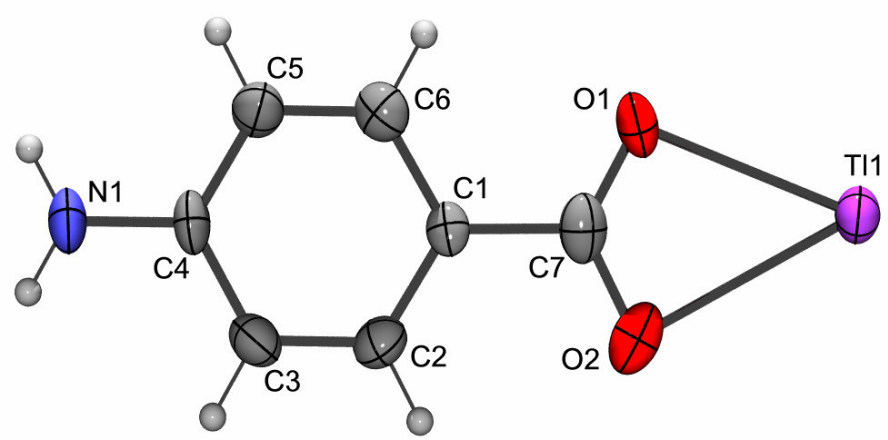

Fig. 2.16 **Molecular structure of the components involved in the thallium – 4-aminobenzoate, with displacement ellipsoids drawn at the 50% probability level. H-atoms are shown.**

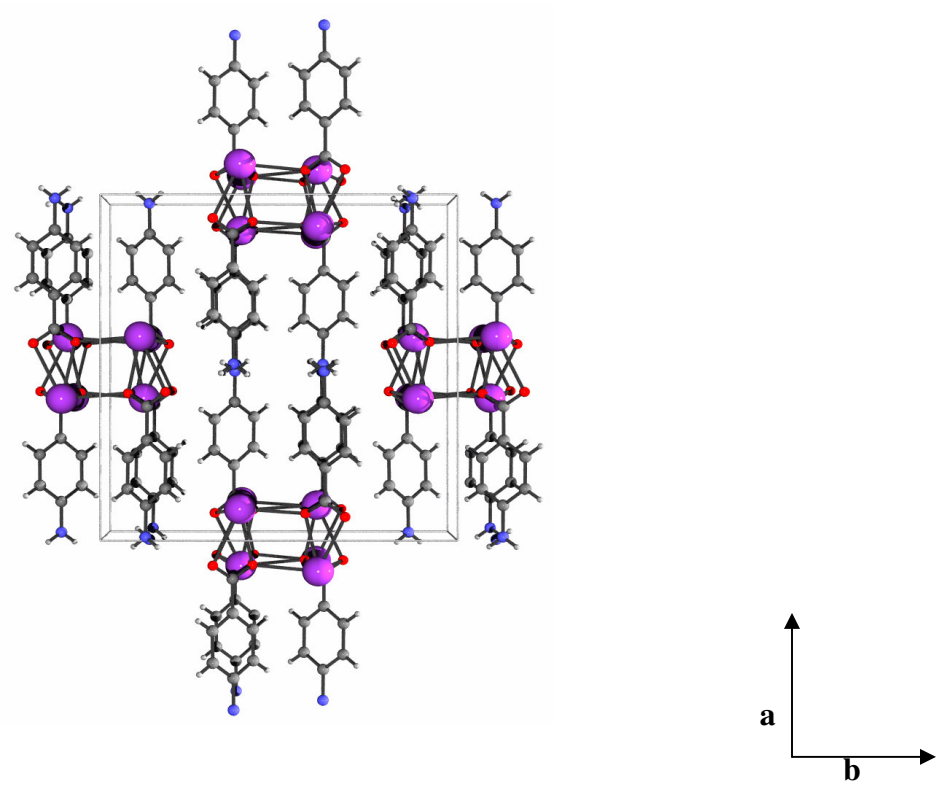

Fig. 2.17 **Molecular packing of the thallium – 4-aminobenzoate viewed along the direction of the c axis. The direction of the a and b axes are shown above.**

CRYSTAL STRUCTURE TABLES FOR THALLIUM – 4-AMINOBENZOATE

Identification code	nb13a_abs1	
Empirical formula	$C_7 H_6 N O_2 Tl$	
Formula weight	340.50	
Temperature	293(2) K	
Wavelength	0.71073 Å	
Crystal system	Orthorhombic	
Space group	I b a 2	
Unit cell dimensions	a = 14.6579(14) Å	α= 90º.
	b = 15.1020(14) Å	β= 90º.
	c = 6.9606(6) Å	γ = 90º.
Volume	1540.8(2) $Å^3$	
Z	8	
Density (calculated)	2.936 Mg/m^3	
Absorption coefficient	20.908 mm^{-1}	
F(000)	1216	
Crystal size	0.12 x 0.10 x 0.08 mm^3	
Theta range for data collection	2.70 to 26.35º.	
Index ranges	-18<=h<=18, -18<=k<=16, -8<=l<=3	
Reflections collected	3916	
Independent reflections	980 [R(int) = 0.0414]	
Completeness to theta = 25.00º	99.3 %	
Absorption correction	Semi-empirical from equivalents	
Max. and min. transmission	0.188 and 0.086	
Refinement method	Full-matrix least-squares on F^2	
Data / restraints / parameters	980 / 1 / 101	
Goodness-of-fit on F^2	1.049	
Final R indices [I>2σ(I)]	R1 = 0.0269, wR2 = 0.0664	
R indices (all data)	R1 = 0.0273, wR2 = 0.0668	

Absolute structure parameter	0.04(2)
Extinction coefficient	0.0058(3)
Largest diff. peak and hole	1.343 and -1.594 e.Å^{-3}

* $w = 1/ [\sigma^2 (F_0^2) + (0.0707P)^2 + 0.0977P]$ where $P = (F_0^2 + 2Fc^2)/ 3$

$\Delta\rho$ max = 1.2 e.Å^{-3} (0.5Å from C1)

$\Delta\rho$ min = -1.69e.Å^{-3}

Table 2.25 Crystal data and structure refinement for thallium – 4-aminobenzoate.

Tl(1)-O(1)	2.628(6)	N(1)-H(1B)	0.8600
Tl(1)-O(1)#1	2.785(7)		
Tl(1)-O(2)	2.796(7)	O(1)-Tl(1)-O(1)#1	70.9(2)
O(1)-C(7)	1.235(15)	O(1)-Tl(1)-O(2)	48.08(18)
O(1)-Tl(1)#2	2.898(7)	O(1)#1-Tl(1)-O(2)	112.21(16)
O(2)-C(7)	1.278(16)	C(7)-O(1)-Tl(1)	98.7(6)
O(2)-Tl(1)#3	2.837(7)	C(7)-O(1)-Tl(1)#1	117.7(8)
C(1)-C(2)	1.395(10)	Tl(1)-O(1)-Tl(1)#1	102.5(2)
C(1)-C(6)	1.417(11)	C(7)-O(1)-Tl(1)#2	115.7(9)
C(1)-C(7)	1.495(11)	Tl(1)-O(1)-Tl(1)#2	106.2(2)
C(2)-C(3)	1.383(10)	Tl(1)#1-O(1)-Tl(1)#2	113.1(2)
C(2)-H(2)	0.9300	C(7)-O(2)-Tl(1)	89.7(6)
C(3)-C(4)	1.411(13)	C(7)-O(2)-Tl(1)#3	105.3(8)
C(3)-H(3)	0.9300	Tl(1)-O(2)-Tl(1)#3	103.4(2)
C(4)-C(5)	1.380(13)	C(2)-C(1)-C(6)	116.6(6)
C(4)-N(1)	1.380(9)	C(2)-C(1)-C(7)	122.8(8)
C(5)-C(6)	1.372(9)	C(6)-C(1)-C(7)	120.6(8)
C(5)-H(5)	0.9300	C(3)-C(2)-C(1)	121.6(7)
C(6)-H(6)	0.9300	C(3)-C(2)-H(2)	119.2
N(1)-H(1A)	0.8600	C(1)-C(2)-H(2)	119.2

C(2)-C(3)-C(4)	120.6(7)	C(5)-C(6)-C(1)	121.8(7)
C(2)-C(3)-H(3)	119.7	C(5)-C(6)-H(6)	119.1
C(4)-C(3)-H(3)	119.7	C(1)-C(6)-H(6)	119.1
C(5)-C(4)-N(1)	121.4(9)	O(1)-C(7)-O(2)	123.5(9)
C(5)-C(4)-C(3)	118.2(7)	O(1)-C(7)-C(1)	119.5(10)
N(1)-C(4)-C(3)	120.4(8)	O(2)-C(7)-C(1)	116.7(10)
C(6)-C(5)-C(4)	121.1(8)	C(4)-N(1)-H(1A)	120.0
C(6)-C(5)-H(5)	119.4	C(4)-N(1)-H(1B)	120.0
C(4)-C(5)-H(5)	119.4	H(1A)-N(1)-H(1B)	120.0

Symmetry transformations used to generate equivalent atoms:

#1 -x+2,-y+1,z #2 x+0,-y+1,z-1/2 #3 x+0,-y+1,z+1/2

Table 2.26 Bond lengths [Å] and angles [º] for thallium – 4-aminobenzoate.

D-H...A	d(D-H)	d(H...A)	d(D...A)	<(DHA)
N(1)-H(1B)...O(2)#4	0.86	2.40	3.063(9)	133.7

Symmetry transformations used to generate equivalent atoms:

#1 -x+2,-y+1,z #2 x+0,-y+1,z-1/2 #3 x+0,-y+1,z+1/2

#4 -x+3/2,y-1/2,z

Table 2.27 Hydrogen bonds for thallium – 4-aminobenzoate [Å and º].

2.5.4 RESULTS FOR THE 2Tl(I), 2(TU) 2(Tph) 2H_2O (Tph = terephthalate benzene-1,4-dicarboxylate) COMPLEX CRYSTAL ANALYSIS

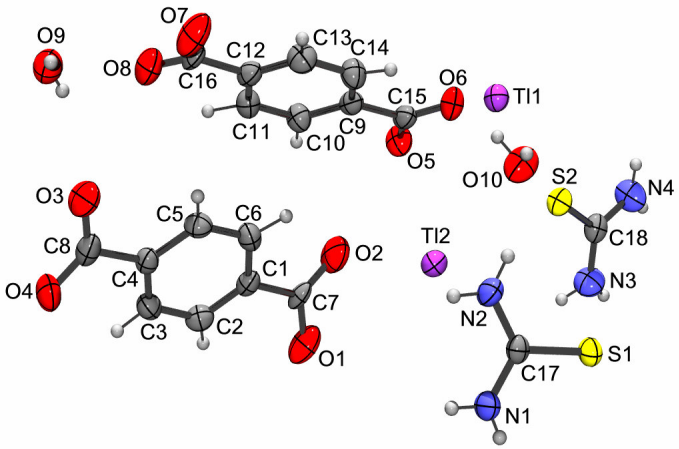

Fig. 2.18 **Molecular structure of the components involved in the 2Tl(I), 2(TU) 2(Tph) 2H_2O (Tph = terephthalate benzene-1,4-dicarboxylate) complex, with displacement ellipsoids drawn at the 50% probability level. H-atoms are shown.**

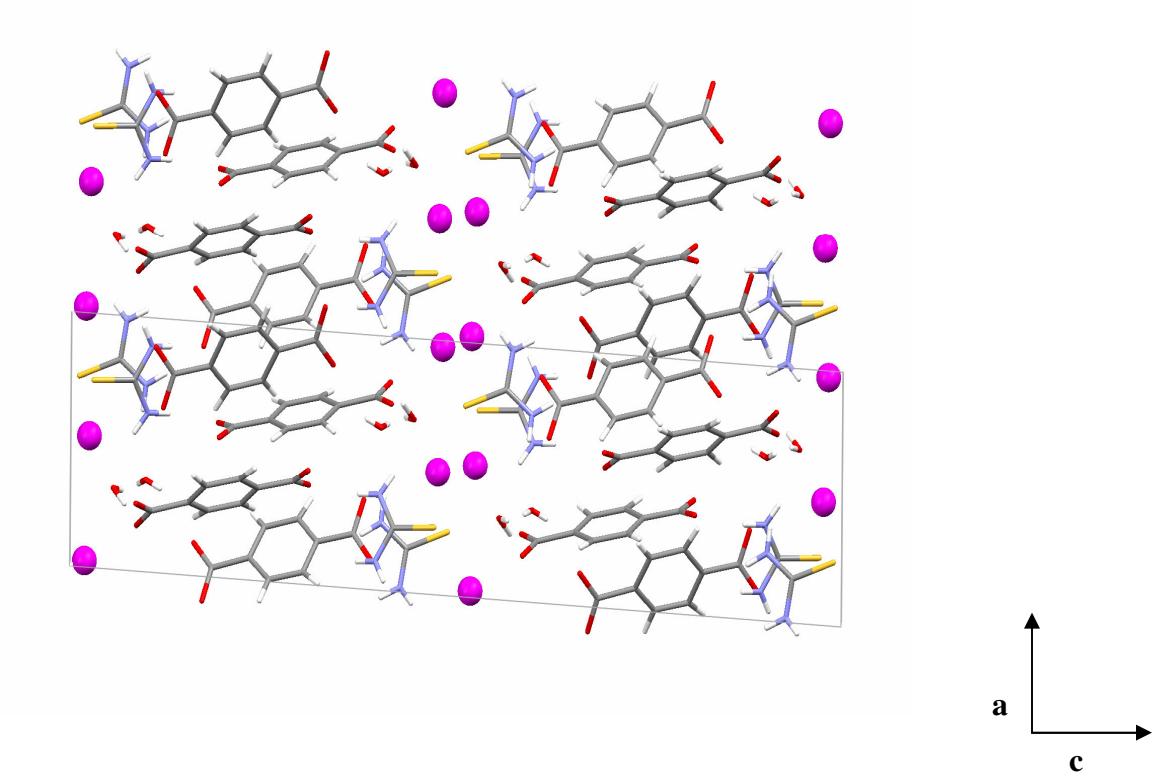

Fig. 2.19 **Molecular packing of 2Tl(I), 2(TU) 2(Tph) 2H_2O (Tph = terephthalate benzene-1,4-dicarboxylate) complex viewed along the direction of the b axis. The direction of the a and c axes are shown above.**

CRYSTAL STRUCTURE TABLES FOR 2Tl(I), 2(TU) 2(Tph) 2H_2O (Tph = terephthalate benzene-1,4-dicarboxylate) COMPLEX

Identification code	nb12a_abs	
Empirical formula	C_{18} H_{20} N_4 O_{10} S_2 Tl_2	
Formula weight	925.24	
Temperature	293(2) K	
Wavelength	0.71073 Å	
Crystal system	Monoclinic	
Space group	P 21/c	
Unit cell dimensions	a = 8.4682(4) Å	α= 90º.
	b = 9.6750(5) Å	β= 93.2990(10)º.
	c = 30.4239(16) Å	γ = 90º.
Volume	2488.5(2) Å^3	
Z	4	
Density (calculated)	2.470 Mg/m^3	
Absorption coefficient	13.162 mm^{-1}	
F(000)	1720	
Crystal size	0.26 x 0.22 x 0.18 mm^3	
Theta range for data collection	2.50 to 26.57º.	
Index ranges	-3<=h<=10, -12<=k<=11, -38<=l<=36	
Reflections collected	13135	
Independent reflections	4748 [R(int) = 0.0298]	
Completeness to theta = 25.00º	99.5 %	
Absorption correction	Semi-empirical from equivalents	
Max. and min. transmission	0.094 and 0.061	
Refinement method	Full-matrix least-squares on F^2	
Data / restraints / parameters	4748 / 0 / 406	
Goodness-of-fit on F^2	1.139	
Final R indices [I>2σ(I)]	R1 = 0.0295, wR2 = 0.0767	

R indices (all data)	R1 = 0.0323, wR2 = 0.0785
Extinction coefficient	0.00370(13)
Largest diff. peak and hole	1.534 and -0.834 e.Å^{-3}

* $w = 1/ [\sigma^2 (F_0^2) + (0.0707P)^2 + 0.0977P]$ where $P = (F_0^2 + 2Fc^2)/ 3$

$\Delta\rho$ max = 1.2 e.Å^{-3} (0.5Å from C1)

$\Delta\rho$ min = -1.69e.Å^{-3}

Table 2.28 Crystal data and structure refinement for 2Tl(I), 2(TU) 2(Tph) 2H_2O (Tph = terephthalate benzene-1,4-dicarboxylate).

Tl(1)-O(5)	2.792(4)	N(1)-H(1A)	0.84(6)
Tl(1)-S(2)	3.1303(13)	N(1)-H(1B)	0.67(6)
Tl(1)-S(1)#1	3.6870(12)	N(2)-C(17)	1.310(6)
Tl(2)-S(1)	3.2962(13)	N(2)-H(2A)	0.84(6)
Tl(2)-S(2)	3.3623(13)	N(2)-H(2B)	0.83(6)
S(1)-C(17)	1.717(4)	N(3)-C(18)	1.315(7)
S(2)-C(18)	1.714(5)	N(3)-H(3A)	0.91(6)
O(1)-C(7)	1.204(7)	N(3)-H(3B)	0.84(9)
O(2)-C(7)	1.225(6)	N(4)-C(18)	1.314(7)
O(3)-C(8)	1.244(7)	N(4)-H(4A)	0.79(6)
O(4)-C(8)	1.250(7)	N(4)-H(4B)	0.78(5)
O(5)-C(15)	1.255(6)	C(1)-C(6)	1.373(7)
O(6)-C(15)	1.252(6)	C(1)-C(2)	1.380(8)
O(7)-C(16)	1.211(7)	C(1)-C(7)	1.465(6)
O(8)-C(16)	1.216(7)	C(2)-C(3)	1.379(8)
O(9)-H(9A)	0.97(11)	C(2)-H(2)	0.94(6)
O(9)-H(9B)	0.64(7)	C(3)-C(4)	1.376(7)
O(10)-H(10A)	0.68(7)	C(3)-H(3)	0.91(7)
O(10)-H(10B)	1.01(13)	C(4)-C(5)	1.389(7)
N(1)-C(17)	1.325(6)	C(4)-C(8)	1.532(6)

C(5)-C(6)	1.373(7)
C(5)-H(5)	0.82(6)
C(6)-H(6)	0.94(5)
C(9)-C(14)	1.367(7)
C(9)-C(10)	1.398(7)
C(9)-C(15)	1.519(6)
C(10)-C(11)	1.385(8)
C(10)-H(10)	0.91(5)
C(11)-C(12)	1.361(7)
C(11)-H(11)	1.03(6)
C(12)-C(13)	1.376(8)
C(12)-C(16)	1.457(6)
C(13)-C(14)	1.389(7)
C(13)-H(13)	0.86(6)
C(14)-H(14)	0.96(6)

O(5)-Tl(1)-S(2)	87.66(9)
O(5)-Tl(1)-S(1)#1	111.31(9)
S(2)-Tl(1)-S(1)#1	147.46(3)
S(1)-Tl(2)-S(2)	143.85(3)
C(17)-S(1)-Tl(2)	101.37(16)
C(18)-S(2)-Tl(1)	101.75(17)
C(18)-S(2)-Tl(2)	103.00(18)
Tl(1)-S(2)-Tl(2)	80.05(3)
C(15)-O(5)-Tl(1)	95.4(3)
H(9A)-O(9)-H(9B)	119(9)
H(10A)-O(10)-H(10B)	109(9)
C(17)-N(1)-H(1A)	125(4)
C(17)-N(1)-H(1B)	127(5)
H(1A)-N(1)-H(1B)	108(6)
C(17)-N(2)-H(2A)	115(4)
C(17)-N(2)-H(2B)	122(4)
H(2A)-N(2)-H(2B)	124(6)
C(18)-N(3)-H(3A)	124(3)
C(18)-N(3)-H(3B)	116(7)
H(3A)-N(3)-H(3B)	116(8)
C(18)-N(4)-H(4A)	119(4)
C(18)-N(4)-H(4B)	117(4)
H(4A)-N(4)-H(4B)	123(6)
C(6)-C(1)-C(2)	123.2(5)
C(6)-C(1)-C(7)	119.4(5)
C(2)-C(1)-C(7)	117.3(5)
C(3)-C(2)-C(1)	117.3(5)
C(3)-C(2)-H(2)	126(4)
C(1)-C(2)-H(2)	116(4)
C(4)-C(3)-C(2)	121.3(5)
C(4)-C(3)-H(3)	122(4)
C(2)-C(3)-H(3)	117(4)
C(3)-C(4)-C(5)	119.6(5)
C(3)-C(4)-C(8)	120.1(5)
C(5)-C(4)-C(8)	120.3(5)
C(6)-C(5)-C(4)	120.5(5)
C(6)-C(5)-H(5)	120(4)
C(4)-C(5)-H(5)	120(4)
C(5)-C(6)-C(1)	118.1(5)
C(5)-C(6)-H(6)	128(3)
C(1)-C(6)-H(6)	114(3)
O(1)-C(7)-O(2)	123.7(5)
O(1)-C(7)-C(1)	118.5(5)
O(2)-C(7)-C(1)	117.8(4)
O(3)-C(8)-O(4)	126.7(5)
O(3)-C(8)-C(4)	117.4(5)

O(4)-C(8)-C(4)	115.9(5)	C(9)-C(14)-C(13)	121.1(5)
C(14)-C(9)-C(10)	119.3(5)	C(9)-C(14)-H(14)	119(3)
C(14)-C(9)-C(15)	121.4(5)	C(13)-C(14)-H(14)	119(3)
C(10)-C(9)-C(15)	119.2(5)	O(6)-C(15)-O(5)	123.9(4)
C(11)-C(10)-C(9)	120.0(5)	O(6)-C(15)-C(9)	117.9(5)
C(11)-C(10)-H(10)	117(3)	O(5)-C(15)-C(9)	118.2(5)
C(9)-C(10)-H(10)	122(3)	O(7)-C(16)-O(8)	123.0(5)
C(12)-C(11)-C(10)	119.1(5)	O(7)-C(16)-C(12)	118.7(5)
C(12)-C(11)-H(11)	116(3)	O(8)-C(16)-C(12)	118.4(5)
C(10)-C(11)-H(11)	125(3)	N(2)-C(17)-N(1)	118.3(5)
C(11)-C(12)-C(13)	122.3(5)	N(2)-C(17)-S(1)	121.5(4)
C(11)-C(12)-C(16)	118.8(5)	N(1)-C(17)-S(1)	120.2(4)
C(13)-C(12)-C(16)	118.9(5)	N(4)-C(18)-N(3)	118.0(5)
C(12)-C(13)-C(14)	118.2(5)	N(4)-C(18)-S(2)	121.3(4)
C(12)-C(13)-H(13)	120(4)	N(3)-C(18)-S(2)	120.7(4)
C(14)-C(13)-H(13)	121(4)		

Symmetry transformations used to generate equivalent atoms:

#1 x+1,y,z

Table 2.29 **Bond lengths [Å] and angles [º] for 2Tl(I), 2(TU) 2(Tph) $2H_2O$ (Tph = terephthalate benzene-1,4-dicarboxylate.**

D-H...A	d(D-H)	d(H...A)	d(D...A)	<(DHA)
N(1)-H(1A)...O(3)#2	0.84(6)	2.08(7)	2.915(6)	177(6)
N(1)-H(1B)...S(1)#3	0.67(6)	2.88(6)	3.552(5)	172(6)
N(2)-H(2A)...O(4)#2	0.84(6)	2.24(7)	3.001(6)	152(6)
N(2)-H(2B)...O(9)#4	0.83(6)	2.36(6)	3.184(7)	168(5)
N(3)-H(3A)...O(8)#5	0.91(6)	2.30(6)	3.171(7)	160(5)
N(3)-H(3B)...O(10)#6	0.84(9)	2.10(9)	2.915(8)	164(9)
N(4)-H(4A)...O(4)#7	0.79(6)	2.07(7)	2.829(7)	161(6)
N(4)-H(4B)...O(6)#8	0.78(5)	2.13(5)	2.891(7)	163(5)
O(9)-H(9A)...O(5)#9	0.97(11)	1.94(11)	2.872(6)	160(8)
O(9)-H(9B)...O(3)	0.64(7)	2.27(7)	2.854(6)	153(9)
O(10)-H(10A)...O(9)#9	0.68(7)	2.21(7)	2.873(7)	164(7)
O(10)-H(10B)...O(6)	1.01(13)	1.80(13)	2.763(7)	159(10)

Symmetry transformations used to generate equivalent atoms:

#1 x+1,y,z #2 -x,y-1/2,-z+3/2 #3 -x,-y,-z+2

#4 -x+1,y-1/2,-z+3/2 #5 x,-y+1/2,z+1/2 #6 -x+1,-y+1,-z+2

#7 x+1,-y+1/2,z+1/2 #8 -x+2,-y+1,-z+2 #9 -x+1,y+1/2,-z+3/2

Table 2.30 Hydrogen bonds for 2Tl(I), 2(TU) 2(Tph) $2H_2O$ (Tph = terephthalate benzene-1,4-dicarboxylate) [Å and º].

2.6 STRUCTURAL ANALYSIS FOR THE REMAINING COMPLEXES

2.6.1 PF_6^- COMPLEX

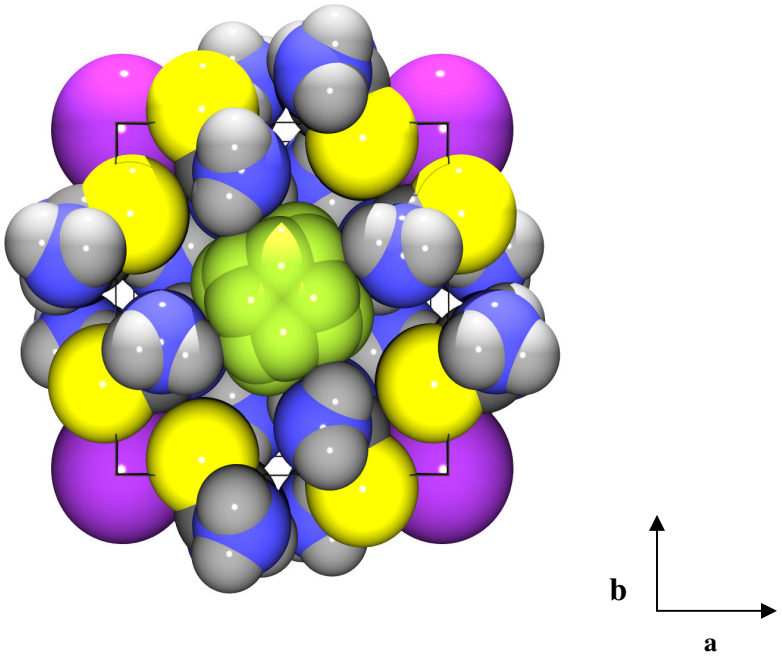

Fig. 2.20 **Space filling drawing showing the efficient packing of the PF_6^- complex viewed along the direction of the c axis. The direction of the a and b axes are shown above.**

As can be seen from Fig. 2.20, 24 phosphorus-fluorine bonds are seen to be generated rather than the expected 6 bonds of the PF_6^- molecule. The reason behind this is disorder that the 4-fold axis of symmetry does not run directly through the F-P-F bonds. Instead the entire PF_6^-molecule is tilted and the 4-fold axis runs through the P-atom and the molecule as shown below.

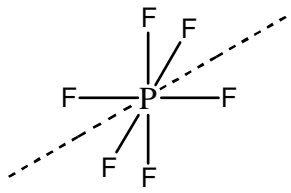

Fig2.21 **Position of 4-fold axis**

Due to this occurrence 24 F atoms are generated with fractional site occupancies. The fact that the PF_6^- is tilted is an interesting phenomenon as it is further proof that the channel with in the

complex remains approximately the same size relative to the substituents added based on the isostructural nature of the complexes.

The PF_6^- anion had to be refined as a rigid body and C(1) could not be refined satisfactorily with anisotropic thermal parameters.
Some evidence for H-bonding was observed from the close contacts between the (N)H…..F atoms. Table 2.31 lists these short contacts, and this is supportive of the observations in the Raman and IR studies (see chapter 3).

H-bonding :
N1…..F2 = 3.070Å (HN1B…..F2 = 2.597Å)
N1…..F6 = 3.149Å (HN1B…..F6 = 2.465Å)
N2…..F3 = 2.868Å (HN2B…..F3 = 2.292Å)
N2…..F1 = 2.770Å (HN2B…..F1 = 2.293Å)
N2…..F5 = 3.061Å (HN2B…..F5 = 2.443Å)

Table 2.31 Close contacts between N(H)…..F atoms

2.6.2 BF_4^- COMPLEX

It is of interest to note that the PF6 and BF4 complexes crystallise in different tetragonal space groups but with almost identical unit cell parameters. The unit cell volumes differ by less than 16 Å.

2.6.3 THALLIUM - 4-AMINOBENZOATE

The unequal Tl – O distances observed are also reflected in all the related structures in the Cambridge Database Version 5.26, also included 2005 updates during Feb., May, Aug.[4]. The shorter distance of 2.628(6) Å compares favourably with 2.597 Å calculated as the average of the 12 shorter contacts. The larger distance of 2.796(7) Å also compares well with the average of the

12 larger contacts (2.810 Å). For the 4-aminobenzoate complex this difference can be explained in terms of the fact that the oxygen with the larger Tl – O distance is also hydrogen bonded to the one thiourea NH_2 group.

2.6.4 2Tl(I), 2(TU) 2(Tph) $2H_2O$ (Tph = terephthalate benzene-1,4-dicarboxylate) COMPLEX

The asymmetric unit containing 2Tl(I), 2(TU) 2(Tph) and $2H_2O$ molecules are included as waters of crystallization. The two H_2O molecules are hydrogen bonded to each other (Table 2.31) as well as to two of the four carboxylate groups, and to both of the two amino groups of thiourea. The carboxylate group containing O1 and O2 are not hydrogen bonded to any other donor/receptor, but all three other carboxylate groups are hydrogen bonded to thiourea. All four thiourea NH_2 groups are involved in hydrogen bonding.

There is a short contact of 2.792(4) Å between Tl 1 and O5. This distance is comparable with the values of 2.628(6) Å and 2.796(7) Å observed for the 4-aminobenzoate complex without thiourea.

All hydrogen atoms were located from experimental data, and included in the refinement without any restrictions. Even the four hydrogen atoms for the $2H_2O$ molecules were located and refined under similar conditions. The refinement proceeded smoothly and no significant residual peaks that could be ascribed to additional hydrogen atoms were observed. The areas around the carboxylate groups were especially studied. If the two thallium atoms are both Tl^+ the remaining 2 hydrogen atoms will have to be placed in theoretical positions at two carboxylate oxygen atoms. When comparing the different C-O distances in the carboxylate functional groups, the following distances are observed:

C7 – O1:	1.204(7) Å	C7 - O2:	1.225(6) Å
C8 – O3:	1.244(7) Å	C8 - O4:	1.250(7) Å
C15 – O5:	1.255(6) Å	C15 - O6:	1.252(6) Å

C16 – O7 1.211(7) Å C16 - O8 : 1.216(7) Å

These distances are relatively similar and do not clearly indicate possible oxygen atoms for the addition of the two hydrogen atoms not observer experimentally.

Both thallium1 and thallium 2 are in close contact with sulphur, oxygen and the carbonyl carbon atom (see Table 2.32).

ATOM 1	ATOM 2	SYMM. OP. 1	SYMM. OP. 2	LENGTH (Å)
Tl1	S1	x,y,z	1+x, -1+y, z	3.687
Tl1	S1	x,y,z	1-x, 1-y, 2-z	3.376
Tl1	S2	x,y,z	x,y,z	3.13
Tl1	S2	x,y,z	2-x, 1-y, 2-z	3.434
Tl1	O1	x,y,z	1+x, y, z	3.103
Tl1	O5	x,y,z	x,y,z	2.792
Tl1	O6	x,y,z	x,y,z	2.918
Tl1	C15	x,y,z	x,y,z	3.168
Tl2	S1	x,y,z	x, -1+y, z	3.296
Tl2	S1	x,y,z	1-x, 1-y, 2-z	3.401
Tl2	S2	x,y,z	x,y,z	3.362
Tl2	S2	x,y,z	1-x, 1-y, 2-z	3.23
Tl2	O2	x,y,z	x,y,z	3.113
Tl2	O5	x,y,z	x,y,z	2.926
Tl2	C15	x,y,z	x,y,z	3.625
Tl2	O10	x,y,z	1-x, 1-y, 2-z	2.893

Table 2.32 Symmetry operations and close contacts of the two thallium atoms with S, O and C (carbonyl) atoms.

2.7 POWDER DIFFRACTION STUDY

All benzoic acid derivative complexes were analysed using x-ray powder diffraction. The instrument used for this analysis was a Siemens D-501 Automated diffractometer using a Cu target (λ = 1.5406 Å) operated at 40 KV and 40 mA. The instrument was equipped with a diffracted beam graphite monochromator, divergence slot of 1º, receiving slit of 0.05º and a scintillation counter. A sample spinner was used. The samples were step scanned at 2θ from 5˚ to 70˚ with steps of 0.01˚ at Ψ with a fixed counting time of 1.15 sec at a mean temperature of 25˚C.

The diffraction patterns of all the complexes including the four diffraction quality single crystals are shown in Fig 2.22 – 2.29. They can be split into eight different groupings. These are (1) the four complexes for which the single crystal structures were obtained, (2) eight complexes with only 2- and 4-substituted benzoates, (3) three groups of pairs of similar complexes, and (4) three complexes with no similarity to the others.

The reason for the remaining complexes falling into different powder patter groupings may be due to the fact that they crystallise as different crystal structures giving rise to different diffraction patterns. No further analysis of the powder data was done, but these results clearly suggest that a project to investigate the structure of the eight compounds with very similar powder patterns could prove of importance. A powder pattern of the 4-amino complex with no thiourea was also run to ensure none of the synthesised complexes had formed without thiourea. The results showed that the non thiourea 4-amino complex gave a completely different powder pattern to any of the other complexes.

2.7.1 EXPERIMENTAL POWDER X-RAY DIFFRACTION PATTERNS

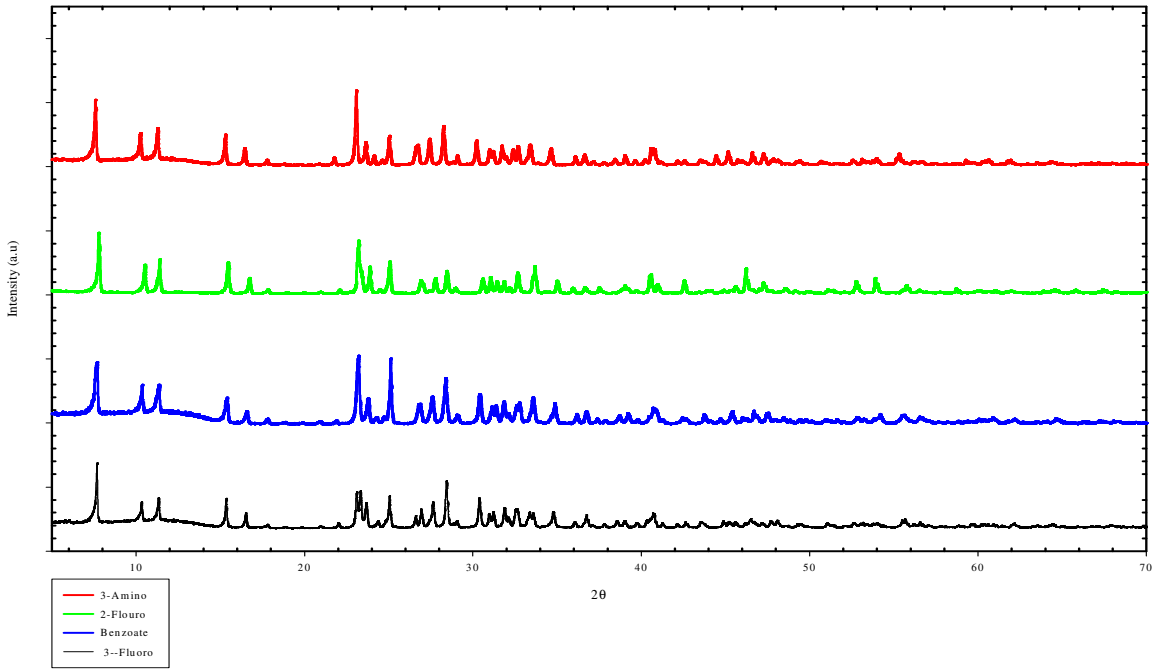

Fig. 2.22 **Experimental powder x-ray diffraction patterns of the 3-amino, 2-fluoro, 3-fluoro, benzoate complexes showing identical position and intensity of reflections**

The theoretical powder diffraction patterns were compared with the experimental powder diffraction patterns and the excellent agreement is shown in Fig 2.23 – 2.26.

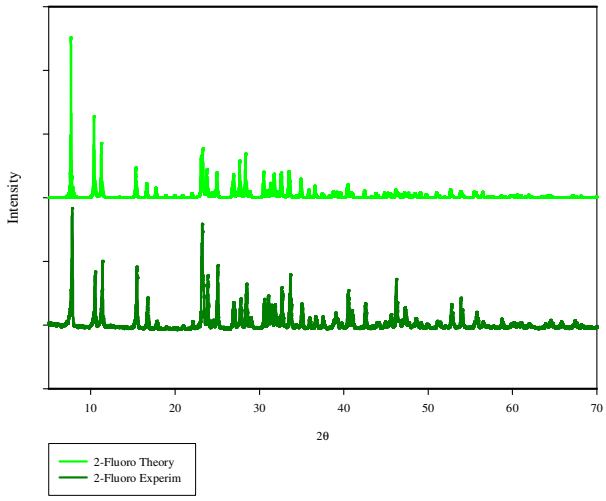

Fig. 2.23 **Comparison of experimental and theoretical powder patterns of the 2-fluoro complex**

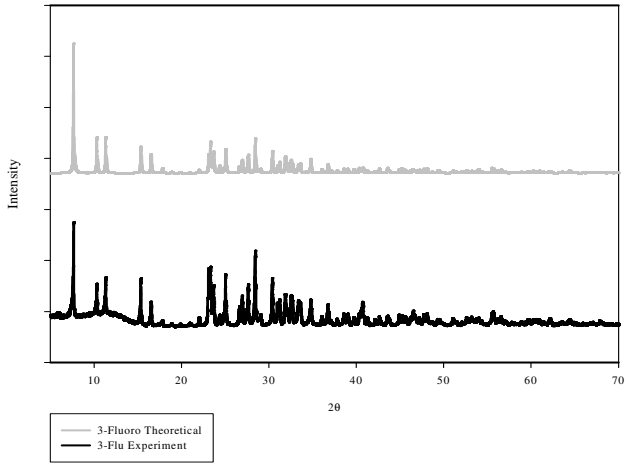

Fig. 2.24 **Comparison of experimental and theoretical powder patterns of the 3-fluoro complex**

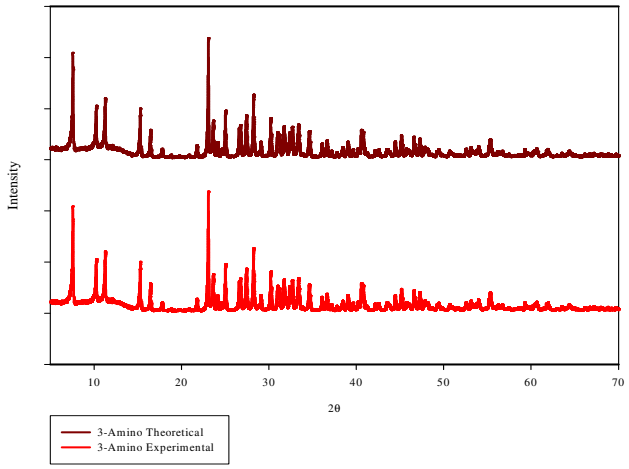

Fig. 2.25 **Comparison of experimental and theoretical powder patterns of the 3-amino complex**

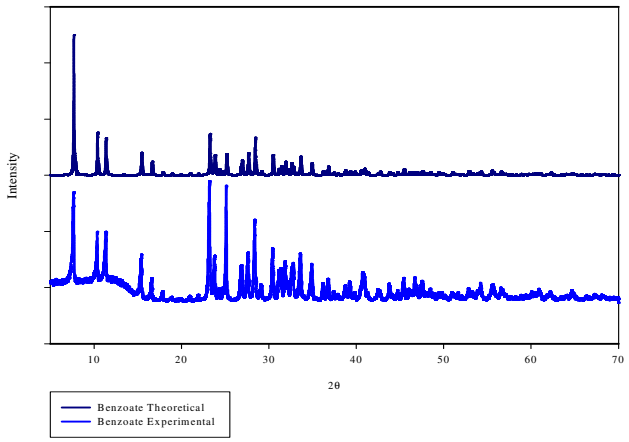

Fig. 2.26 **Comparison of experimental and theoretical powder patterns of the benzoate complex**

The group of eight compounds in Fig. 2.27 could also crystallise with the same crystal structure, based on the agreement between the various powder spectra.

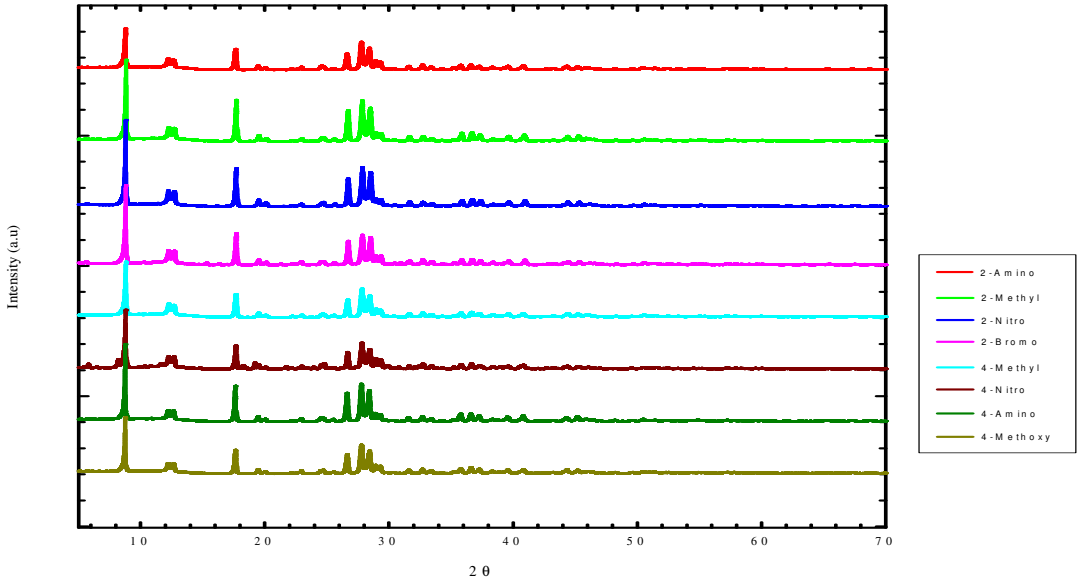

Fig. 2.27 **Experimental powder x-ray diffraction patterns of the eight complexes showing similarity in position and intensity of the reflections**

The same could be said for the next three groups of two compounds each, as depicted in Fig.2.28

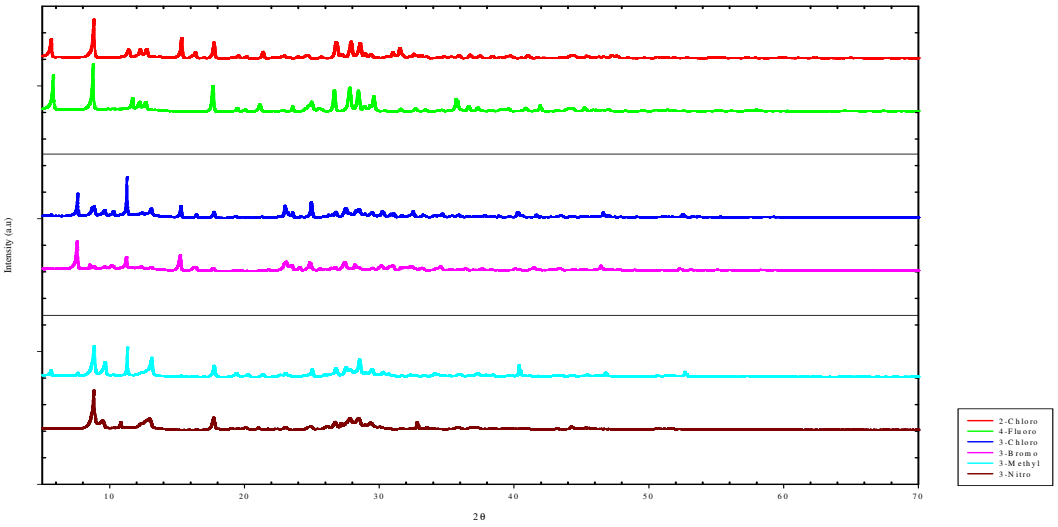

Fig. 2.28 **Experimental powder x-ray diffraction patterns of three groups of two complexes which show similarities in position and intensity of reflections**

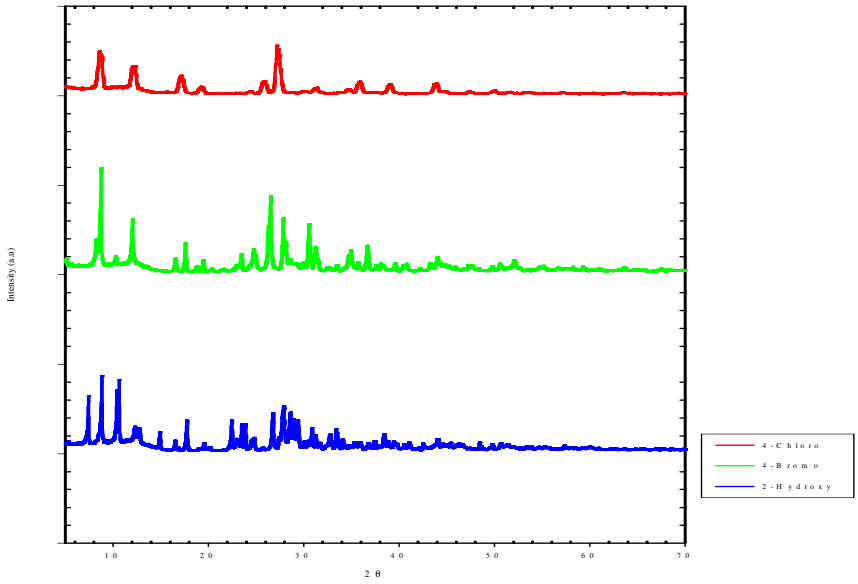

Fig. 2.29 **Experimental powder x-ray diffraction patterns of three complexes which are not similar in position and intensity of the reflections to any other complexes**

2.8 CONCLUSION

Both single crystal and powder diffraction data suggests that the 2-fluoro, 3-fluoro, 3-amino benzoate complexes, as well as the unsubstituted benzoate complex, are isostructural. The single crystal diffraction studies show that these four benzoate complexes all crystallise in the same space group and have almost identical crystal structures. The volumes of the four unit cells differ by less than 28 $Å^3$. This indicates that displacement of a hydrogen atom by a fluoro or amino group, as substituent on the benzoate, does not alter the packing requirements. The influence of the Tl…S interaction in packing in the solid state seems to be of importance as well.

The experimental and theoretical powder diffraction patterns for these four complexes are also almost identical in position and intensity, underlining the similarity in the crystal structures. None of the remaining complexes' powder diffraction patterns match those of the four benzoates listed above. However, of importance is the fact that some groups of compounds also have almost identical powder diffractograms – that is very similar 2θ˚ and intensity values. This may be a result of very similar crystal structures with in these groups. The main group of eight complexes is such a group. This group included electron withdrawing, electron donating and bulky groups, in both the ortho position as well as the para position. There are a further three groups with pairs of complexes that also both yield the same powder diffraction pattern. The powder diffraction patterns for 18 complexes were not all unique: one group of four, one group of eight, and three groups of two complexes had very closely related spectra. There were three complexes giving spectra that showed no clear correlation with any of the other spectra measured.

2.9 REFERENCES

CHAPTER 2

1. L. H. W. Verhoef and J. C. A. Boeyens, Acta Cryst. 1969, **B25**, 607
2. Olof Kristiansson, Eur. J. Inorg. Chem., 2002, 2355-2361
3. F. H. Herbstein and J. C. A. Boeyens, Inorg. Chem. 1967, **6(7)**, 1408 – 1425
4. The Cambridge Database : a quarter of a million crystal structures and rising, F. H. Allen, Acta Crystallogr. 2002, **B58**, 380-388 (version 5.26, as well as the 2005 updates during February, May, August)
5. Bruker, 2001. SMART, SAINT, SADABS and SHELXTL (Version 6.12). Bruker AXS Inc., Madison, Wisconsin, USA
6. Sheldrick, G. M. 1997, SHELXS 97 and SHELXL 97, University of Gottingen, Germany
7. Farringia, L. J., J. Appl. Cryst. 1997, **30**, 565
8. The POV-ray Team, 2004. POV-Ray. URL: http://www.povray.org/download/.
9. F. Wiesbrock and H. Schmidbaur, J. Am. Chem. Soc., Vol. 125, NO. 12, 2003, 3624

2.10 APPENDIX – ADDITIONAL CRYSTALLOGRAPHIC DATA FOR THE COMPLEXES

2.10.1 Tl^{+1} 4(TU) 2-Fluorobenzoate complex

	x	y	z	U(eq)
Tl(1)	0	0	0	47(1)
S(1)	1070(1)	1245(1)	2500	39(1)
C(1)	2134(2)	1045(2)	2500	36(1)
N(1)	2559(2)	965(2)	1105(3)	49(1)
S(2)	1423(1)	9049(1)	2500	43(1)
C(2)	1173(2)	8072(2)	2500	41(1)
N(2)	1073(2)	7680(2)	1116(4)	61(1)
O(1)	695(2)	6055(2)	2500	55(1)
C(3)	0	3174(3)	2500	78(2)
C(4)	753(5)	3567(3)	2500	86(2)
C(5)	743(3)	4396(3)	2500	57(1)
C(6)	0	4818(4)	2500	38(1)
C(7)	0	5720(3)	2500	36(1)
F(1)	1429(3)	4646(3)	2500	106(3)

Table 2.33 **Atomic coordinates (x 10^4) and equivalent isotropic displacement parameters ($Å^2$x 10^3) for Tl^{+1} 4(TU) 2-Fluorobenzoate. U(eq) is defined as one third of the trace of the orthogonalized U^{ij} tensor.**

	U^{11}	U^{22}	U^{33}	U^{23}	U^{13}	U^{12}
Tl(1)	49(1)	46(1)	46(1)	-6(1)	0	0
S(1)	27(1)	45(1)	44(1)	0	0	2(1)

C(1)	31(2)	31(1)	47(2)	0	0	1(1)
N(1)	32(1)	70(2)	45(1)	1(1)	2(1)	8(1)
S(2)	57(1)	31(1)	42(1)	0	0	-7(1)
C(2)	41(2)	35(2)	47(2)	0	0	-3(1)
N(2)	95(2)	39(1)	50(2)	-3(1)	-3(1)	-17(1)
O(1)	36(2)	30(1)	99(2)	0	0	-6(1)
C(3)	145(8)	25(3)	64(3)	0	0	0
C(4)	132(6)	38(3)	87(3)	0	0	42(3)
C(5)	57(3)	38(2)	76(2)	0	0	16(2)
C(6)	48(3)	22(2)	45(3)	0	0	0
C(7)	30(2)	22(2)	56(2)	0	0	0
F(1)	29(2)	35(3)	254(8)	0	0	2(2)

Table 2.34 **Anisotropic displacement parameters ($Å^2 x\ 10^3$)for Tl^{+1} 4(TU) 2-Fluorobenzoate. The anisotropic displacement factor exponent takes the form: $-2p^2[\ h^2 a^{*2} U^{11} + ... + 2\ h\ k\ a^*\ b^*\ U^{12}\ ]$**

	x	y	z	U(eq)
H(1A)	3110(20)	873(15)	1160(30)	48(7)
H(1B)	2420(40)	1020(30)	290(50)	54(14)
H(2A)	910(20)	7250(30)	1250(40)	59(9)
H(2B)	1140(30)	7810(30)	410(60)	54(13)
H(3)	0	2650(60)	2500	90(20)
H(4)	1230(40)	3250(30)	2500	70(13)

Table 2.35 **Hydrogen coordinates ($x\ 10^4$) and isotropic displacement parameters ($Å^2 x\ 10^3$) for Tl^{+1} 4(TU) 2-Fluorobenzoate.**

2.10.2 Tl^{+1} 4(TU) 3-Fluorobenzoate complex

	x	y	z	U(eq)
Tl(1)	0	0	0	45(1)
S(1)	1068(1)	1222(1)	2500	38(1)
C(1)	2142(2)	1034(2)	2500	36(1)
N(1)	2574(2)	961(2)	3895(3)	49(1)
S(2)	1432(1)	9062(1)	2500	44(1)
C(2)	1187(2)	8090(2)	2500	41(1)
N(2)	1089(2)	7702(2)	1108(3)	61(1)
C(3)	0	3228(3)	2500	51(1)
C(4)	763(3)	3637(2)	2500	55(1)
C(5)	764(2)	4449(2)	2500	46(1)
C(6)	0	4857(3)	2500	38(1)
C(7)	0	5745(3)	2500	37(1)
O(1)	-704(2)	6082(2)	2500	54(1)
F(1)	1451(3)	3255(3)	2500	90(2)

Table 2.36 **Atomic coordinates (x 10^4) and equivalent isotropic displacement parameters ($Å^2$x 10^3) for Tl^{+1} 4(TU) 3-Fluorobenzoate. U(eq) is defined as one third of the trace of the orthogonalized U^{ij} tensor.**

	U^{11}	U^{22}	U^{33}	U^{23}	U^{13}	U^{12}
Tl(1)	46(1)	44(1)	43(1)	-6(1)	0	0
S(1)	29(1)	44(1)	42(1)	0	0	1(1)
C(1)	32(2)	32(2)	44(2)	0	0	0(1)
N(1)	34(1)	70(2)	43(1)	1(1)	-1(1)	5(1)

S(2)	59(1)	31(1)	40(1)	0	0	-5(1)
C(2)	42(2)	35(2)	46(2)	0	0	0(1)
N(2)	97(2)	38(1)	49(1)	-3(1)	-5(1)	-14(1)
C(3)	60(3)	28(2)	64(3)	0	0	0
C(4)	58(2)	33(2)	73(3)	0	0	10(2)
C(5)	36(2)	32(2)	69(2)	0	0	1(2)
C(6)	41(3)	24(2)	48(3)	0	0	0
C(7)	31(2)	23(2)	55(2)	0	0	0
O(1)	37(1)	34(1)	91(2)	0	0	6(1)
F(1)	55(3)	39(2)	175(6)	0	0	18(2)

Table 2.37 **Anisotropic displacement parameters ($Å^2 x\ 10^3$)for Tl^{+1} 4(TU) 3-Fluorobenzoate. The anisotropic displacement factor exponent takes the form: $-2p^2[\ h^2a^{*2}U^{11} + ... + 2\ h\ k\ a^*\ b^*\ U^{12}\ ]$**

	x	y	z	U(eq)
H(1A)	3140(20)	928(16)	3840(30)	51(8)
H(1B)	2400(30)	1010(30)	4680(40)	53(12)
H(2A)	920(20)	7250(20)	1200(40)	60(9)
H(2B)	1130(30)	7920(30)	240(40)	58(12)
H(4)	1270(30)	4760(30)	2500	42(10)
H(6)	0	2730(40)	2500	66(18)

Table 2.38 **Hydrogen coordinates ($x\ 10^4$) and isotropic displacement parameters ($Å^2 x\ 10^3$) for Tl^{+1} 4(TU) 3-Fluorobenzoate.**

2.10.3 Tl^{+1} 4(TU) 3-Aminobenzoate complex

	x	y	z	U(eq)
Tl(1)	0	0	0	42(1)
S(1)	1074(1)	1218(1)	2500	34(1)
S(2)	1433(1)	9060(1)	2500	37(1)
O(1)	705(2)	6094(2)	2500	49(1)
C(1)	2155(2)	1023(2)	2500	32(1)
C(3)	0	3237(3)	2500	42(1)
N(1)	2581(2)	946(1)	1113(3)	44(1)
C(5)	763(2)	4453(2)	2500	39(1)
C(7)	0	5748(2)	2500	34(1)
C(6)	0	4863(3)	2500	36(1)
N(2)	1080(2)	7697(2)	1116(3)	57(1)
C(4)	776(3)	3634(2)	2500	43(1)
C(2)	1177(2)	8087(2)	2500	36(1)
N(3)	1474(5)	3234(4)	2500	60(2)

Table 2.39 **Atomic coordinates (x 10^4) and equivalent isotropic displacement parameters ($Å^2$x 10^3) for Tl^{+1} 4(TU) 3-Aminobenzoate. U(eq) is defined as one third of the trace of the orthogonalized U^{ij} tensor.**

	U^{11}	U^{22}	U^{33}	U^{23}	U^{13}	U^{12}
Tl(1)	45(1)	41(1)	41(1)	-6(1)	0	0
S(1)	27(1)	35(1)	39(1)	0	0	1(1)
S(2)	47(1)	27(1)	36(1)	0	0	-4(1)
O(1)	36(1)	28(1)	84(2)	0	0	-4(1)

C(1)	30(2)	26(1)	40(1)	0	0	-1(1)
C(3)	50(3)	21(2)	55(2)	0	0	0
N(1)	33(1)	63(1)	36(1)	1(1)	1(1)	6(1)
C(5)	36(2)	23(2)	58(2)	0	0	0(1)
C(7)	30(2)	22(2)	51(2)	0	0	0
C(6)	40(3)	23(2)	45(3)	0	0	0
N(2)	90(2)	34(1)	46(1)	-4(1)	-2(1)	-13(1)
C(4)	46(2)	27(2)	55(2)	0	0	7(1)
C(2)	34(2)	32(2)	42(1)	0	0	-3(1)
N(3)	39(4)	21(3)	119(7)	0	0	3(3)

Table 2.40 **Anisotropic displacement parameters ($Å^2 x\ 10^3$) for Tl^{+1} 4(TU) 3-Aminobenzoate. The anisotropic displacement factor exponent takes the form: $-2p^2[\ h^2 a^{*2} U^{11} + ... + 2\ h\ k\ a^*\ b^*\ U^{12}\ ]$**

	x	y	z	U(eq)
H(5)	1240(30)	4730(30)	2500	34(8)
H(1A)	3100(20)	901(15)	1110(30)	40(7)
H(3)	0	2740(40)	2500	52(15)
H(2A)	928(18)	7250(20)	1200(30)	47(8)
H(1B)	2390(30)	1000(20)	310(50)	44(10)
H(2B)	1090(30)	7920(30)	270(40)	54(12)
H(3A)	1490(50)	2900(40)	2500	21(19)
H(3B)	1800(50)	3480(40)	2500	28(19)

Table 2.41 **Hydrogen coordinates ($x\ 10^4$) and isotropic displacement parameters ($Å^2 x\ 10^3$) for Tl^{+1} 4(TU) 3-Aminobenzoate.**

2.10.4 Tl^{+1} 4(TU) Benzoate complex

	x	y	z	U(eq)
Tl(1)	0	0	0	45(1)
S(1)	1078(1)	1235(1)	2500	36(1)
C(1)	2160(2)	1029(2)	2500	33(1)
N(1)	2580(2)	947(2)	3900(3)	44(1)
S(2)	1453(1)	9052(1)	2500	40(1)
C(2)	1188(2)	8075(2)	2500	38(1)
N(2)	1086(2)	7685(2)	1112(4)	57(1)
O(1)	708(2)	6061(2)	2500	49(1)
C(3)	0	3190(3)	2500	50(1)
C(4)	769(3)	3586(2)	2500	52(1)
C(5)	765(2)	4414(2)	2500	40(1)
C(6)	0	4826(4)	2500	35(1)
C(7)	0	5721(3)	2500	31(1)

Table 2.42 **Atomic coordinates (x 10^4) and equivalent isotropic displacement parameters ($Å^2$x 10^3) for Tl^{+1} 4(TU) Benzoate. U(eq) is defined as one third of the trace of the orthogonalized U^{ij} tensor.**

	U^{11}	U^{22}	U^{33}	U^{23}	U^{13}	U^{12}
Tl(1)	46(1)	44(1)	45(1)	-6(1)	0	0
S(1)	26(1)	40(1)	42(1)	0	0	3(1)
C(1)	28(2)	29(1)	43(2)	0	0	1(1)
N(1)	26(1)	62(1)	43(1)	2(1)	0(1)	7(1)
S(2)	54(1)	28(1)	39(1)	0	0	-5(1)
C(2)	39(2)	30(2)	46(2)	0	0	-1(1)

N(2)	90(2)	36(1)	45(2)	-2(1)	-3(1)	-14(1)
O(1)	32(2)	28(1)	85(2)	0	0	-5(1)
C(3)	65(4)	24(2)	60(3)	0	0	0
C(4)	51(3)	30(2)	75(3)	0	0	13(2)
C(5)	31(2)	26(2)	63(2)	0	0	2(1)
C(6)	39(3)	22(2)	44(3)	0	0	0
C(7)	22(2)	23(2)	49(2)	0	0	0

Table 2.43 **Anisotropic displacement parameters ($Å^2 x\ 10^3$) for Tl^{+1} 4(TU) Benzoate. The anisotropic displacement factor exponent takes the form: $-2p^2[\ h^2 a^{*2} U^{11} + ... + 2\ h\ k\ a^*\ b^*\ U^{12}\ ]$**

	x	y	z	U(eq)
H(1A)	3040(20)	886(15)	3850(30)	35(8)
H(1B)	2360(40)	960(30)	4810(40)	40(13)
H(2A)	940(20)	7200(20)	1260(40)	50(8)
H(2B)	1140(30)	7830(30)	330(50)	41(12)
H(3)	0	2600(50)	2500	90(20)
H(4)	1300(30)	3280(30)	2500	55(11)
H(5)	1290(30)	4670(30)	2500	45(10)

Table 2.44 **Hydrogen coordinates ($x\ 10^4$) and isotropic displacement parameters ($Å^2 x\ 10^3$) for Tl^{+1} 4(TU) Benzoate.**

2.10.5 Tl^{+1} 4(TU) PF_6^- complex

	x	y	z	U(eq)
Tl(1)	0	0	1280(4)	50(1)
S(1)	411(6)	2570(5)	3840(20)	55(1)
C(1)	-1040(20)	3320(20)	3720(60)	51(6)
N(1)	-1390(20)	3790(30)	5310(30)	68(9)
N(2)	-1888(19)	3500(20)	2520(30)	38(5)
P	5000	5000	4030(50)	81(7)
F(1)	5020(60)	5910(30)	2540(60)	111(11)
F(2)	4970(60)	4070(30)	5540(60)	111(11)
F(3)	3624(14)	4530(30)	3550(70)	111(11)
F(4)	6369(14)	5450(30)	4530(90)	111(11)
F(5)	5600(30)	3900(30)	2980(70)	111(11)
F(6)	4400(30)	6080(30)	5100(70)	111(11)

Table 2.45 **Atomic coordinates (x 10^4) and equivalent isotropic displacement parameters ($Å^2$x 10^3) for Tl^{+1} 4(TU) PF_6^-. U(eq) is defined as one third of the trace of the orthogonalized U^{ij} tensor.**

	U^{11}	U^{22}	U^{33}	U^{23}	U^{13}	U^{12}
Tl(1)	52(1)	52(1)	45(1)	0	0	0
S(1)	76(4)	52(3)	36(2)	-4(6)	-4(8)	-4(2)
N(1)	24(10)	130(20)	48(14)	-38(15)	-32(11)	14(13)
N(2)	42(11)	50(11)	22(8)	13(9)	26(9)	23(9)
P	104(7)	104(7)	40(20)	0	0	0

Table 2.46 **Anisotropic displacement parameters ($Å^2$x 10^3)for Tl^{+1} 4(TU) PF_6^-. The anisotropic displacement factor exponent takes the form: $-2\pi^2[h^2a^{*2}U^{11} + ... + 2 h k a^* b^* U^{12}]$**

	x	y	z	U(eq)
H(1A)	3979	-2582	2561	57
H(1B)	3375	-1680	1390	57
H(2A)	4056	-2073	5231	117
H(2B)	3527	-863	5906	117

Table 2. 47 **Hydrogen coordinates (x 10^4) and isotropic displacement parameters ($Å^2$x 10^3) for Tl^{+1} 4(TU) PF_6^{-1} .**

2.10.6 Tl^{+1} 4(TU) BF_4^- complex

	x	y	z	U(eq)
Tl(1)	0	0	2500	51(1)
S(1)	-403(4)	2592(2)	0	92(1)
C(1)	1063(13)	3347(7)	0	99(4)
N(1)	1654(8)	3648(5)	-1383(5)	125(3)
B(1)	5000	5000	0	250(50)
F(1)	5170(20)	6135(13)	660(30)	246(13)

Table 2.48 **Atomic coordinates (x 10^4) and equivalent isotropic displacement parameters ($Å^2$x 10^3) for Tl^{+1} 4(TU) BF_4^-. U(eq) is defined as one third of the trace of the orthogonalized U^{ij} tensor.**

U^{11}	U^{22}	U^{33}	U^{23}	U^{13}	U^{12}

Tl(1)	54(1)	54(1)	45(1)	0	0	0
S(1)	184(2)	57(1)	36(1)	0	0	7(1)
C(1)	219(12)	37(3)	41(4)	0	0	-39(5)
N(1)	256(8)	77(3)	41(2)	2(2)	4(3)	-66(4)

Table 2.49 **Anisotropic displacement parameters ($Å^2 x\ 10^3$) for Tl^{+1} 4(TU) BF_4^-. The anisotropic displacement factor exponent takes the form: $-2p^2[\ h^2 a^{*2} U^{11} + ... + 2\ h\ k\ a^*\ b^*\ U^{12}$**

	x	y	z	U(eq)
H(1)	2393	4025	-1363	149
H(2)	1297	3466	-2298	149

Table 2.50 **Hydrogen coordinates (x 10^4) and isotropic displacement parameters (□^{2}x 10^3) for Tl^{+1} 4(TU) BF_4^-.**

2.10.7 thallium – 4-aminobenzoate

	x	y	z	U(eq)
Tl(1)	8900(1)	5903(1)	4311(2)	35(1)
O(1)	9257(5)	4250(4)	3394(10)	43(1)
O(2)	8157(4)	4300(4)	5574(10)	48(2)
C(1)	8701(5)	2894(4)	4613(9)	25(2)
C(2)	8148(5)	2435(5)	5907(10)	35(2)
C(3)	8159(5)	1521(5)	6014(11)	37(2)
C(4)	8724(7)	1020(5)	4785(15)	32(2)
C(5)	9273(5)	1468(5)	3501(12)	37(2)
C(6)	9262(5)	2375(5)	3396(12)	36(2)
C(7)	8700(6)	3881(6)	4460(30)	37(3)
N(1)	8732(5)	108(5)	4895(13)	47(2)

Table 2.51 **Atomic coordinates (x 10^4) and equivalent isotropic displacement parameters (Å^{2}x 10^3) for thallium – 4-aminobenzoate.. U(eq) is defined as one third of the trace of the orthogonalized U^{ij} tensor.**

	U^{11}	U^{22}	U^{33}	U^{23}	U^{13}	U^{12}
Tl(1)	47(1)	26(1)	33(1)	1(1)	1(1)	3(1)
O(1)	54(3)	24(2)	50(3)	8(2)	3(3)	-4(3)
O(2)	54(3)	36(3)	55(4)	-10(3)	-5(3)	10(3)
C(1)	32(3)	24(3)	19(5)	-1(3)	-9(3)	-3(3)
C(2)	38(4)	36(4)	32(4)	-7(3)	2(3)	2(3)
C(3)	39(4)	37(4)	36(3)	4(3)	5(3)	-7(3)
C(4)	42(4)	18(3)	36(6)	4(3)	-8(3)	-2(3)
C(5)	30(3)	35(4)	45(3)	-2(3)	2(3)	-1(3)

C(6)	34(4)	39(4)	35(4)	-1(3)	-5(3)	-5(3)
C(7)	36(3)	30(3)	45(8)	3(5)	-15(7)	1(3)
N(1)	53(4)	19(3)	68(6)	-1(3)	11(3)	-4(3)

Table 2.52 **Anisotropic displacement parameters ($Å^2 x\ 10^3$)for thallium – 4-aminobenzoate. The anisotropic displacement factor exponent takes the form: $-2p^2[\ h^2 a^{*2} U^{11} + ... + 2\ h\ k\ a^*\ b^*\ U^{12}\ ]$**

	x	y	z	U(eq)
H(2)	7763	2752	6717	42
H(3)	7791	1233	6905	45
H(5)	9658	1150	2694	44
H(6)	9633	2658	2502	43
H(1A)	9084	-194	4153	56
H(1B)	8384	-159	5704	56

Table 2.53 **Hydrogen coordinates ($x\ 10^4$) and isotropic displacement parameters ($Å^2 x\ 10^3$) for thallium – 4-aminobenzoate.**

2.10.8 2Tl(I), 2(TU) 2(Tph) $2H_2O$ (Tph = terephthalate benzene-1,4-dicarboxylate) complex

	x	y	z	U(eq)
Tl(1)	9746(1)	2829(1)	9815(1)	40(1)
Tl(2)	4813(1)	2552(1)	9761(1)	42(1)
S(1)	2487(1)	-133(1)	9887(1)	35(1)
S(2)	7377(1)	4713(1)	10293(1)	38(1)
O(1)	1144(6)	2402(5)	8904(1)	63(1)
O(2)	3478(5)	3144(6)	8805(1)	67(1)
O(3)	1278(5)	4154(5)	6608(1)	63(1)
O(4)	-947(5)	3005(5)	6717(1)	57(1)
O(5)	7365(5)	2436(4)	9153(1)	46(1)
O(6)	8209(4)	4599(4)	9142(1)	47(1)
O(7)	6097(6)	4845(5)	6915(1)	69(1)
O(8)	5520(6)	2700(6)	6926(1)	68(1)
O(9)	3601(5)	4615(5)	5981(2)	50(1)
O(10)	6821(6)	6976(6)	9443(2)	59(1)
N(1)	178(5)	-522(5)	9277(2)	41(1)
N(2)	2642(6)	-463(5)	9027(1)	41(1)
N(3)	6263(6)	3563(6)	10999(2)	52(1)
N(4)	8872(6)	4039(6)	11051(2)	53(1)
C(1)	1710(6)	3008(5)	8201(2)	34(1)
C(2)	480(6)	2217(6)	8022(2)	38(1)
C(3)	87(6)	2377(5)	7578(2)	37(1)
C(4)	879(5)	3300(5)	7326(2)	32(1)
C(5)	2115(6)	4073(5)	7520(2)	36(1)
C(6)	2542(5)	3929(6)	7960(2)	38(1)
C(7)	2132(6)	2836(5)	8671(1)	31(1)
C(8)	365(6)	3507(6)	6840(2)	41(1)

C(9)	7139(5)	3643(5)	8469(2)	33(1)
C(10)	6453(6)	2494(6)	8255(2)	39(1)
C(11)	6069(6)	2542(6)	7806(2)	39(1)
C(12)	6368(5)	3718(6)	7580(2)	36(1)
C(13)	7021(6)	4872(6)	7783(2)	44(1)
C(14)	7407(6)	4812(6)	8232(2)	42(1)
C(15)	7602(5)	3554(6)	8958(2)	37(1)
C(16)	5977(5)	3758(6)	7108(1)	34(1)
C(17)	1724(5)	-385(5)	9358(1)	30(1)
C(18)	7518(6)	4055(5)	10817(2)	37(1)

Table 2.54 **Atomic coordinates (x 10^4) and equivalent isotropic displacement parameters (Å^{2}x 10^3) for 2Tl(I), 2(TU) 2(Tph) 2H_2O (Tph = terephthalate benzene-1,4-dicarboxylate). U(eq) is defined as one third of the trace of the orthogonalized U^{ij} tensor.**

	U^{11}	U^{22}	U^{33}	U^{23}	U^{13}	U^{12}
Tl(1)	44(1)	41(1)	36(1)	4(1)	0(1)	1(1)
Tl(2)	43(1)	44(1)	40(1)	0(1)	5(1)	1(1)
S(1)	34(1)	41(1)	28(1)	-1(1)	-3(1)	-2(1)
S(2)	45(1)	36(1)	33(1)	5(1)	2(1)	2(1)
O(1)	95(3)	60(3)	34(2)	9(2)	13(2)	13(2)
O(2)	66(3)	100(4)	34(2)	-5(2)	-7(2)	16(3)
O(3)	67(2)	90(4)	31(2)	14(2)	4(2)	-8(2)
O(4)	54(2)	72(3)	42(2)	-10(2)	-14(2)	-1(2)
O(5)	55(2)	48(2)	35(2)	9(2)	-3(2)	-3(2)
O(6)	58(2)	49(2)	35(2)	-7(2)	-2(2)	0(2)
O(7)	94(3)	77(3)	35(2)	6(2)	5(2)	29(3)
O(8)	77(3)	91(4)	36(2)	-7(2)	3(2)	-10(3)

O(9)	54(2)	52(3)	44(3)	-6(2)	2(2)	2(2)
O(10)	82(3)	43(3)	55(3)	7(2)	15(2)	-1(2)
N(1)	36(2)	57(3)	28(2)	-2(2)	-1(2)	-2(2)
N(2)	39(2)	55(3)	29(2)	-5(2)	5(2)	2(2)
N(3)	58(3)	55(3)	45(3)	14(2)	8(2)	-5(2)
N(4)	53(3)	58(3)	46(3)	21(3)	-7(2)	0(2)
C(1)	38(2)	37(3)	26(2)	0(2)	2(2)	10(2)
C(2)	41(3)	36(3)	39(3)	7(2)	7(2)	2(2)
C(3)	35(2)	37(3)	41(3)	-3(2)	0(2)	-2(2)
C(4)	33(2)	33(3)	29(2)	-1(2)	-2(2)	6(2)
C(5)	35(2)	37(3)	37(3)	7(2)	6(2)	-3(2)
C(6)	36(2)	40(3)	37(3)	-3(2)	-4(2)	-2(2)
C(7)	45(3)	32(3)	17(2)	3(2)	5(2)	16(2)
C(8)	48(3)	44(3)	30(2)	-4(2)	-2(2)	14(2)
C(9)	30(2)	41(3)	29(2)	3(2)	1(2)	4(2)
C(10)	41(3)	38(3)	36(3)	5(2)	-3(2)	-1(2)
C(11)	41(3)	37(3)	37(3)	-2(2)	-3(2)	1(2)
C(12)	35(2)	45(3)	28(2)	2(2)	4(2)	5(2)
C(13)	49(3)	43(3)	40(3)	11(2)	3(2)	-4(2)
C(14)	49(3)	38(3)	38(3)	1(2)	-1(2)	-7(2)
C(15)	30(2)	50(3)	29(2)	0(2)	2(2)	2(2)
C(16)	38(2)	46(3)	17(2)	3(2)	6(2)	7(2)
C(17)	35(2)	25(2)	30(2)	-2(2)	0(2)	1(2)
C(18)	48(3)	27(2)	35(2)	2(2)	0(2)	3(2)

Table 2.55 **Anisotropic displacement parameters ($Å^2 x\ 10^3$) for 2Tl(I), 2(TU) 2(Tph) $2H_2O$ (Tph = terephthalate benzene-1,4-dicarboxylate). The anisotropic displacement factor exponent takes the form: $-2p^2[\ h^2a^{*2}U^{11} + ... + 2\ h\ k\ a^*\ b^*\ U^{12}\ ]$**

	x	y	z	U(eq)
H(2)	90(60)	1530(70)	8207(19)	54(17)
H(3)	-770(70)	1890(70)	7470(20)	62(19)
H(5)	2600(60)	4620(70)	7370(19)	57(18)
H(6)	3350(60)	4400(60)	8124(16)	37(13)
H(10)	6100(50)	1760(50)	8407(15)	26(12)
H(11)	5610(60)	1720(70)	7621(19)	52(16)
H(13)	7190(60)	5600(70)	7633(19)	50(16)
H(14)	7710(60)	5650(70)	8386(18)	47(15)
H(1A)	-260(70)	-640(70)	9030(20)	52(18)
H(1B)	-390(70)	-390(70)	9420(20)	50(20)
H(2A)	2160(70)	-600(70)	8780(20)	54(18)
H(2B)	3620(70)	-370(60)	9061(18)	47(16)
H(3A)	6300(60)	3120(60)	11260(20)	42(15)
H(3B)	5480(110)	3390(110)	10830(30)	120(40)
H(4A)	8940(60)	3620(70)	11280(20)	44(16)
H(4B)	9600(60)	4380(60)	10947(17)	33(15)
H(9A)	3420(110)	5550(120)	5870(30)	130(40)
H(9B)	3300(80)	4430(90)	6160(20)	60(30)
H(10A)	6900(70)	7600(70)	9340(20)	40(20)
H(10B)	7460(130)	6270(130)	9290(40)	160(40)

Table 2.56 **Hydrogen coordinates (x 10^4) and isotropic displacement parameters (Å^{2}x 10^3) for 2Tl(I), 2(TU) 2(Tph) 2H_2O (Tph = terephthalate benzene-1,4-dicarboxylate).**

University of Pretoria etd – Brennan, NF (2006)

CHAPTER 3
INFRARED AND RAMAN SPECTROSCOPY

3.1 INTRODUCTION

Raman and infrared spectroscopy measure the energy difference between vibrational energy levels in molecules. The main difference between these two spectroscopic techniques is that IR active vibrations cause a change in the dipole moment of the molecule, whereas a vibration is Raman active if it changes the molecular polarizability. Therefore, whether or not a vibrational mode is active or inactive depends on the symmetry of the molecules [1].

The position of a given stretch vibration in both Raman and infrared spectra can be related to two factors namely the masses of the atoms involved (light atoms vibrate at higher frequencies than heavier ones) and the relative strength of the bond. The wavenumber position of a specific vibration associated with a bond between the same atoms therefore decrease in the following order $sp > sp^2 > sp^3$.

Furthermore the position of a vibrational mode is dependent on the environment of a molecule. Molecular substituents, molecular geometry and hydrogen bonding affect the vibrational force constant, which dictates the vibrational energy (position of band).

Infrared and Raman spectroscopy are therefore useful methods to study intermolecular interactions and can give useful information about the geometry of crystalline compounds, as both methods are sensitive to changes in bond lengths and symmetry of molecules. Furthermore the formation of new bonds upon complexation can be monitored through Raman and IR spectroscopy by the appearance of new bands in the spectra.

In the complexes under study the polarizable thiourea ligands act as bridges between the separated anions and cations. Vibrational spectra of the thiourea ligand are sensitive to structural changes and have been used extensively to obtain more information about covalent metal-thiourea coordination compounds and thiourea

inclusion compounds [6, 7]. The cation-thiourea columns are identical in all of the complexes, therefore the differences in crystal structure are a direct consequence of the ionic strength, size and morphology of the anions.

The FT-Raman and FTIR spectra of all the thiourea complexes were obtained and the spectra are used to illustrate the ionic nature of the intermolecular interactions and confirm the presence of hydrogen bonding in the complexes.

3.2 EXPERIMENTAL DETAIL

The instrumentation used to collect the required transmission infrared vibrational data was a Perkin Elmer Spectrum RX-1, FT-IR System. The analysis was carried out in the solid state. 2 mg of each complex and ~100 mg KBr powder were grounded together using a pestle and mortar until a fine homogeneous powder remained. The KBr is used as a diluting agent, as it does not absorb above 250 cm^{-1} [2] which means that all bands seen in the spectrum relate to the complex. The fine powder is then pressed using a hydraulic press until a clear pellet is produced for analysis. In each interferogram 32 scans were signal averaged, with a spectral resolution of 4 cm^{-1}.

In order to reduce the fluorescence experienced with 514.5 nm laser excitation, a FT-Raman Spectrometer was used which contained an Nd:YAG laser to excite the Raman effect. The Nd:YAG laser has a wavelength of 1064 nm and at this wavelength there are less electronic transitions [3], which in many instances are responsible for a high fluorescence background. The laser power was 500 mW and 512 scans were accumulated with a resolution of 4 cm^{-1}.

As with the IR experiments, the analysis was carried out in the solid state, however, unlike the infrared studies there was very little sample preparation required. A small amount of each complex was placed in a test tube and loaded into the sample compartment. The only necessary and important factor to be considered is that the sample must be in the foci of the laser beam and collection lens [3].

Section 3.3 includes the analysis of the spectra obtained for thiourea (TU), benzoate complex $[(C_6H_5COO)Tl{\cdot}4(SCN_2H_4)]$, 3-amino complex $[(C_6H_6NCOO)Tl{\cdot}4(SCN_2H_4)]$, 2-fluoro complex $[(C_6H_4FCOO)Tl{\cdot}4(SCN_2H_4)]$ and the 3-fluoro complex $[(C_6H_4FCOO)Tl{\cdot}4(SCN_2H_4)]$. These four complexes were the only

complexes where accurate structural data was obtained (see Chapter 2), thus allowing the possibility to correlate the crystallographical and spectroscopic data. The assignments of the bands for the other complexes was guided by this analysis and information obtained in the literature and are given in 3.5 and 3.7.

3.3 DISCUSSION

According to past crystallographic studies carried out on $[(C_6H_5COO)Tl{\cdot}4(SCN_2H_4)]$, it is known that hydrogen bonding occurs between the oxygen atoms of the benzoate ions and the amino hydrogen atoms of the thiourea molecules [4]. Due to the preferred orientation in the packing of the complexes in the solid state there are two different N-H…O approaches, 2.92 Å and 3.03 Å. These are discussed in greater depth in the crystallographic chapter, but suffice to say those of 2.92 Å are stronger hydrogen bonds than those of 3.03 Å and may well be indicated in the spectra by a larger shift [4].

In IR and Raman spectra hydrogen bonding is observed mainly by a broadening of the spectral bands in question as well by a shift of the bands to lower frequencies [5].

It is indicated that some of the complexes that were synthesised are isostructural, and if this is true then the hydrogen bond distances will be very similar to the $[(C_6H_5COO)Tl{\cdot}4(SCN_2H_4)]$ and it is expected that the IR and Raman spectra of the complexes will be very similar.

In Figures 3.1 and 3.2 the FT-Raman and FT-IR spectra of four of the complexes and thiourea are presented. The complexes are the 2-fluoro, 3-fluoro, 3-amino benzoates and the unsubstituted benzoate, which were selected as they were the only complexes which produced single crystal diffraction quality crystals. These four complexes turned out to be isostructural (Chapter 2).

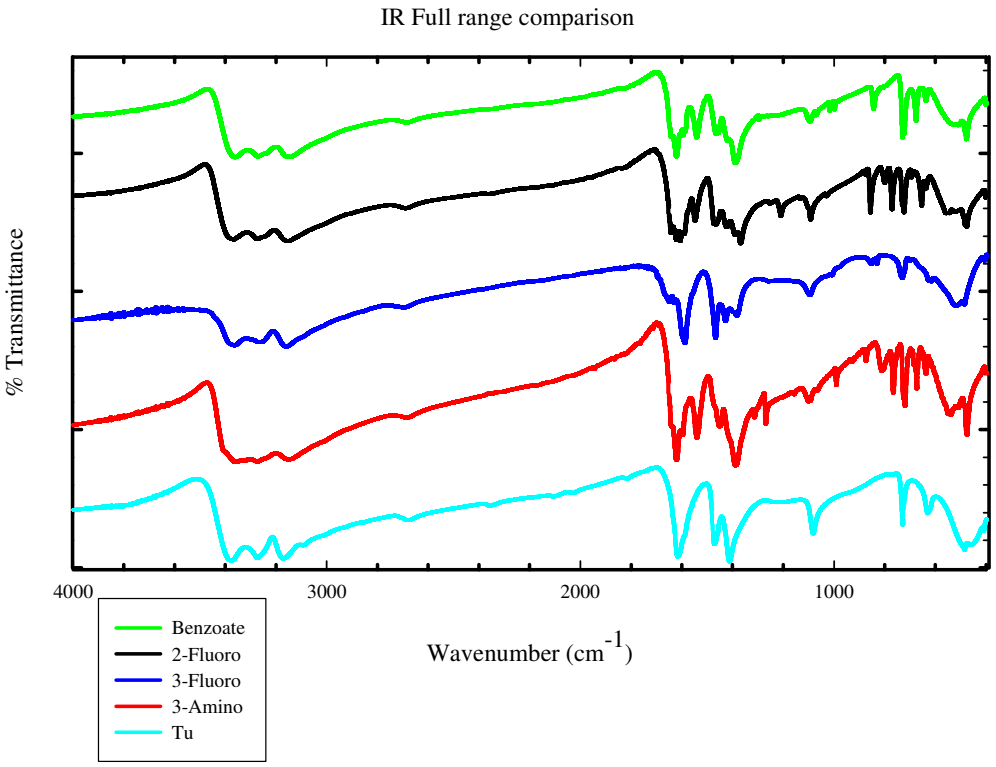

Fig 3.1 **IR spectra of 2-fluoro, 3-fluoro, 3-amino, benzoate complexes and thiourea**

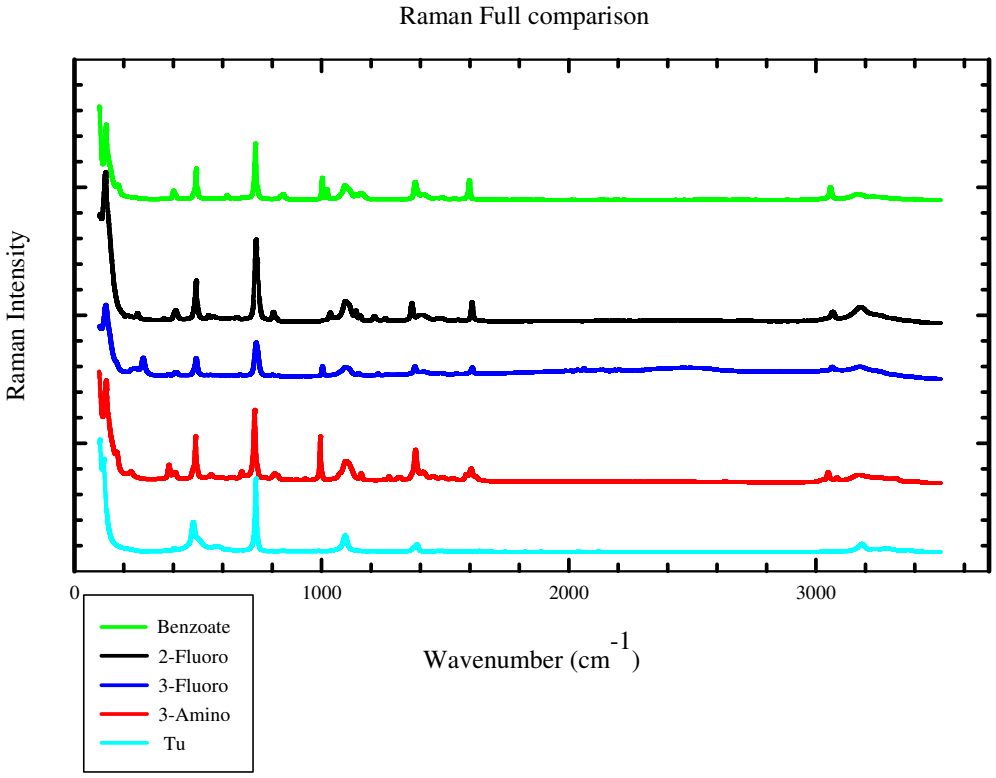

Fig 3.2 **Raman spectra of 2-fluoro, 3-fluoro, 3-amino, benzoate complexes and thiourea**

It is important to note that the C, N and S atoms of the thiourea molecule are co-planar and due to resonance structures the thiourea molecule has complex vibrational dynamics, arising from the mixture of its normal modes of vibration. Therefore, some contradictory interpretations and assignments of vibrational bands are found in the literature for thiourea and its complexes. The comprehensive assignments given in references [6, 7] were used throughout the chapter as these are the most thorough and complete thiourea IR and Raman references that were available.

In all the spectra (including those of the complexes that did not produce crystals suitable for single crystal analysis) the majority of the thiourea bands are in most instances easily identified as can be seen in Fig. 3.1 and 3.2.

It is not with in the scope of this study to do a full analysis of the very complex spectra of the benzoate anions, which is influenced by the position and type of substituents. The main focus is on the comparison of the thiourea bands in the coordination metal – thiourea complexes in order to study the hydrogen bonding, as well as the ionic nature of these complexes.

For convenience sake the FT-Raman and IR spectra of the complexes can be divided into three wavenumber regions, namely: 3500-3000 cm^{-1} (N-H and C-H stretching), 1700-400 cm^{-1} and below 400 cm^{-1}. The low frequency region is important for this study as the thallium – thiourea bands would be expected in this region if a formal covalent bond is formed between thallium and thiourea [6, 7].

3.3.1 THE REGION 3500 – 3000 cm^{-1} (Table 3.1)

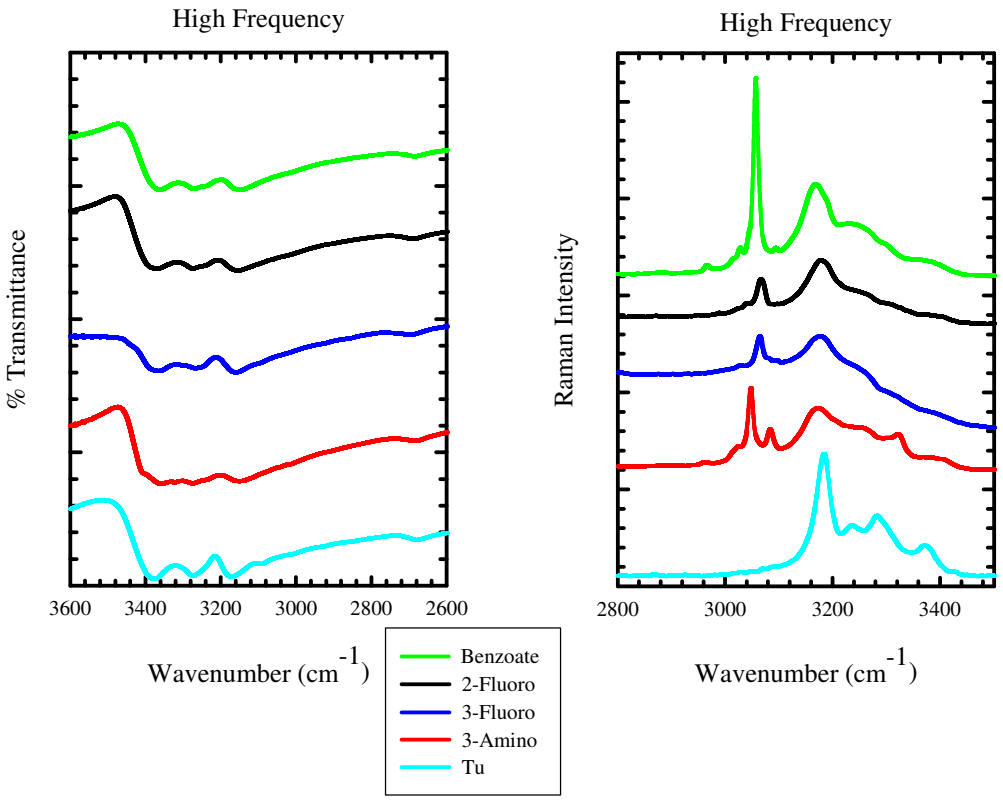

Fig. 3.3 **IR and Raman spectra of 2-fluoro, 3-fluoro, 3-amino, benzoate complexes and thiourea in the region of 3500-3000 cm^{-1}**

This is an important region which contains the N-H stretch of the amine groups of thiourea and C-H stretch vibrations of the aromatic ring of benzoate ions [8]. The spectra are very similar and dominated by the bands originating from thiourea.

N-H region

It is generally agreed that the band in the thiourea spectrum at 3377 cm^{-1} is the antisymmetric stretch vibration, the peak at 3273 cm^{-1} represents the first overtone of the NH_2 antisymmetric bending component and the band at 3172 cm^{-1} represents N-H symmetric stretching [6, 9]. The spectrum of the 3-amino complex shows an extra band at 3323 cm^{-1} which can be attributed to the NH_2 group bonded to the benzoate ion [6, 8].

In both IR and Raman spectra there is a general shift to lower wavenumbers and broadening of the NH_2 vibrations which can best be observed in the Raman

spectrum (Table 3.1 and Fig. 3.3). The shifting and broadening are indicative of an increase in hydrogen bonding in the complexes, compared to thiourea. This is in contrast to coordination metal – thiourea complexes, where a decrease in hydrogen bonding is observed (shift to higher wavenumbers). In these complexes a marked increase of intensity of the NH_2 bands is also observed and attributed to hydrogen bond weakening due to covalent metal – sulphur bonding that exists. The opposite is observed for the compounds of this study, indicative of the different bonding seen in these complexes..

As there are two different NH…..O approaches in the complexes a larger shift for the smaller approach value is expected as it is involved in stronger hydrogen bonding but the two hydrogen bonds were not resolved in the spectra.

C-H region

The C-H ring vibration is most clearly seen in the Raman spectra as a strong, sharp band between 3047-3083 cm^{-1} which is of course not seen in the pure thiourea spectrum, therefore must be attributed to the C-H vibrations of the ring [8, 10].

In the IR spectra these bands are less prominent as they are masked by the broad N-H band between 3143-3160 cm^{-1}.

THIOUREA		BENZOATE COMPLEX		2-FLUORO COMPLEX		3-FLUORO COMPLEX		3-AMINO COMPLEX		
IR	**RAMAN**	**IR**	**RAMAN**	**IR**	**RAMAN**	**IR**	**RAMAN**	**IR**	**RAMAN**	
3377ms	3370w	3365ms		3367ms		3365ms		3339w		1
								3323w	3321w	2
3273ms	3282w	3273ms		3275ms		3269ms		3274mw		3
			3231w							4
3172ms	3183ms	3143ms	3167m	3160ms	3177ms	3160ms	3175ms	3150m	3172m	5
					3066m		3064m		3083w	6
			3057ms						3047m	7

1 = N-H stretch/Ar-NH_2, 2-5 = N-H stretch, 6-7 = C-H stretch

Table 3.1 **IR and Raman spectra wavenumbers for benzoate, 2-fluoro, 3-fluoro, 3-amino complexes and thiourea**

3.3.2 THE REGION 1700 – 400 cm^{-1} (Table 3.3)

Within this region there are a number of bands present in both the IR and Raman spectra of the 3 complexes.

In terms of IR results, the thiourea band at 1617 cm^{-1}, which represents the NH_2 bending vibration overlaps with small weaker bands in the spectra of the 2-fluoro and 3-fluoro complexes. This is attributed to the aromatic C=C ring stretch of the complex which also occurs in this region. Thus it is difficult to determine exact assignments for these bands [6, 7, 9, 10]. The same main band is present in the spectra of the benzoate complex and the 3-amino complex, however, with little or no splitting. But due to the broadness of the band in both spectra the assignment may be NH_2 or C=C or both, as these bands may be masked. No prominent shifts in wavenumbers are seen relative to the thiourea.

The Raman spectrum of the thiourea shows a very weak band in the region at 1636 cm^{-1}, relating to the symmetric and antisymmetric-coupled bending mode $\delta(NH_2)$ [6, 7]. The strong NH_2 bands in the IR are absent and the assignment of the aromatic C=C stretch is unambiguous. The spectra of the 2-fluoro, 3-fluoro and the benzoate complexes all show a single sharp band at 1607 cm^{-1}, 1608 cm^{-1} and 1596 cm^{-1} respectively, which are attributed to the C=C stretch of the benzoate ion [10]. In the 3-amino complex spectrum this band occurs at 1603 cm^{-1}, however, it overlaps with the aromatic NH_2 which is also found in this region [8, 10].

The IR spectra of the 3-amino and benzoate complexes all possess a strong to medium band, 2-fluoro has a weak band and 3-fluoro has no band between 1550 - 1541 cm^{-1}. As this band is not seen in the thiourea spectrum, it is assigned to the COO^- of the benzoate ion, which occurs in this region [11, 12].

The Raman spectra shows very weak broad bands in this region which makes assignment difficult.

The IR spectra of thiourea and the 4 complexes (Fig. 3.5) show a band at 1473 cm^{-1} with a slight increasing shift visible in the Raman spectra (Fig. 2.6). This band is attributed to the antisymmetric (NCN) stretching of the thiourea [6, 7, 9]. At slightly lower wavenumbers (1450 cm^{-1}), the benzoate and amino complexes show medium to weak bands which can be assigned to ring vibrations as they are not present in thiourea spectrum [10, 13]. The strong IR band at 1413 cm^{-1} in pure

thiourea is also seen in the IR (Fig. 3.5) and Raman (Fig. 3.6) spectra of the three complexes and according to literature values can be assigned to the C=S vibration [8, 9].

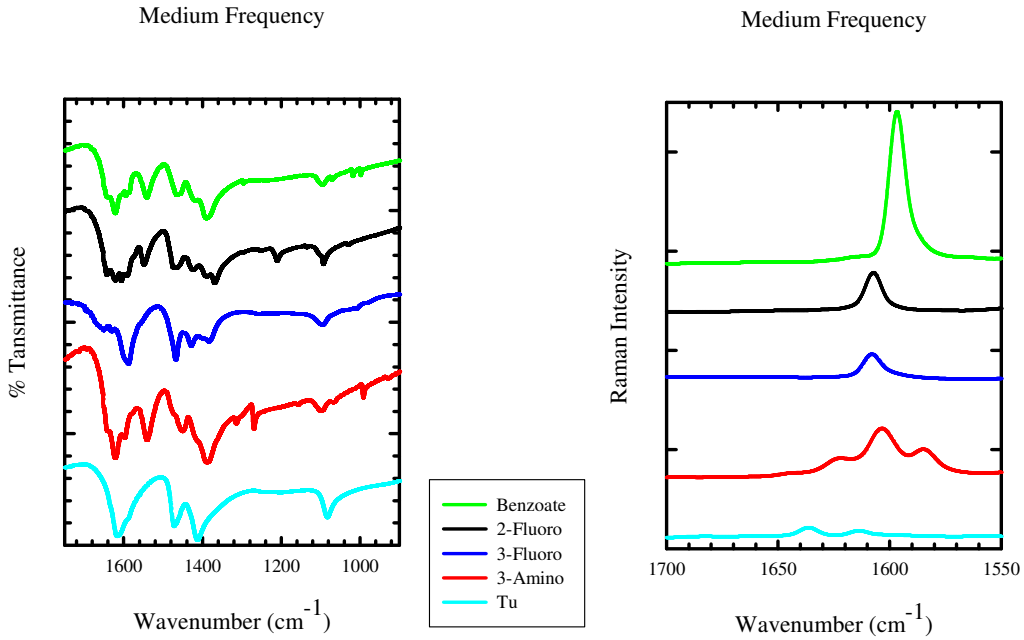

Fig. 3.4 **IR (region 1760 cm^{-1}-920 cm^{-1}) and Raman (region 1698 cm^{-1}-1554 cm^{-1}) spectra of 2-fluoro, 3-fluoro, 3-amino, benzoate complexes and thiourea**

The Raman spectrum (Fig. 3.6) of thiourea shows a band at 1384 cm^{-1} with a shoulder at 1374 cm^{-1}. This band is present in the complexes as a single band with a shift to lower wavenumbers. It is assigned to a vibration that affects the whole thiourea molecule and has contributions from ν(CN), δ(NCN), δ(CNH) and ν(CS) [6, 7]. Note : ν = stretch δ = bend

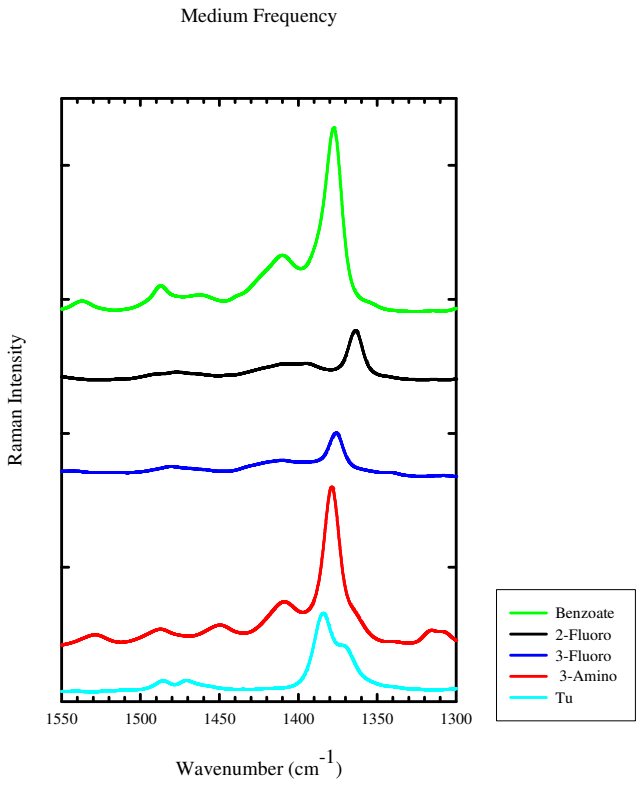

Fig. 3.5 **Raman (region 1550-1300 cm^{-1}) spectra of 2-fluoro, 3-fluoro, 3-amino, benzoate complexes and thiourea**

Within the region of 1098-1083 cm^{-1} the bands are both IR and Raman active for both the thiourea and the 4 complexes.

Both the IR and Raman spectra of the complexes have a relatively strong band at approximately 1090 cm^{-1}. The Raman band at 1093 cm^{-1} in the thiourea arises from a mixed normal mode with contributions from ν(CN) and ρ(HNH) [6, 7, 8, 9, 10].

Between wavenumber values of 1030-486 cm^{-1} all the bands bar 3 are weak and correspond to C-H vibration of the aromatic ring [8, 10]. The first band of real importance is a strong band at 729 cm^{-1} and is present in both the Raman and IR spectra of both the thiourea and the 4 complexes. The band relates to a pure C=S stretch vibration of the thiourea and is relatively broad [5, 6, 8, 9, 14].

A large shift to lower wavenumbers is observed for the C=S stretch vibration of thiourea - metal coordination complexes where a coordination bond is formed between the metal and the sulphur atoms, as the double bond character of the C=S disappears upon coordination [6, 7]. No shift is observed for the complexes under investigation.

When discussing the C=S bond it is important to also take into consideration the interatomic distance between the metal and sulphur atoms. But it is also worth noting that because there are two different NH.....benzoic acid hydrogen bonds, this leads to two different S.....Tl interactions with in the complexes. The pairs of different S…..Tl distances observed for the four crystal structures determined in this study, as well as the results from the previously reported benzoate crystal structure [4], are given in Table 3.2.

COMPLEX	Tl(1) – S(1) Å	Tl(1) – S(2)#1 Å
2-Fluoro #2	3.3792(7)	3.4235(8)
3-Fluoro #2	3.3537(7)	3.4142(8)
3-Amino #2	3.3588(6)	3.4209(7)
Benzoate #2	3.3642(7)	3.4345(9)
Benzoate #3	3.450	3.380

Table 3.2 Table showing the two different Tl – S interatomic distances

Note: #1 = Symmetry transformations used to generate equivalent atoms: x, y-1, z
#2 = This study
#3 = Ref. [4]

These complexes have Tl-S distances of similar magnitude. However, when one measures the Tl-S bond length in a coordination complex the bond length is only 2.45 Å (a considerable difference relative to the complexes in question) and which results in shifts up to 50 cm^{-1} in the spectra [6, 7]. As there are no shifts present in the complexes one is able to deduce that ionic interactions are dominant and little or no coordination character could be shown [15]. This is in accordance to the paper by Boeyens, on the crystal structure of the $C_6H_5COOTl{\cdot}4(SCN_2H_4)$, where it is stated that there is no formal Tl-S bond [16]. However, in a subsequent study of the chlorate complex, the Tl-S interatomic distances vary from 3.33 Å to 3.51 Å, and this is described as polymeric bonds [17]. In an earlier publication on ionic complexes of thiourea, it states that the average Tl-S distance 3.43 Å, which is considerably longer than the separation between sulphur atoms of coordinated ligands and metal atoms. As the sum of the thallium and sulphur atom radii is 2.70 Å and the sum of the ionic

radii is 3.3 Å it is clear that the complexes are ionic and the main cohesive interactions are ion-dipole interactions [16].

The second band occurs in the IR of thiourea at 631 cm^{-1} and is of medium intensity. It is seen in the benzoate complex and is assignable to NCN [18].

The third band of importance is a large, prominent band in both IR and Raman spectra in the complexes at approximately 485 cm^{-1}. It is also present in the Raman and IR of thiourea at 479 cm^{-1} and 486 cm^{-1} respectively which corresponds to the published assignment [6, 8]. It usually shifts to lower wavenumbers upon coordination, but in our case shifts to higher wavenumbers with 10 cm^{-1}. This opposite shift could be indicative of the fundamental difference between covalent and ionic metal – thiourea complexes.

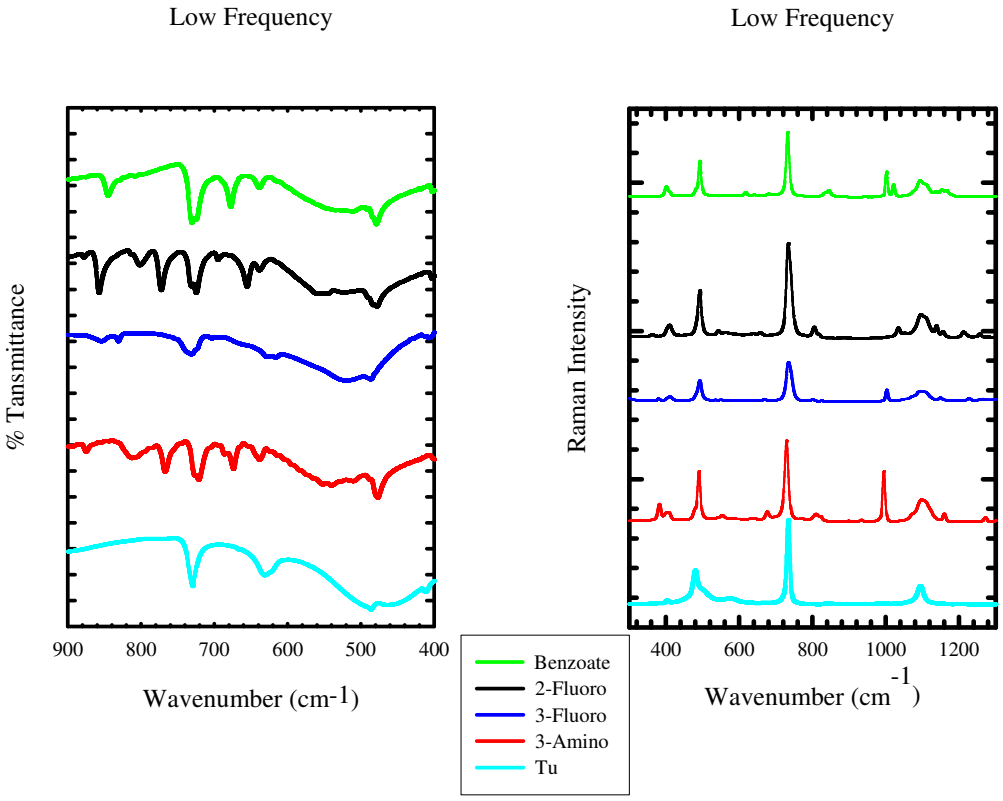

Fig 3.6 **IR (region 900 cm^{-1}-400 cm^{-1}) and Raman (region 1240 cm^{-1}- 320 cm^{-1}) spectra of 2-fluoro, 3-fluoro, 3-amino, benzoate complexes and thiourea**

3.3.3 THE REGION 300 – 100 cm^{-1}

Only Raman spectra are available for this region and the metal – sulphur symmetric stretch bands expected to occur in this region (220 – 260 cm^{-1}) are not observed, which is supportive of the ionic nature of the complexes, which excludes the formation of a formal covalent bond between the thallium and sulphur atoms.

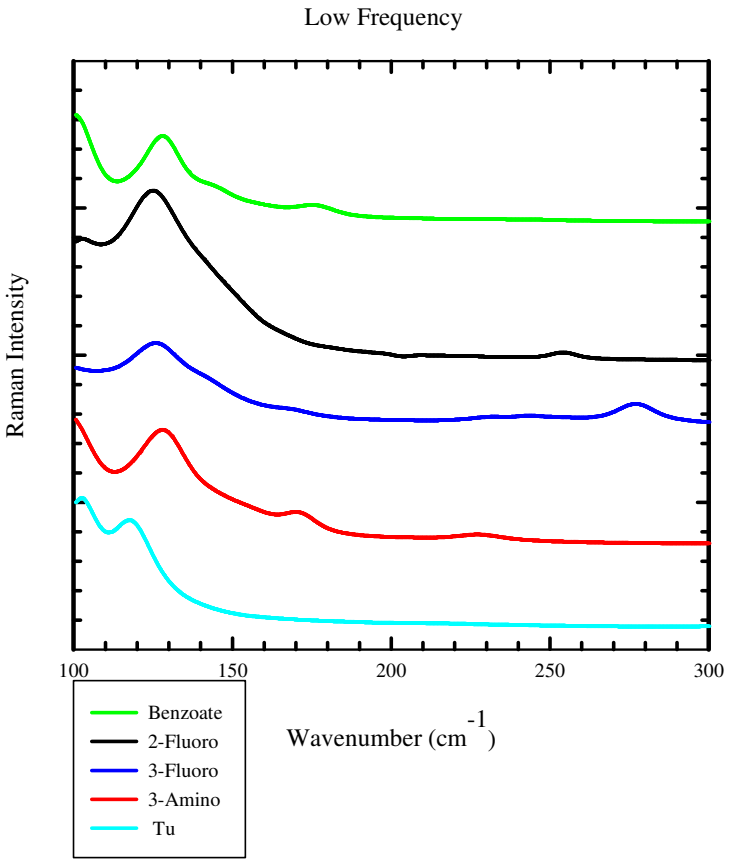

Fig. 3.7 **Raman (region 100-300 cm^{-1}) spectra of 2-fluoro, 3-fluoro, 3-amino, benzoate complexes and thiourea**

THIOUREA		BENZOATE COMPLEX		2-FLUORO COMPLEX		3-FLUORO COMPLEX		3-AMINO COMPLEX	
IR	**RAMAN**	**IR**	**RAMAN**	**IR**	**RAMAN**	**IR**	**RAMAN**	**IR**	**RAMAN**
	1636w			1644w		1652w			
1617s		1623s		1621w		1631w		1621s	
		1596w	1596s	1597ms	1607m	1589s	1608w	1598w	1603m
		1542m	1537w	1550w	1550w			1541ms	1528w
1473ms	1471w		1487w	1469m	1477w	1468s	1481w		1487w
		1457m						1450mw	1449w
1413s			1410w	1427mw	1395w	1429mw	1410w		1409w
	1384m	1390s	1377s	1370m	1365ms	1384mw	1376m	1388s	1378s
1083s	1093ms	1098mw	1093ms	1094m	1095ms	1096m	1093s	1098mw	1096ms
			1020m		1030w				
			1001ms				1002ms	992w	994s
		845w	843mw	858mw		855w			
				801w	803w			809mw	
				773w				767m	
729m	734s	731ms	732s	731m	733s	732m	734s	721m	729s
		678mw						674mw	
631m		639w							
			616w			617w			
	573w								
486ms	479s	479m	492s	484m	492s	486s	491s	477ms	490s

1-2 = NH_2, 3 = NH_2/C=C/Ar-NH_2, 4 = COO^-, 5 = NCN/C=C, 6 = C=C, 7-8 = C=S, 9 = NH_2/C=S/C-N/C-H, 10-14 = C-H, 15 = C=S, 16 = NH_2/C=S/NCN, 18-19 = C-H, 20 = NCN/C=S

Table 3.3 **IR and Raman wavenumbers for benzoate, 2-fluoro, 3-fluoro, 3-amino complexes and thiourea**

3.4 RAMAN AND IR SPECTRA OF THE OTHER 17 COMPLEXES

IR and Raman spectra for the full list of complexes that was synthesised were obtained. The main bands were all very similar in all the spectra as can be seen from the tables in 3.6. The detailed analysis confirmed the same increase in hydrogen bonding as observed for the previous four samples (similar shifts in thiourea bands), as well as the ionic nature of the metal – sulphur band. Thus, it was concluded that the solid state structures of all complexes are in fact quite similar. The bands that are expected to be different are discussed below.

Ar-NO_2 Delocalized NO_2 stretching vibrations seen at1338 cm^{-1}. The vibrations do not correspond exactly to literature values as substituted nitrobenzenes are affected by inductive effects,

resonance effects and hydrogen bond formation related to the benzene ring substituents [8].

HALOGENS — The complexes which contain halogen substitution, i.e. 2/3/4-fluoro, 2/3/4-bromo, 2/3/4-chloro complexes do not show well defined C-X (X = halogen) absorptions as halogen substituted aromatics result in absorptions that occur in a spectral region that is crowded by other important group frequencies [10].

2/3/4-METHYL
4-METHOXY
2-HYDROXY

All are difficult to identify due to overlapping of other important bands in the region they occur.

As has been stated in chapter one, all the complexes were initially synthesised and analysed with $TlNO_3$ as the starting material before being resynthesised with Tl_2CO_3 and reanalysed. Due to the presence of NO_3 in some of the complexes in the first batch, there was an uncertainty in the infrared band assignment at 1384 cm^{-1} as TU and NO_3 overlap. In the second batch with no NO_3 or CO_3 it can be seen that the band in question relates to TU, specifically C=S.

Note : Proof of no CO_3 contamination is assured. The complete absence of the characteristic CO_3 band at 1039 cm^{-1} from all the complex IR spectra proved that there was no carbonate present in any of these samples.

3.5 CONCLUSION

The FT-Raman and FT-IR bands in the spectra of all the complexes have been assigned according to literature data. The complexity of the spectra, which contain bands originating from the anions, as well as thiourea, makes some of the assignments ambiguous as indicated in the tables and figures.

Some important conclusions could be drawn from the spectra.

- An increase in hydrogen bonding, reflected by the observed changes relative to the thiourea spectra, is observed for all the complexes measured. The presence of hydrogen bonding indicated broadening and shifting to lower wavenumbers in the IR and Raman spectra. This is also supported by the observation that two different hydrogen bonds were observed in the single crystal study of the four benzoate structures. It was however not possible to distinguish between the two bonds of 2.92 Å and 3.03 Å.
- The absence of a band due to covalently bonded Tl-S is in accordance with the ionic nature of the complexes. The Tl-S distances as measured in the crystallographic study also supports the observation from this spectroscopic study that thallium is not covalently bonded to sulphur and the ionic model as suggested in references [16, 17] is correct.

3.6 IR AND RAMAN BANDS FOR ALL THE COMPLEXES

The following complexes did not give Raman spectra of sufficient quality for interpretation bar the one band at approximately 733 cm^{-1} which is characteristic of C=S : 2-bromo, 2-hydroxy, 3-nitro, 4-fluoro,2/3/4-chloro

2-AMINO COMPLEX		3-AMINO COMPLEX		4-AMINO COMPLEX		ASSIGNMENT
IR	RAMAN	IR	RAMAN	IR	RAMAN	
3376ms		3339w		3368m		N-H stretch
		3323w	3321w			N-H stretch
3276ms		3274mw		3275m		N-H stretch
3164s	3185ms	3150m	3172mw	3171m	3184m	N-H stretch
			3083w			C-H stretch
			3047mw			C-H stretch
1598s	1607w	1621ms	1603m	1599ms	1607w	Ar-NH_2/C=C/NH_2
		1598w				NH2/C=C/Ar-NH2
		1541ms	1528w			COO^-
1469ms	1474w		1487w	1469mw	1474w	C=C/NCN
		1450mw	1449w			C=C
1433w			1409w	1433w		C=S
1384w	1393w	1388s	1378ms	1383w	1394w	NH_2/C=S/NCN
1094mw	1106m	1098w	1096ms	1095m	1105m	NH_2/C=S/C-N/C-H
		992w	994s			C-H
853w		809mw		850ms		C-H
		767mw				C-H
732m	740s	721mw	729s	730s	740s	C=S
		674mw				C-H
486s	493s	477s	490s	483s	492s	NCN/C=S

Table 3.4 IR and Raman wavenumbers for 2/3/4-amino complexes

2-NITRO COMPLEX		3-NITRO COMPLEX		4-NITRO COMPLEX		ASSIGNMENT
IR	RAMAN	IR	RAMAN	IR	RAMAN	
3338w		3366w		3368m		N-H stretch
3289m		3279m		3279m		N-H stretch
3161ms	3183ms	3161ms		3163ms	3184m	N-H stretch
					3076w	C-H stretch
1600s	1606w	1599s		1599s	1594ms	NH_2 /C=C
1471ms	1476w	1470m		1470ms		C=C/NCN
1428w		1429w		1432w		C=S
1385ms	1398w	1383m		1385mw	1387m	NH_2/C=S/NCN
	1336w				1338m	Ar-NO_2
1092ms	1106m	1097m		1094m	1106m	NH_2/C=S/C-N/C-H
	1050w					C-H
861m				853w		C-H
				801mw		C-H
730ms	740s	725ms		732m	740s	C=S
484ms	493ms	487m		487m	492ms	NCN/C=S

Table 3.5 IR and Raman wavenumbers for 2/3/4-nitro complexes

2-FLUORO COMPLEX		3-FLUORO COMPLEX		4-FLUORO COMPLEX		ASSIGNMENT
IR	RAMAN	IR	RAMAN	IR	RAMAN	
3367ms		3365ms		3367ms		N-H stretch
3275ms		3269ms		3273ms		N-H stretch
3160ms	3177ms	3160ms	3175ms	3162ms		N-H stretch
	3066m		3064m			C-H stretch
1644w		1652w				NH2
1621w		1631w				NH2
1597ms	1607m	1589s	1608w	1602s		NH_2/C=C
1550w	1550w			1553mw		COO^-
1469m		1468ms		1469m		C=C/NCN
1427mw	1395w	1429mw		1431mw		C=S
1370m	1365ms	1384ms	1376w	1387s		C=S
1094m	1095ms	1096m	1093m	1084mw		NH2/C=S/CN/C-H
	1030w		1002mw			C-H
858mw		855w		856mw		C-H
801w						C-H
773w				782w		C-H
731m	733s	732m	733s	733mw		C=S
		617w				C-H
484m	492s	486s	491s	486m		NCN/C=S

Table 3.6 IR and Raman wavenumbers for 2/3/4-fluoro complexes

2-BROMO COMPLEX		3-BROMO COMPLEX		4-BROMO COMPLEX		ASSIGNMENT
IR	RAMAN	IR	RAMAN	IR	RAMAN	
3366ms		3367ms		3360ms		N-H stretch
3277ms		3267ms		3259ms		N-H stretch
3162s		3157ms	3169m	3159s	3174m	N-H stretch
			3078mw		3088ms	C-H stretch
			3048m		3071ms	C-H stretch
		1622m				$C=C/NH_2$
1599s		1601mw	1587ms	1587s	1586ms	NH_2/C=C
		1543ms	1535w	1543m		COO^-
1470ms		1467ms	1464w	1466m	1480w	NCN/C=C
1429mw				1429mw		C=S
			1405w	1404m		C=S
1387mw		1371s	1366s	1384s	1372s	NH_2/C=S/NCN
1097mw		1096mw	1091s	1093w	1108mw	NH_2/C=S/C-H/CN
				1074w	1071s	C-H
			999s		1014w	C-H
855w		858mw	858w	838w		C-H
			830w		837mw	C-H
		768mw		770mw		C-H
730m		724m	732s	729mw	731s	C=S
			650mw			C-H
488m		489ms	489s	486ms	485s	NCN/C=S

Table 3.7 IR and Raman wavenumbers for 2/3/4-bromo complexes

2-CHLORO COMPLEX		3-CHLORO COMPLEX		4-CHLORO COMPLEX		ASSIGNMENT
IR	RAMAN	IR	RAMAN	IR	RAMAN	
3367ms		3367ms		3359m		N-H stretch
3270ms		3274ms		3253m		N-H stretch
3162ms		3162ms		3157m		N-H stretch
1594s		1600m		1589s		NH_2/C=C
		1545m		1545m		COO^-
1468ms		1468m		1467m		C=C/NCN
1430mw				1428w		C=S
1384mw		1375ms		1386s		NH_2/C=S/NCN
1094mw		1098w		1099m		NH_2/C=S/CN/C-H
				1012w		C-H
		869w				C-H
				839w		C-H
		769mw		774m		C-H
732m		738m		729m		C=S
487s		479m		485w		NCN/C=S

Table 3.8 **IR wavenumbers for 2/3/4-chloro complexes**

2-METHYL COMPLEX		3-METHYL COMPLEX		4-METHYL COMPLEX		ASSIGNMENT
IR	RAMAN	IR	RAMAN	IR	RAMAN	
3366ms		3366ms		3366ms		N-H stretch
3276ms		3274ms		3278ms		N-H stretch
3161ms	3185ms	3159ms	3179ms	3161ms	3184ms	N-H stretch
			3042w			C-H stretch
1598s	1607w	1599s	1602w	1598s	1607w	NH_2/C=C
1472m		1469m		1470m		C=C/NCN
1430w				1431w		C=S
1383w	1393w	1383s	1386w	1382w	1393w	NH_2/C=S/NCN
1093m	1106m	1098m	1106m	1093ms	1106m	NH_2/C=S/CN/C-H
			1005mw			C-H
854mw				852m		C-H
733m	740s	731ms	737s	730m	740s	C=S
485m	493s	490m	490s	483m	493m	NCN/C=S

Table 3.9 **IR and Raman wavenumbers for 2/3/4-methyl complexes**

4-METHOXY COMPLEX		2-HYDROXY COMPLEX		BENZOATE COMPLEX		ASSIGNMENT
IR	**RAMAN**	**IR**	**RAMAN**	**IR**	**RAMAN**	
3369ms		3366ms		3365m		N-H stretch
3277ms		3268ms		3273ms		N-H stretch
					3231w	N-H stretch
3164s	3185ms	3158s		3143ms	3167m	N-H stretch
					3057ms	C-H stretch
				1623s		NH_2
1599s	1607w	1589s		1596w	1596s	NH_2/C=C
				1542m	1537w	COO^-
1470m	1475w	1468m		1457m	1487w	C=C/NCN
1433w		1430w			1410w	C=S
1383w	1389w	1382m		1390s	1377s	NH_2/C=S/NCN
1093m	1106m	1093mw		1098mw	1093ms	NH_2/C=S/CN/C-H
					1020m	C-H
					1001ms	C-H
853mw		862w		845w	843mw	C-H
733m	740s	730mw		731ms	732s	C=S
				678mw		C-H
				639w		NH_2/C=S/NCN
					616w	C-H
486m	493s	486m		479m	492s	NCN/C=S

Table 3.10 IR and Raman wavenumbers for 4-methoxy, 2-hydroxy, benzoate complexes

3.7 REFERENCES

CHAPTER 3

1. www.cem.msu.edu/~cem472/ramanir.pdf
2. www.wpi.edu/Academics/Depts/Chemistry/Courses/CH2670/infrared page 15
3. Introduction to FT-Raman Spectroscopy, FT-Raman Users Manual, page 7-18
4. L. H. W. Verhoef and J. C. A. Boeyens, Acta Cryst. 1969, **B25**, 607
5. D. Gambino, E. Kremer, E. J. Baron, Spectrochimica Acta, Part A, 2002, **58**, 3087-3090
6. J. M. Alia, H. G. M. Edwards, M. D. Stoev, Spectrochimica Acta, Part A, 1999, **55**, 2423-2435
7. J. M. Alia, H. G. M. Edwards, F. J. Garcia-Navarro, Journal of Molecular Structure, 1999, **508,** 51-58.
8. D. Lin-Vien, N. B. Colthup, W. G. Fateley, J. G. Grasselli, The Handbook of Infrared and Raman Characteristic Frequencies of Organic Molecules, Academic Press, Boston, MA, 1991, page 155-284
9. G. M. S. El-Bahy, B. A. El-Sayed, A. A. Shabana, Vibrational Spectroscopy, 2003, **31**, 104
10. John Coates, Interpretation of Infrared Spectra, A Practical Approach, Coates Consulting, Newtown, USA, page 8-13
11. W. Lewandowski, L. Fuks, M. Kalinowska, P. Koczon, Spectrochimica Acta Part A, 2003, **59,** 3413
12. P. Koczon, W. Lewandowski, A. P. Mazurek, Vibrational Spectroscopy, 1999, **20,** 145
13. B. Dasiewicz, L. Fuks, W. Lewandowski, Journal of Molecular Structure, 2001, **565-566**, 2
14. P. Bombiez, I. Mutikainen, M. Krunks, T. Leskela, J. Madarasz, L. Niinisto, Inorganica Chimica, Acta, 2004, **357,** 522
15. J. C. A. Boeyens, G. Gafner, The Journal of Chemical Physics, 1968, **49,** 2435
16. J. C. A. Boeyens, F. H. Herbstein, Nature, 1966, **211**, 589
17. J. Mitchell, J. C.A. Boeyens, Acta Cryst,. 1970, **B26**, 1122
18. M. M. El-Etri, W. M. Scovell, Inorganica Chimica Acta, 1991, **187**, 205

University of Pretoria etd – Brennan, NF (2006)

CHAPTER 4
UV/VIS SPECTROSCOPY

4.1 INTRODUCTION

UV/VIS Spectroscopy was another analytical technique used in the solid state mainly to prove the formation of the complexes. Any shifting of the bands would also be an indication of hydrogen bonding with in the complexes. An added use of this technique was to identify if charge transfer reactions were taking place, this is discussed later.

Before any details as to the theory behind UV and the results and discussion of the analysed complexes, it is important to note that in this study the results of UV are of relatively little importance if not combined with the results of infrared spectroscopy and NMR (Nuclear Magnetic Resonance) Spectroscopy. However, when combined, valid structural proposals can be made [1]. Hence the reason why the other chapters focus on both IR and NMR along with other useful structural determination techniques.

The principles of UV centre on the fact that molecules have the ability to absorb ultraviolet or visible light. This absorption corresponds to the excitation of outer electrons in the molecules concerned. It is these transitions of electrons which are important to understand.

When a molecule absorbs energy an electron is promoted from the Highest Occupied Molecular Orbital (HOMO) to the Lowest Unoccupied Molecular Orbital (LUMO).

It must be noted that occupied molecular orbitals with the lowest energy are the σ orbitals, then at a slightly higher energy are the π orbitals and non-bonding orbitals (those with unshared pairs of electrons) at still a higher energy. The highest energy orbitals belong to π^* and σ^*, i.e. the unoccupied or as otherwise known as, the antibonding orbitals [1].

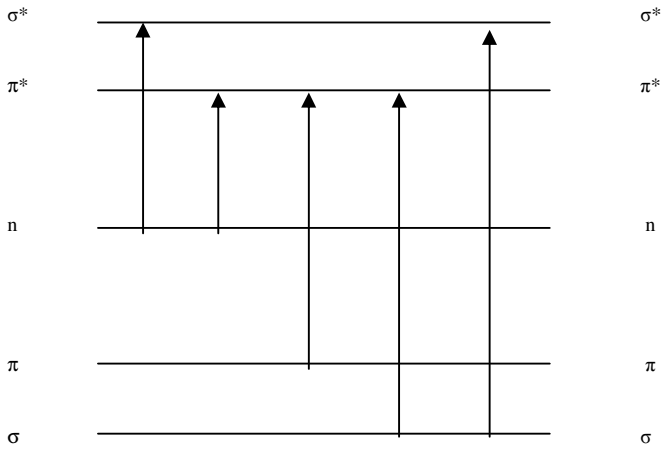

Fig. 4.1 Electronic energy levels and transitions [1]

4.2 INSTRUMENTATION

The actual instrument used to determine the ultra violet spectra of the complexes was the Milton Roy Spectronic GENESYS 5.

As with any UV/VIS spectrophotometer, three of the main elements are a UV-light source, a monochromator and a detector. The monochromator works as a diffraction grating to dispense the beam of light into the various wavelengths. The detectors role is to record the intensity of the light which has been transmitted [1].

Before the samples are run, a reference must first be taken. This calibrates the spectra to screen out ant spectral interference. In the case of liquid samples the solvent which has been used to dissolve the sample is used. However, there are certain criteria that solvents must pass before they can be deemed as suitable solvents. The main criterion is that the solvent should not absorb ultraviolet radiation in the same region as the sample being analysed [1].

In the case of solid-state UV/VIS spectroscopy the reference is normally KBr as the KBr does not absorb radiation in the same region as most complexes.

4.3 PREPARATION OF SAMPLE

The complexes that were analysed were in the solid state. A KBr reference pellet was first made by grinding up pure KBr in a pestle and mortar until a fine powder remained. This was then placed in a high pressure press and left for approximately 5 minutes at approximately 8 tons, until a thin, clear pellet was formed. The complexes were also pressed into pellets. A mixture of KBr and each complex were ground then pressed to form pellets.

4.4 CHARGE TRANSFER

As with Infrared and Raman spectroscopy, the absence of bands can at times provide as much, if not more information than the presence of bands.

Of particular relevance to the UV spectra of the synthesized complexes is the fact that only the expected bands are visible, i.e. there are no extra bands. An extra band would indicate a charge transfer state [2]. This takes place when n electrons are able to be excited to π^* orbitals. The aromatic ring gains an electron while the atom or molecule from which the n electron was removed loses an electron – becomes electron deficient [1].

4.5 UV OF AROMATIC COMPOUNDS

The electronic energy levels involved in aromatic compounds are of the type, $\pi \longrightarrow \pi^*$. Due to electron – electron repulsions and symmetry operations, three electronic transitions take place to these excited states. In the liquid state, bands at 184 nm and 202 nm are known as primary bands while a band at 253 nm is known as a secondary band [1]. Benzene exhibits two intense absorption bands at 180 nm and 200 nm and a weak absorption band at 260 nm, all of which are linked with the π-system of the benzene ring.

The bands at 180 nm and 200 nm can be ascribed to transitions to dipolar excited states, while the band at 260 nm is ascribed as the forbidden transition to a homonuclear excited state.

Different nomenclatures are used to describe these three bands, i.e. the 180 nm band is also known as $A_{1g} \longrightarrow E_{1u}$, while the 200 nm band as $A_{1g} \longrightarrow B_{1u}$ an the 260 nm band as $A_{1g} \longrightarrow B_{2u}$.

However, the 180 nm band is beyond the range of most instruments and therefore for the remainder of this chapter the words primary and secondary will be used to describe the bands at 200 nm and 260 nm respectively [3].

The 184 nm band as it is beyond the range of most instruments and so what is generally seen are the primary and secondary bands at 202 nm and 253 nm respectively.

When substituents are added to the ring system other possible energy level transitions must be considered. These are of the type $n \longrightarrow \pi^*$, however, these particular bands are hidden by the secondary benzene band at 253 nm. Another feature of adding substituents to benzene is that the bands shift to larger wavelengths depending on the nature of the substituents, i.e. their electron donating or withdrawing nature [1].

An example of this is when COOH (electron withdrawing group) is added to a benzene ring to form benzoic acid. A noticeable bathochromic or red shift of both the primary and secondary bands is clearly seen [1, 3, 4].

SPECTRA OF BENZENE AND BENZOIC ACID

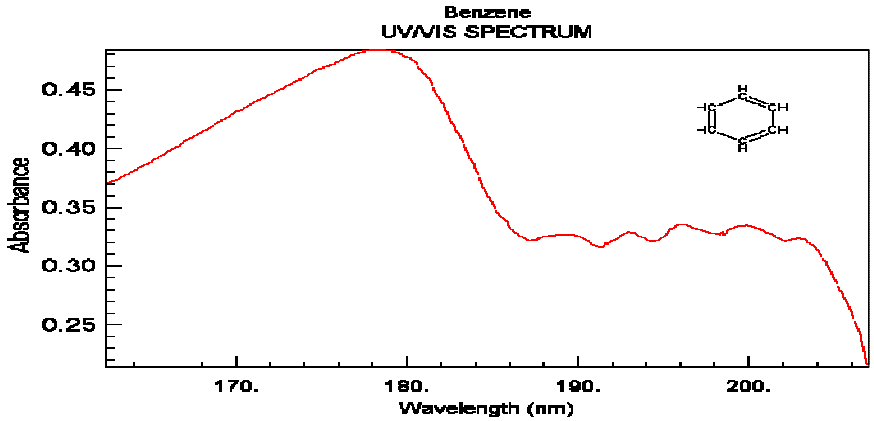

Fig. 4.2 UV Spectrum of benzene [5]

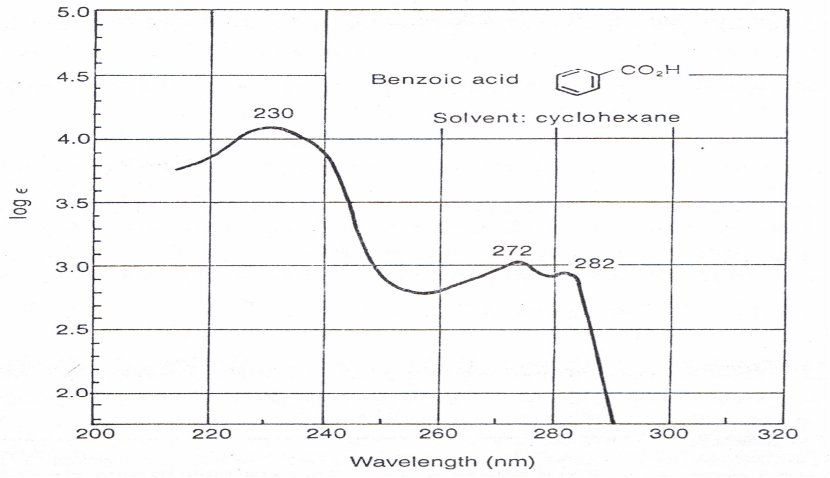

Fig. 4.3 UV Spectrum of benzoic acid [1]

Also of particular interest to the complexes that were synthesized are the literature values for the shifts present in chloro, nitro, amino and hydroxy benzoic acids. All show marked shifts of the primary and secondary bands relative to benzoic acid which are shown in Table 4.1.

SUBSTITUENT ON BENZOIC ACID	**PARA-DERIVATIVES**	**META-DERIVATIVES**		**ORTHO-DERIVATIVES**	
	WAVELENGTHS ABSORBED (nm)				
		200 nm	**260 nm**	**200 nm**	**260 nm**
Cl	241	231.5	283	229	280
NO_2	264.5	_	_	_	_
NH_2	284	250	310	248	327
OH	255	236.5	296	237	302

Table 4.1 [3] Literature values for wavelengths absorbed, indicating the shifting of the primary and secondary bands

The values listed in Table 4.1 refer to data obtained for the wavelengths absorbed for the benzoic acids (non-complexed) in solution. These values differ from

the results obtained in this study, mainly due to the fact that the data for these complexes was obtained in the solid state.

4.6 SOLVENT EFFECTS

The shifting of peaks that is caused by the effects of particular solvents is most prominent when in the case of benzene, the added substituents are polar, e.g. OH group. Notable shifting can also take place due to solute – solvent hydrogen bonding[1].

Although the complexes that were synthesized were analysed in the solid state and hence no solvents effects were involved, the general shifts and trends are similar to those that occur in the liquid state. Yet it is important to remember that solid and liquid state values will most certainly be different in terms of the specific amounts of shifting that complexes undergo due to the added substituent.

4.7 DISUBSTITUTED BENZENE DERIVATIVES

Depending on the electronic nature of the substituents and their positioning relative to each other on the benzene ring, the degree of shifting differs. i.e. in multi-substituted benzene derivatives the position of the electronic transitions depends on the relative position of the substituents on the ring [4].

If both the substituted groups are electron withdrawing in nature and are para to each other (4-nitro complex), the primary band will shift to an approximate value of 268 nm while the secondary band will remain unshifted.

If both substituents are para to each other but one group is electron withdrawing while the other is donating (all the other para complexes), then the shift of the primary band is greater than the sum of the shift brought about by the individual groups.

The final permutation which incorporates the remainder of the complexes is if both groups are ortho or meta to each other. In this case the shift of the primary band is equal to the sum of the shifts of the individual groups [1].

4.8 UV SPECTRA OBTAINED FROM COMPLEXES

All the complexes show a bathochromic or red shift of the two expected bands – the primary and secondary bands and are shown in Figs. 4.4 – 4.22.

The primary band has shifted to with in the range of 223 nm - 253 nm and the secondary band has shifted to with in the range of 274 nm - 307 nm . The shifts that are seen in the solid state are slightly different to those quoted in the literature for the liquid state.

All complexes analysed were found to be closely related in terms of the degree of shifting. This is further proof of the isostructural nature of the complexes.

The absorbance values of the peaks in all the complexes are also relatively similar. However, the 3-nitro and 3-bromo complexes show a noticeable hyperchromic effect and the 2-chloro and benzoate complexes show a definite hypochromic effect relative to the other complexes.This is most likely due to the fact that absorbance unlike wavelength is related to the concentration of sample analysed.

4.9 CONCLUSION

Prominent shifting of the bands are observed in all the complexes synthesized, relative to the bands observed for uncomplexed benzoic acids. However, the shifting may also, in part, be due to the presence of hydrogen bonding which from the results of the other analytical techniques is known to exist with in the complexes. As there are no extra bands present in the spectra, one can rule out the possibility that charge transfer reactions are occurring.

Thus,

- Substitution was confirmed on the ortho, meta and para positions.
- No clear trend could be observed reflecting the electronic characteristics of substitution, i.e. electron donating or electron withdrawing properties.
- Complexation of benzoic acids shows clear bathochromic shifts for both primary and secondary bands, for all complexes in this study.

4.10 REFERENCES

CHAPTER 4

1. D. L. Pavia, G. M. Lampman, G. S. Kritz, Introduction to Spectroscopy, A guide for students of organic chemistry, 2nd ed., 267-293
2. C. N. R. Rao, Ultraviolet and Visible Spectroscopy, 2nd ed., Butterworths, London, 1967, Chapter 11
3. C. N. R. Rao, Ultraviolet and Visible Spectroscopy, 2nd ed., Butterworths, London, 1967, Chapter 5
4. Prof. Dr. H-H Perkampus, Benzene and Benzene Derivatives-Introduction Institute of Physical Chemistry, Dusseldorf University, pages 2-6
5. www.wooster.edu/chemistry/is/brubaker/uv/uv_spectrum

4.11 WAVELENGTH AND ABSORBANCE AS WELL AS SPECTRA OF ALL THE COMPLEXES

COMPLEX	WAVELENGTH (nm)		ABSORBANCE (log ε)	
2-amino	244	280	1.907	1.737
3-amino	238	277	2.128	1.945
4-amino	247	298	2.290	2.044
2-nitro	250	298	2.666	2.523
3-nitro	244	307	3.391	3.502
4-nitro	250	298	2.405	2.348
2-fluoro	250	298	2.430	2.226
3-fluoro	247	295	2.697	2.781
4-fluoro	250	298	2.084	1.962
2-bromo	247	277	2.140	1.874
3-bromo	244	301	3.389	3.499
4-bromo	250	298	2.750	2.710
2-chloro	223	298	1.725	1.270
3-chloro	250	298	2.841	2.834
4-chloro	247	295	2.436	2.102
2-methyl	250	295	2.776	2.560
3-methyl	247	298	2.654	2.596
4-methyl	247	298	2.403	2.445
4-methoxy	250	298	2.604	2.482
2-hydroxy	253	298	2.809	2.463
Benzoate	238	274	1.725	1.574

Table 4.2 Wavelength and absorbance value for the complexes

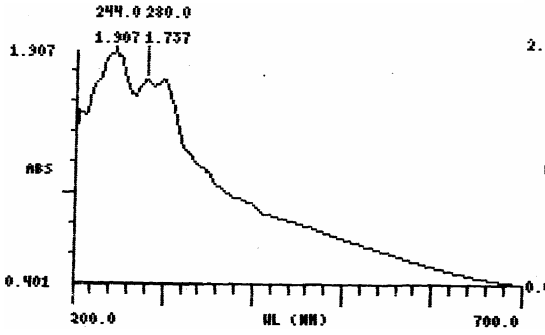

Fig. 4.4 UV spectrum of the 2-amino complex

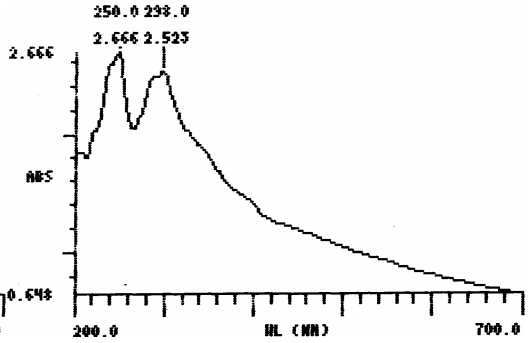

Fig. 4.7 UV spectrum of the 2-nitro complex

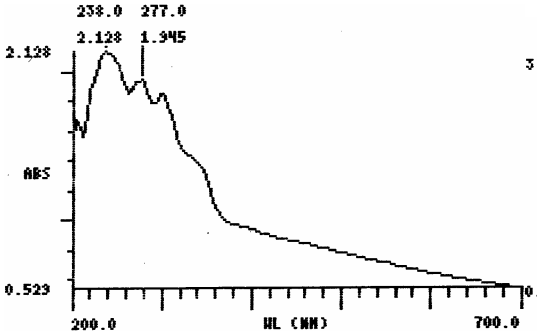

Fig. 4.5 UV spectrum of the 3-amino complex

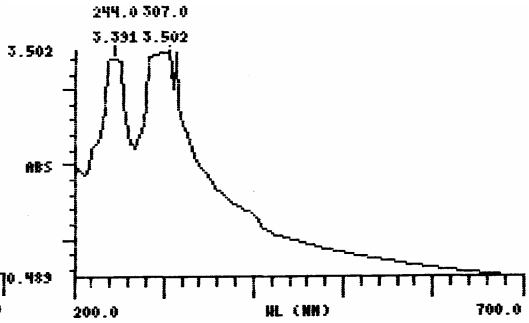

Fig. 4.8 UV spectrum of the 3-nitro complex

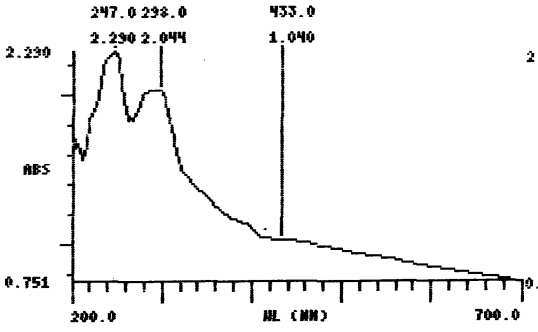

Fig. 4.6 UV spectum of the 4-amino complex

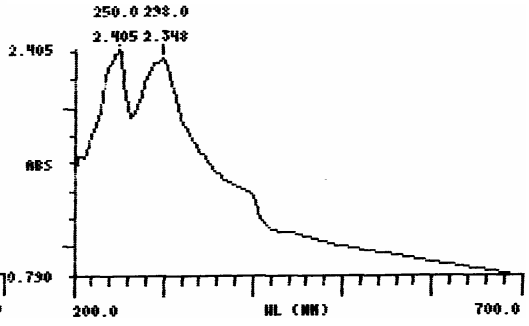

Fig. 4.9 UV spectrum of the 4-nitro complex

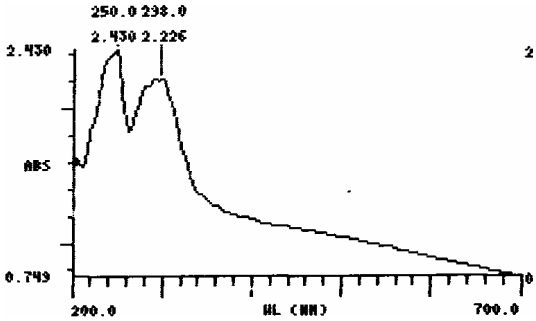

Fig. 4.10 UV spectrum of the 2-fluoro complex

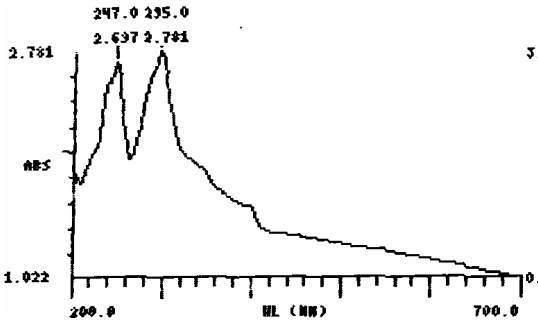

Fig. 4.11 UV spectrum of the 3-fluoro complex

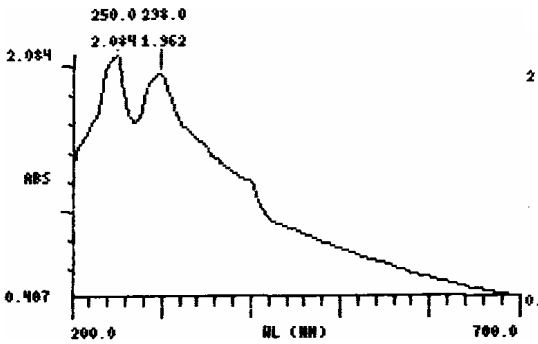

Fig. 4.12 UV spectrum of the 4-fluoro complex

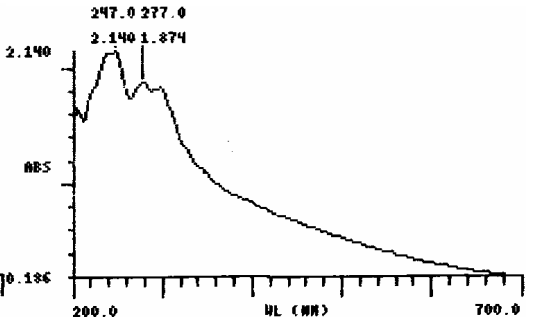

Fig. 4.13 UV spectrum of the 2-bromo complex

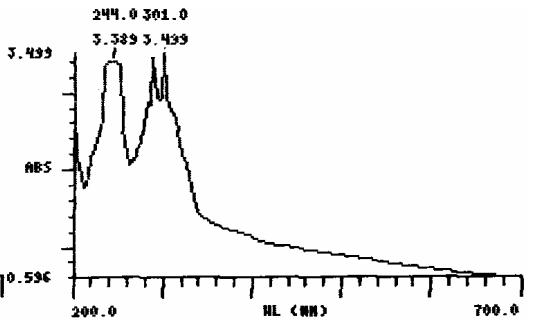

Fig. 4.14 UV spectrum of the 3-bromo complex

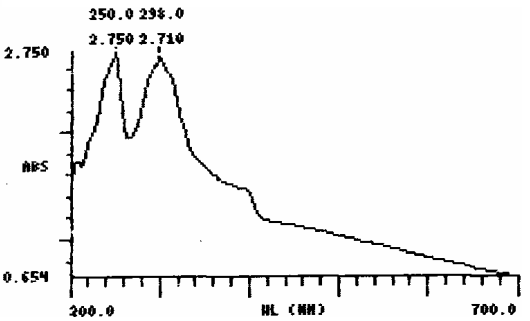

Fig. 4.15 UV spectrum of the 4-bromo complex

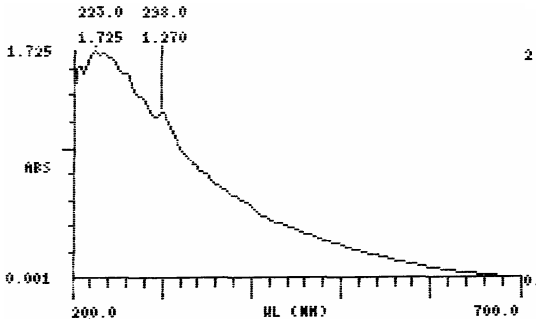

Fig. 4.16 UV spectrum of the 2-chloro complex

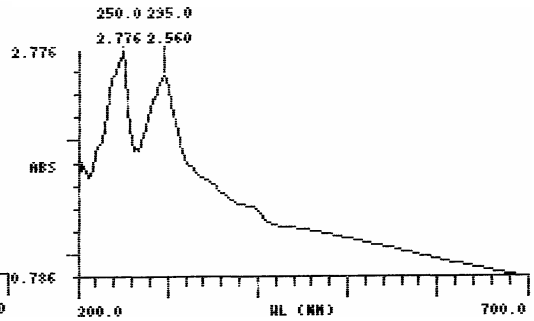

Fig. 4.19 UV spectrum of the 2-methyl complex

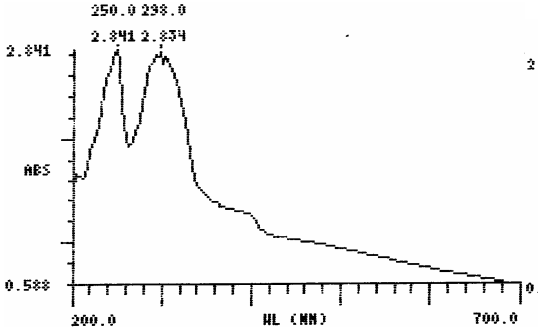

Fig. 4.17 UV spectrum of the 3-chloro complex

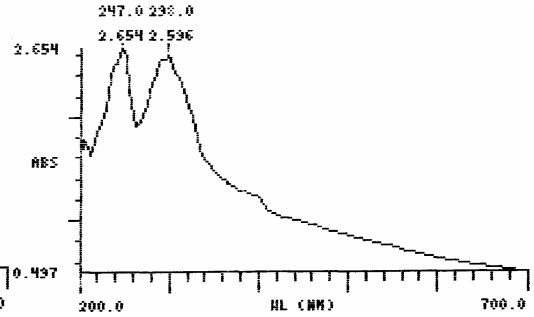

Fig. 4.20 UV spectrum of the 3-methyl complex

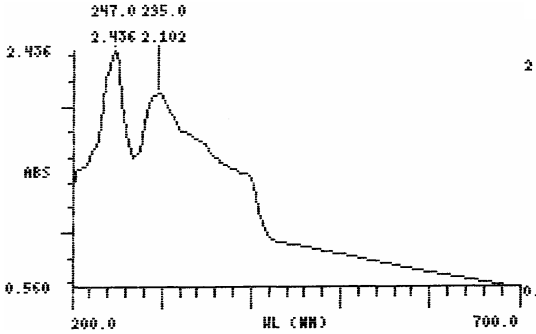

Fig. 4.18 UV spectrum of the 4-chloro complex

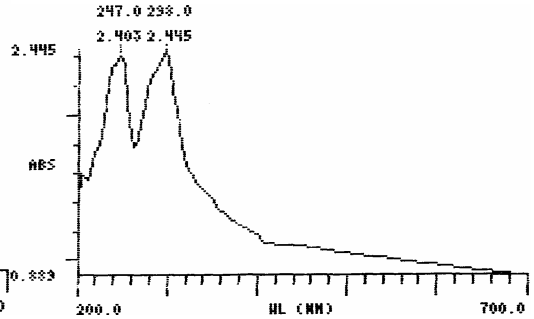

Fig. 4.21 UV spectrum of the 4-methyl complex

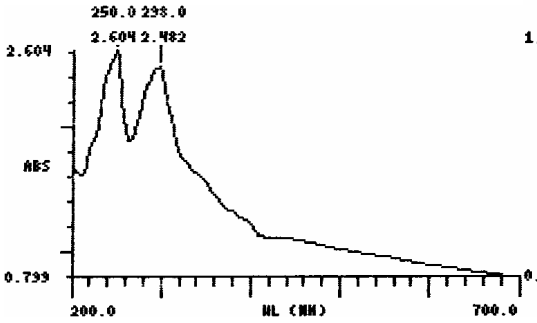

Fig. 4.22 UV spectrum of the 4-methoxy complex

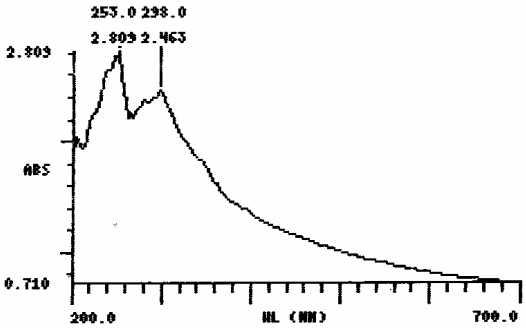

Fig. 4.23 UV spectrum of the 2-hydroxy complex

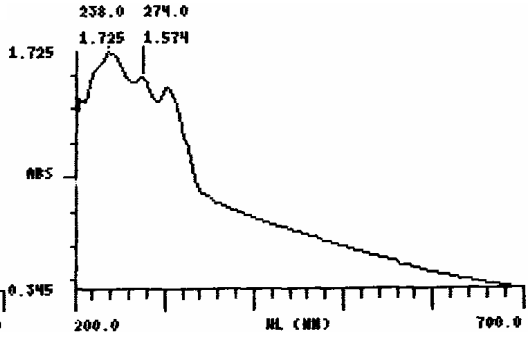

Fig. 4.24 UV spectrum of the benzoate complex

CHAPTER 5

NMR SPECTROSCOPY

5.1 INTRODUCTION

As it is known, Nuclear Magnetic Resonance (NMR) spectroscopy can be incorporated and used in a wide variety of situations and for a wide variety of purposes. In terms of the study at hand there were three main purposes. Firstly, as a means of additional proof that the complexes did in fact form, secondly to study the stoichiometry of the complexes and hence prove that the thiourea and thallium were in a 4:1 ratio to each other, and
thirdly to note any shifting of peaks relative to the values reported in the literature which, would be an indication of hydrogen bonding.
With in the study both proton NMR and COSY NMR will be employed to ensure the correct assignments of the peaks.

5.2 GROUP 13 METALS AND NMR

Before discussing the NMR spectra of the complexes, of interest is how group 13, which of course includes thallium, and NMR can be related to biologically relevant aspects as well as those chemical aspects which include the results and interpretation to come.

The group 13 metals are not considered essential to life, however, they are NMR-active nuclides which can be used in the NMR analysis of biologically relevant systems [1]. For example, there are links between aluminium and Alzheimer's disease. Gallium, although possessing no real metabolic role, is present in human tissue. Thallium of course is of a poisonous nature due to the thallium ions having the ability to mimic alkali metal ions present in the body such as K^+. However, this ability also opens up the opportunity for Tl^+ to be used as a probe in biological system studies of K^+ and Na^+. Protein systems also take advantage of the ability of ^{205}Tl NMR to investigate metals in their particular binding sites [1].

In terms of these metals and their NMR properties, they are all quadropolar

(spin I > 1) except for thallium which has spin I = ½, which in general allows for good structure information to be obtained. Although they are not of a quadropolar nature, ^{203}Tl and ^{205}Tl do possess high receptivities [1].

5.3 ANALYSIS OF COMPLEXES

In all cases the crystalline material obtained (recrystallised) were used. The four complexes which produced single crystals as well as 2-hydroxy, 3-bromo and 4-chloro complexes (a representation of the remaining complexes) were run on the Bruker ARX 300 at 300.13 Mhz. The NMR spectra were recorded at 303 K unless stated otherwise and were referenced relative to the solvent used.

The solvent used for the four single crystal complexes was deuterated dimethyl sulphoxide (DMSO-d_6), while the 2-hydroxy, 3-bromo and 4-chloro complexes were dissolved in deuteriunoxide (D_2O), as these could not be dissolved satisfactorily in DMSO.

The complexes were analysed using proton NMR due to the significant number of different hydrogens in the complexes.

Before discussing the individual spectra, a reference diagram is shown below which has a labelling pattern which will be continually referred to in the following section.

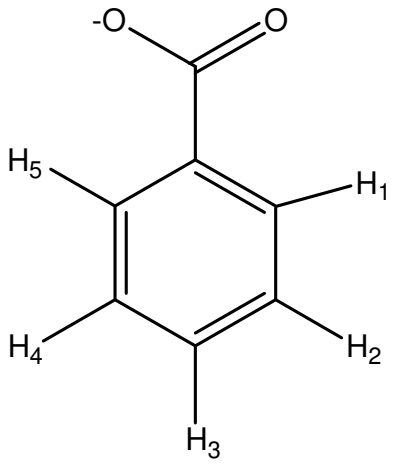

Fig. 5.1 Reference diagram showing the individual hydrogen numbers

It should also be noted that the discussion to follow is centred on the peaks relating to the hydrogen atoms attached to the benzene rings of the complexes, as the splitting patterns vary depending on the position of the substituent.

However, the spectra also show three other main peaks which are at constant positions in all the spectra, as could be expected. The first is the peak relating to the hydrogens of the thiourea molecules. It is a broad singlet peak (hydrogen bonded) at a chemical shift of $\delta = 7.04$ ppm. This is consistent with the literature value which is given at 7.05 ppm [2]. At a chemical shift of $\delta = 3.3$ ppm there is another peak which is present in all the spectra and is consistently at the same value. This broad peak relates to excess water from the synthesis which remained even after the drying of the complexes. Although it must be mentioned that every effort was made to dry the samples as full as possible under high vacuum to remove the majority of the water. Literature also gives a chemical shift value of $\delta = 3.3$ ppm [3].

The third and final consistently present peak is that of the solvent, deuterated DMSO-d_6 at chemical shift of $\delta = 2.49$ ppm [4].

5.4 ANALYSIS OF THE FOUR SINGLE CRYSTAL COMPLEXES

5.4.1 3-AMINO COMPLEX

In this particular spectrum the expected peaks are present, however, the benzoic hydrogens and the thiourea hydrogens resonance occur in the same region and so there is a definite overlap. In order to see the exact splitting pattern of the benzoic hydrogens a D_2O exchange was carried out. There is very little shifting of the peaks in the D_2O exchange spectrum compared to the DMSO spectrum. The chemical shift values given are from the D_2O exchange.

A multiplet with a chemical shift of $\delta = 7.07$ pm which represents H4 is visible, however, the splitting pattern is difficult to identify.

Slightly upfield is a doublet of triplets corresponding to H5 with a chemical shift of $\delta = 7.03$ pm. The coupling constants are as follows:

J (5, 1) 1.29 Hz J (5, 3) 1.29 Hz J (5, 4) 7.71 Hz

H1 is found at a chemical shift of δ = 6.95 ppm and is a triplet of doublets with the following coupling constants:

J (1, 3) 7.53 Hz J (1, 4) 0.39 Hz J (1, 5) 7.53 Hz

At a chemical shift of δ = 6.57 ppm H3 is the final multiplet which is a doublet of doublets of doublets and the 8 peaks are clearly visible. The coupling constants are as follows:

J (3,1) 2.37 Hz J (3, 4) 7.71 Hz J (3, 5) 1.29 Hz

When compared to the literature values of chemical shifts (H4, δ = 7.20 ppm, H5, δ = 7.17 ppm, H1, δ = 7.01 ppm, H3, δ = 6.74 ppm) [5] it is seen that the experimental values for the hydrogen atoms are slightly lower and could be an indication of hydrogen bonding.

A singlet at a chemical shift of 4.0 ppm is also seen which accounts for the hydrogens associated with the NH_2 substituent. It was not seen when the D_2O exchange was run as the hydrogens exchange.

An exact stoichiometric ratio between the thiourea hydrogens and the benzoic hydrogens can not be given as there is a certain amount of overlap, making the use of integration values meaningless.

A two-dimensional (1H-1H) homonuclear chemical shift correlation (COSY) experiment of 3-aminobenzoic acid was run to show the couplings.

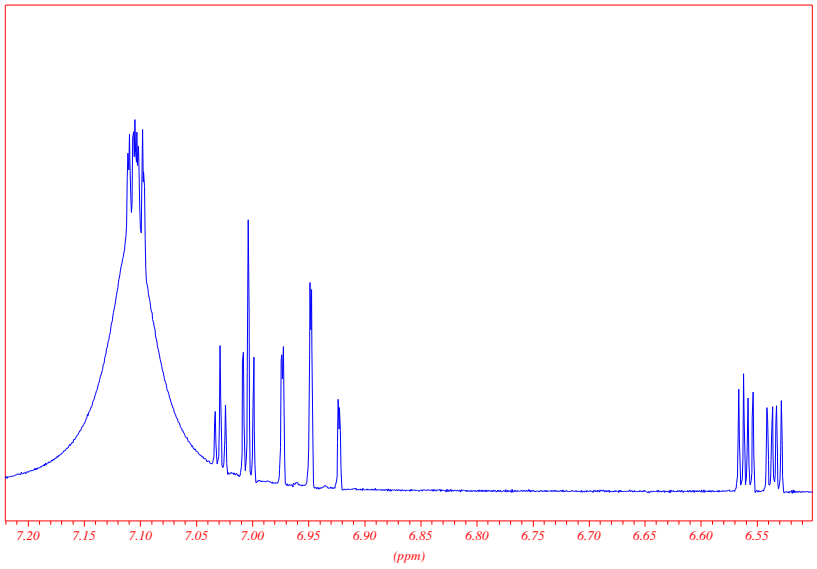

Fig. 5.2 NMR spectrum of the 3-amino complex dissolved in DMSO

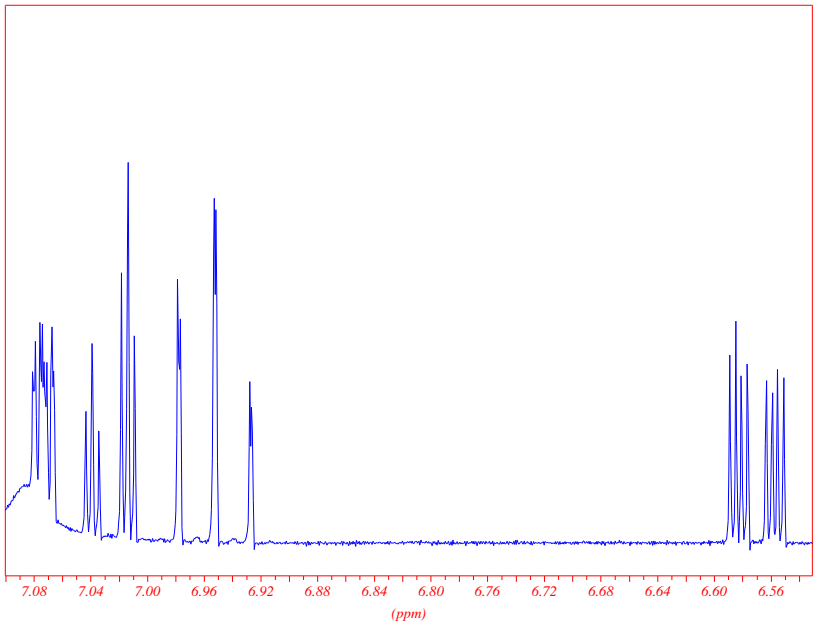

Fig. 5.3 NMR spectrum of the D_2O exchange carried out on the 3-amino complex

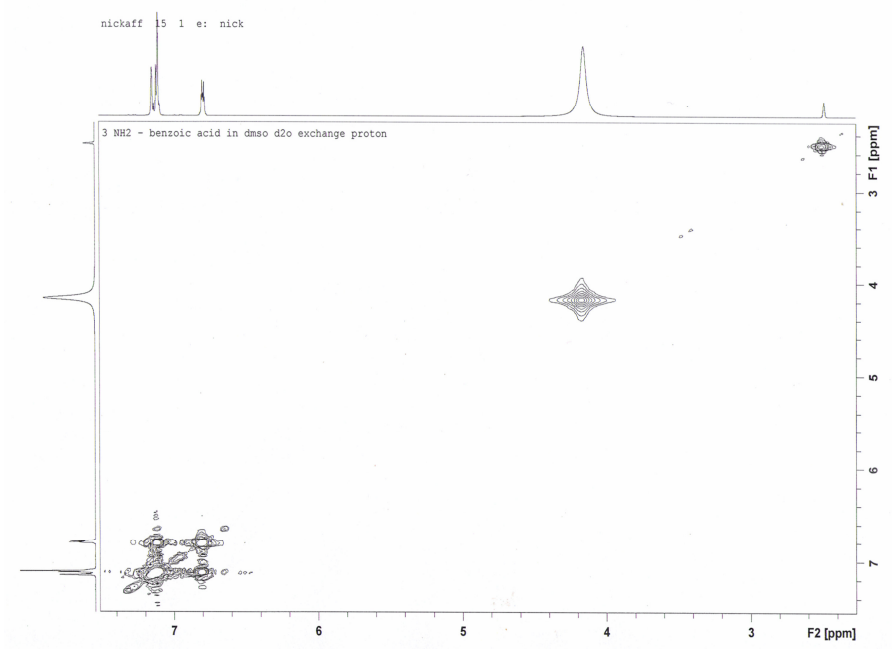

Fig. 5.4 COSY NMR of 3-aminobenzoic acid

5.4.2 2-FLUORO COMPLEX

As with the 3-amino complex, a D_2O exchange was necessary to identify the benzoic hydrogens. The spin = ½ of the fluorine can be seen to influence the spectrum to such an extent that the peak determination is not a simple matter. There is very little shifting of the peaks in the D_2O exchange spectrum compared to the DMSO spectrum. The chemical shift values given are from the D_2O exchange.

At a chemical shift of δ = 7.50 ppm H5 is the most deshielded hydrogen. It can be described as a triplet of doublets, however, coupling constants are difficult to assign.

The next multiplet at a chemical shift of δ = 7.28 ppm is H3. One would expect a doublet of doublets of doublets but the influence of the fluorine means that multiplet identification and coupling constants are not able to be determined.

Upfield to the H3 is a multiplet incorporating H4 and H2. The chemical shift of the multiplet is δ = 7.04 ppm. Unfortunately due to the influence of the fluorine it is not possible to determine exact chemical shift values for the respective hydrogens, nor obtain coupling constants.

The stoichiometric ratio is unable to be obtained as there is a large amount of overlap between the thiourea hydrogens and the benzoic hydrogens.

Note that a ^{19}F NMR was also run on the complex to prove the presence of fluorine as well as a COSY NMR of 2-fluorobenzoic acid to show the coupling.

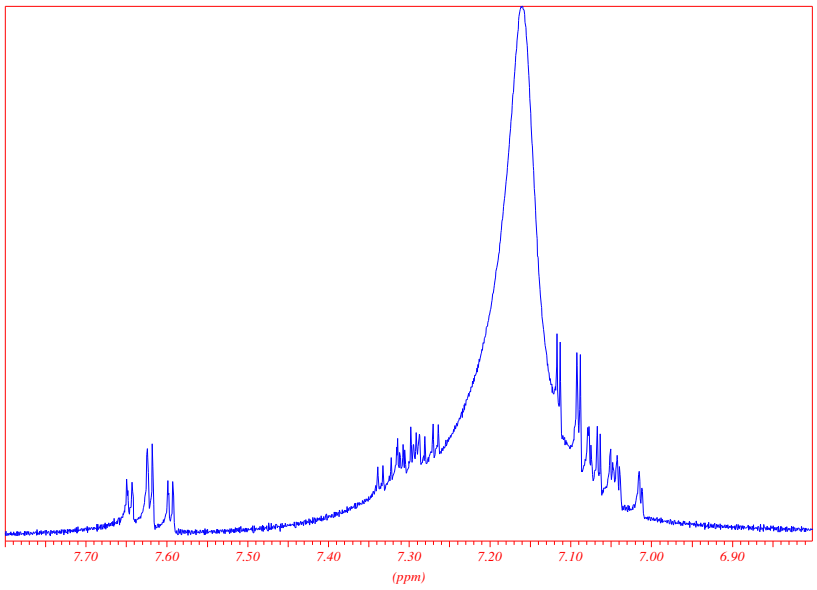

Fig. 5.5 NMR spectrum of the 2-fluoro complex dissolved in DMSO

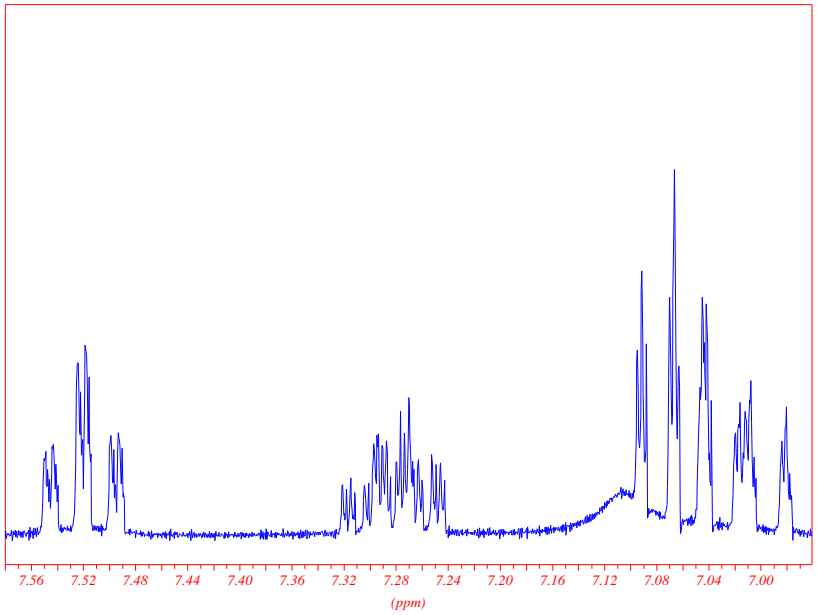

Fig. 5.6 **NMR spectrum of the D_2O exchange carried out on the 2-fluoro complex**

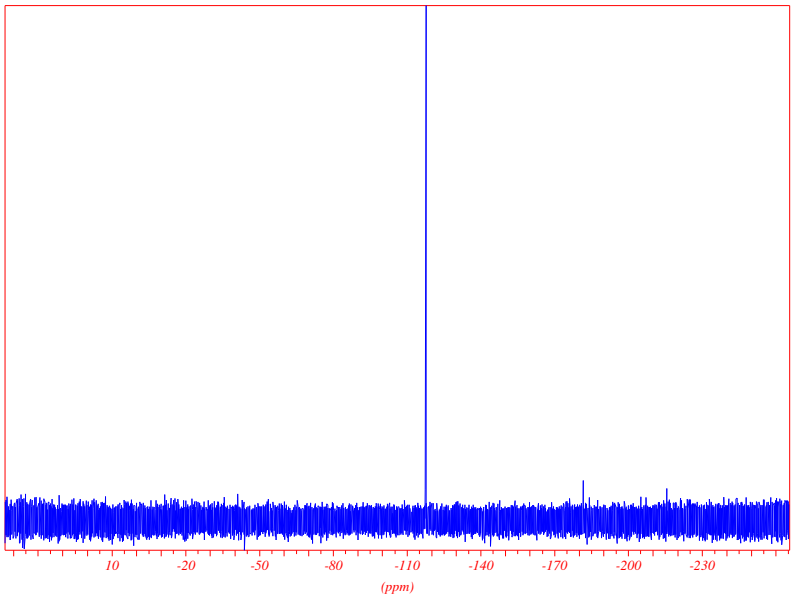

Fig. 5.7 **^{19}F NMR spectrum of the 2-fluoro complex**

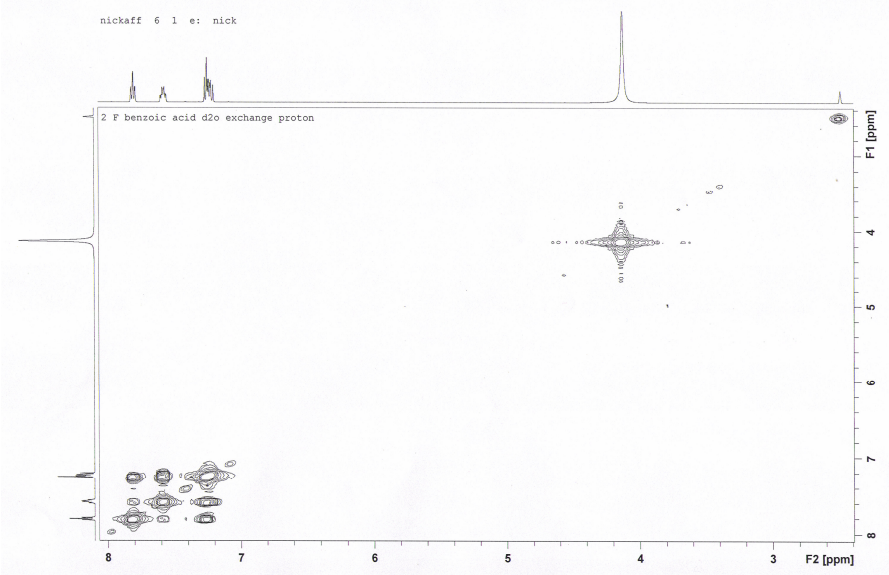

Fig. 5.8 COSY NMR of 2-fluorobenzoic acid

5.4.3 3-FLUORO COMPLEX

Once again the spin = ½ of the fluorine has an effect on the spectrum.

The H5 is represented by a doublet of triplets. The chemical shift is at a value of δ = 7.66 ppm. The fact that this hydrogen is represented by the peaks positioned the furthest downfield is to be expected as it is deshielded the most by the carboxylate group (COO^-).

The coupling constants are as follows,

J (5, 4) 4.59 Hz J (5, 3) 0.63 Hz J (5, 1) 0.66 Hz

At a chemical shift of 7.52 ppm is the second most deshielded hydrogen, H1. This hydrogen couples with the H5, the H3 as well as the fluorine atom. The eight expected peaks of the doublet of doublets of doublets are clearly identifiable.

Coupling constants are as follows,

J (1, 3) 1.74 Hz J (1, 4) 6.06 Hz J (1, 5) 0.84 Hz

The H4 is found at a chemical shift of δ = 7.36 ppm. The splitting pattern should be the same as that for the H1, doublet of doublets of doublets
(8 peaks), however, a certain amount of overlap has occurred and some of the peaks are not visible. This makes it difficult to determine coupling constants.

The fourth and final multiplet in this spectrum is that relating to the H3. In theory, due to its position on the ring, this hydrogen should couple with H5, H4, H1 as well as the fluorine. Therefore what should be seen is a doublet of doublets of doublets of doublets (12 peaks). Unfortunately no information can be obtained as this multiplet occurs in the same chemical shift region as the thiourea hydrogens and is involved in a large amount of overlapping. A D_2O exchange was carried out and the multiplet is indeed visible, however, the peaks are very broad and shifted upfield.

When compared to the literature values [5] of chemical shifts it is seen that the experimental values for the hydrogens are slightly lower. This may well be an indication of hydrogen bonding.

The stoichiometric ratio of the thiourea hydrogens to the benzoic hydrogens is 4:1, based on the integration values.

Note that a ^{19}F NMR was also run on the complex to prove the presence of fluorine as well as a COSY NMR of 3-fluorobenzoic acid to show the coupling.

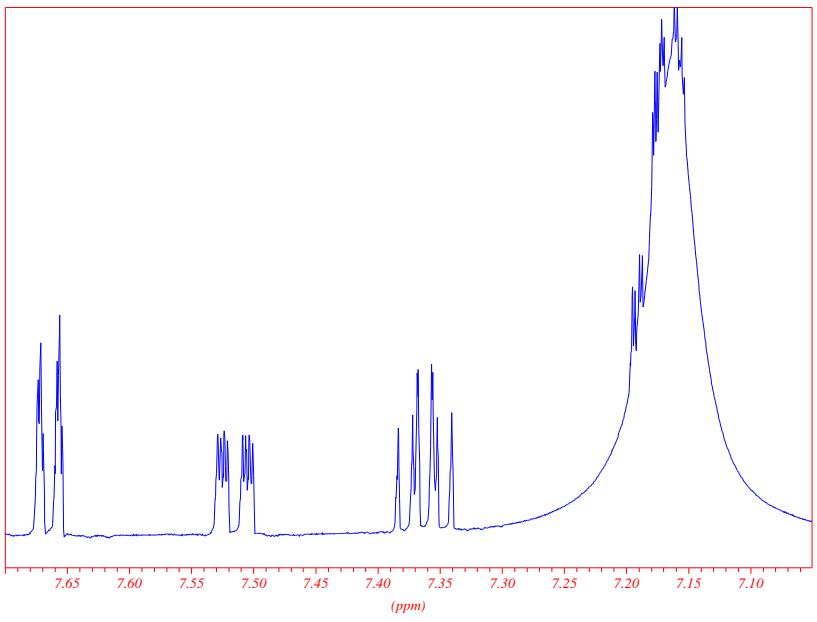

Fig. 5.9 NMR spectrum of the 3-fluoro complex dissolved in DMSO

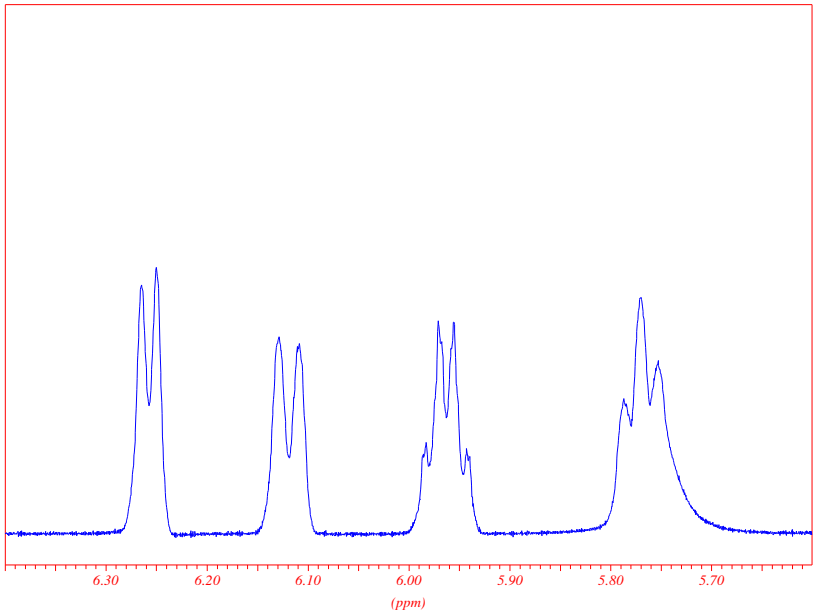

Fig. 5.10 **NMR spectrum of the D_2O exchange carried out on the 3-fluoro complex**

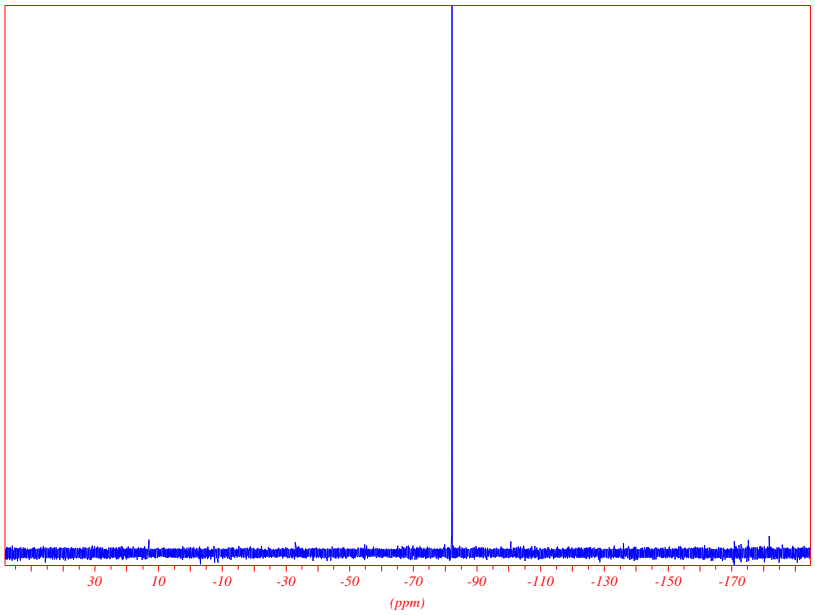

Fig. 5.11 **^{19}F NMR spectrum of the 3-fluoro complex**

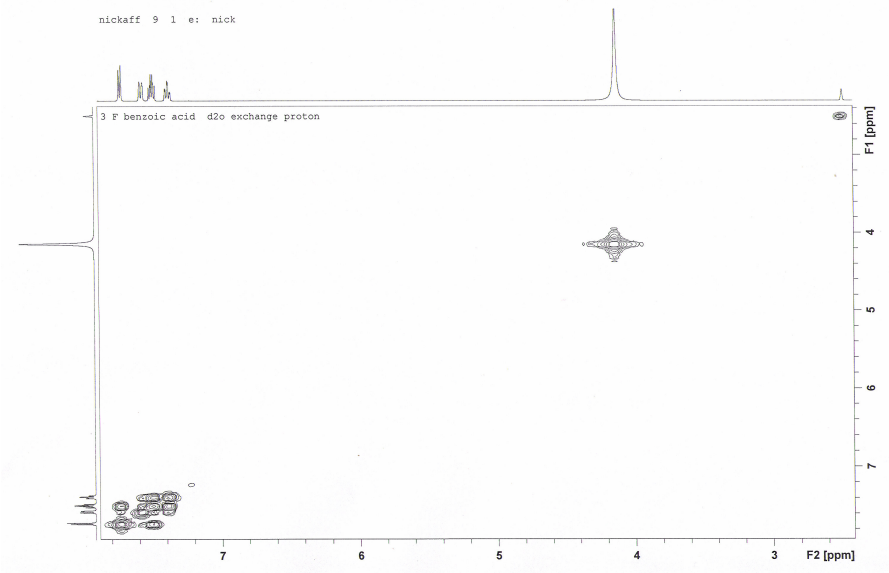

Fig. 5.12 COSY NMR of 3-fluorobenzoic acid

5.4.4 BENZOATE COMPLEX

Unlike the 3-amino and 2-fluoro complexes, D_2O exchange was not required to analyse the benzoic hydrogens.

As there is an element of symmetry to this complex two doublets should be seen representing H1, H5 and H2, H4.

The H1, H5 doublet can be seen at a chemical shift of δ = 7.82 ppm. However, further upfield the expected second doublet of H2, H4 at a chemical shift of δ = 7.28 ppm is not clearly identifiable due to overlap.

H3 has a chemical shift of δ = 7.32 ppm and should be a doublet of doublets but once again the effect of overlap has affected the ability to identify coupling constants.

Shifting of the H2, H3 and H4 indicate the possibility of hydrogen bonding.

The stoichiometric ratio of the thiourea hydrogens to the benzoic hydrogens is 4:1, based on the integration values.

A COSY NMR of benzoic acid was run to show the coupling.

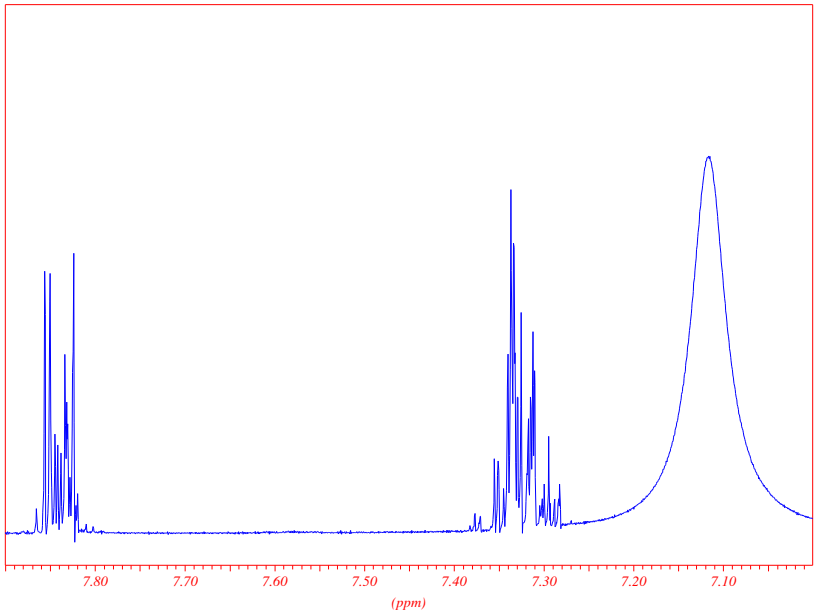

Fig. 5.13 **NMR spectrum of the benzoate complex dissolved in DMSO**

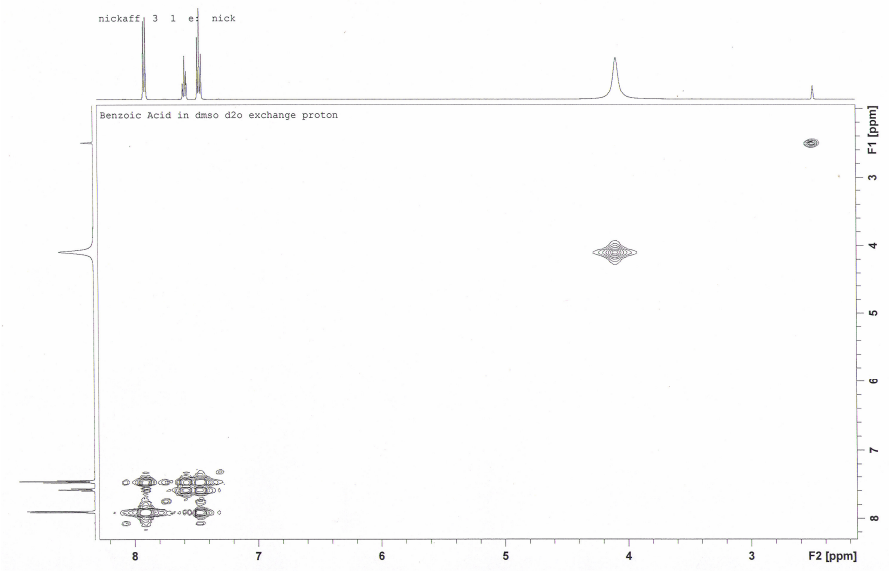

Fig. 5.14 **COSY NMR of benzoic acid**

5.5 ANALYSIS OF THE 2-HYDROXY, 3-BROMO, 4-CHLORO COMPLEXES

As has already been mentioned these three non single crystal quality complexes were analysed as a representation of all the other complexes to ensure the benzoic hydrogens were present.

The complexes were dissolved in D_2O but as they only remained soluble at 60˚C high temperature (60˚C) NMR was run. As a consequence the peaks in all three cases were very broad and therefore coupling constants were unable to be obtained. The chemical shifts were available but the increase in temperature shifted the values relative to the literature values [5].

COMPLEX	ACTUAL δ VALUES (ppm)	UNCOMPLEXED LITERATURE δ VALUES [5] (ppm)	Assignments
2-hydroxy	8.04	7.64	H5
	7.67	7.37	H3
	7.17 (merging)	7.01, 6.92	H4, H2
3-bromo	8.31	7.98	H1
	8.12	7.75	H5
	7.98	7.71	H3
	7.67	7.34	H4
4-chloro	8.13	7.75	H1, H5
	7.76	7.46	H2, H4

Table 5.1 **Table showing the actual and literature chemical shift values of the 2-hydroxy, 3-bromo and 4-chloro complexes**

The thiourea peak in each spectrum is not observed as the thiourea hydrogens exchange with the D_2O. This is also the reason why the hydroxy hydrogen is not seen.

To ensure it was in fact due to the temperature that the chemical shifts increased, the 3-bromo complex without thiourea was analysed as it dissolved readily in D_2O at room temperature. As expected the results showed chemical shift values similar to the literature [5].

COMPLEX	**ACTUAL δ VALUES**	**UNCOMPLEXED LITERATURE δ VALUES**	
	(ppm)	**(ppm)**	**Assignments**
3-bromo (no TU)	7.90	7.98	H1
	7.73	7.75	H5
	7.61	7.71	H3
	7.30	7.34	H4

Table 5.2 **Table showing the actual and literature chemical shift values for the 3-bromo complex without thiourea**

Although the peaks were more split than the 3-bromo complex with thiourea, there was still a large degree of merging which restricted the ability to obtain coupling constants.

5.6 CONCLUSION

The NMR results of all the complexes analysed show the presence of the benzoic hydrogens in the correct splitting patterns as well as the thiourea hydrogens and in the case of the 3-amino complex the NH_2 substituent hydrogens.

With respect to the four single crystal complexes the shifting of the peaks relative to the literature values was small, however, the fact that shifting did occur even in solution is further evidence of some hydrogen bonding, albeit in solution.

The stoichiometry of the benzoate and 3-fluoro complexes hydrogens relative to the thiourea hydrogens was 4:1 which was to be expected. The 2-fluoro and 3-amino complexes were assumed to have the same ratio but as was stated earlier in the chapter the ratios could not be identified due to overlapping of the thiourea hydrogens and the benzoic hydrogens, however, the correct 4:1 ratio was proved in the crystallographic study.

Overall, NMR provided this study with good results, results which further confirm that complexation of all the samples had taken place, as seen by the positioning and shifting of peaks.

5.7 REFERENCES

CHAPTER 5

1. J. P. Andre and H. R. Macke, Journal of Inorganic Biochemistry, 2003, **97**, Issue 4, 1, 2, 3, 4
2. S. Ahmad, A. A. Isab, W. Ashraf, Inorganic Chemistry Communications, 2002, **5**, Issue 10, 3
3. www.chem.ucla.edu/~webspectra/Notesonsolvents
4. www.eclipse.net/~numare/deutsolv
5. C. S. Chemdraw, Chemical Structure Drawing Standard, 1985-2000

University of Pretoria etd – Brennan, NF (2006)

CHAPTER 6
THERMAL ANALYSIS AND MASS SPECTROMETRY

6.1 INTRODUCTION

Thermal analysis in its most general terms can be defined as a group of techniques in which a physical change of a substance is measured as a function of temperature, while the substance is subjected to a controlled temperature change [1].

All the complexes that were synthesized underwent two specific types of thermal analysis, Thermogravimetry (TG) measurements and Differential Scanning Calorimetry (DSC) measurements. TG simply measures the amount of weight lost by the sample over a controlled temperature range, while DSC is concerned with the energy changes occurring in the sample, i.e. whether the reaction in question is endothermic or exothermic ($0 > dH/dt > 0$) [1].

It is important to note that when using TG as a means of analysis, there are potentially a number of sources of error which one must be aware of. These include measurement of weight by the balance, random fluctuations of the balance mechanism and reaction between sample and container or atmosphere, to name but a few. Most of the sources of error can be corrected while others are interrelated and cannot be assessed separately [1].

DSC is also open to various sources of error. These are normally related to the sample and to the instrument itself. Sample factors include, amount of sample, particle size and sample packing, while experimental factors include, heating rate, sample holder materials and atmosphere surrounding sample [1].

DSC focuses on the energy changes that take place, peaks such as the exothermic and endothermic peaks, as well as peaks associated with other types of thermal events are of importance. Glass transition is an indication that the structure has undergone a transition from a rigid to a flexible structure. Crystallisation is a peak which indicates that further crystallisation or recrystallisation has occurred within the complex due to the heating of the sample. This is observed as an exotherm preceding the melting endotherm [1].

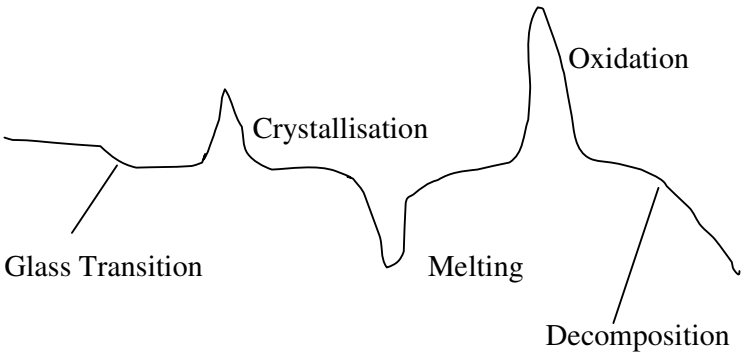

Fig. 6.1 [1] **Important DSC peaks**

It was hoped that, due to the variety of the type of substituents in the benzoate anion, it may be possible to distinguish thermal events as a function of the electronic properties or size of the substituent group. This study would also make it possible to get an indication of the relative energy of dissociation or decomposition of the different groups in the complex. Should these complexes crystallise in more than one crystal system and/or space group, it could be expected that a variety of different enthalpy values for say the release of thiourea could be expected.

6.2 APPLICATIONS OF THERMOGRAVIMETRY (TG) [2]

As a matter of interest, TG has many applications other than for the analysis used in this project. These include:

- Thermal Stability
- Kinetic Studies
- Material Characterisation
- Corrosion Studies
- Simulation of industrial processes
- Compositional Analysis

6.3 EXPERIMENTAL

TG – DSC analysis was carried out on the STA 409 EP NETZCH and TA control system NETZCH with an acquisition rate of 1.5 points/K and a heating rate of 5 K/min in platinum crucibles which were open to air, as some test runs at heating rates of 1, 2, 3, 5 K/min yielded identical results. All complexes were heated to a temperature of 1200 ˚C, to ensure complete decompostion of the complexes.

The TG % mass loss ranges and the actual mass losses were obtained using the standard thermal software. It is known that the software supplied with the equipment has some minor inaccuracies, reflected by the fact that some samples gave a mass loss of more than 100 %. Apart from instrumentation and software problems, the fact that gas flow control during the experiment was done by controlling the valve on the gas bottle could have resulted in some variations in measurements. The presence of water was ruled out as no corresponding peak in the TG was observed at temperatures around 100°C. It should also be noted that the sample which gave one of the highest total mass losses (over 100%) was the 2-fluoro complex which has a known crystal structure described in chapter 2, therefore the inaccuracies are not related to the sample.

6.4 DISCUSSION OF THE RESULTS OF THE THERMAL STUDIES OF THE COMPLEXES

6.4.1 ENDOTHERMIC AND EXOTHERMIC TRANSITIONS

These are the most important transitions recorded by DSC techniques. Typical endothermic effects include melting, boiling and evaporation which require energy to break solid state forces. Exothermic effects include freezing as it involves the release of thermal energy as the sample crystallises from the melt [3]. In terms of the analysis at hand, the melting of the complex is of importance.

6.5 TRENDS IN THERMAL RESULTS

The thermal decomposition of all the complexes is a multi-stage process. The endothermic and exothermic peaks that are seen in the DSC spectra, for the most part, occur at the same temperatures with corresponding mass loss in the TG spectra. Those peaks in the DSC spectrum which are not accompanied by a corresponding peak in the TG spectrum normally, indicate a phase change [4].

Overall the thermographs of all the complexes are relatively similar as is expected due to the similarities in the nature of the complexes. However, important differences and trends are visible when analysed closely.

6.5.1 DSC

In terms of the DSC results all the complexes except the 2-chloro, 2-methyl and 4-methoxy complexes have endothermic peaks relating to their respective melting points. The majority of the complexes show a general trend of having seven distinct endothermic and exothermic peaks. Their relation to the % mass loss are discussed later.

In the temperature region of approximately 340˚C – 800˚C all the complexes are very similar, showing two exothermic peaks at approximately 350˚C (no mass loss) and 400˚C (mass loss) respectively and two endothermic peaks at approximately 630˚C and 800˚C. The differences in the complexes are between room temperature and just over 200˚C.

Firstly the only four complexes which produced diffraction quality single crystals that were shown to be isostructural (see Chapter 2) plus the 3-bromo complex, show one large endothermic peak at 200˚C + which coincides with their melting points. All of the remaining complexes have three peaks in the region at approximately 150˚C , 170˚C and 200˚C. In all cases the peaks at 170˚C and 200˚C are endothermic peaks while the peak at 150˚C is an endothermic peak in most cases but in the 3-nitro, 3-methyl, 3-chloro and 2-hydroxy it is an exothermic peak. The peaks at 150˚C and 200˚C relate to the thiourea molecules while the peak at 170˚C relates to the melting points. The fact that the thiourea molecules come off at different temperatures can be compared with the three water loss steps from hydrated copper

sulphate where by two water molecules are lost at 65˚C, two more at 90˚C and the final molecule at 220˚C [5].

6.5.2 ENTHALPY VALUES OF THE COMPLEXES

COMPLEX	ENTHALPY (kJ/mol) IN THE REGION RT-200˚C
Tl-3-fluorobenzoate-thiourea	437 *
Tl-2-fluorobenzoate-thiourea	536 *
Tl-3-aminobenzoate-thiourea	419 *
Tl-benzoate-thiourea	492 *
Tl-3-bromobenzoate-thiourea	487
Tl-2-methylbenzoate-thiourea	420
Tl-2-aminobenzoate-thiourea	286
Tl-4-aminobenzoate-thiourea	356
Tl-2-nitrobenzoate-thiourea	Not available
Tl-3-nitrobenzoate-thiourea	Not available
Tl-4-nitrobenzoate-thiourea	118
Tl-4-fluorobenzoate-thiourea	305
Tl-2-bromobenzoate-thiourea	244
Tl-4-bromobenzoate-thiourea	288
Tl-2-chlorobenzoate-thiourea	319
Tl-3-chlorobenzoate-thiourea	295
Tl-4-chlorobenzoate-thiourea	313
Tl-3-methylbenzoate-thiourea	233
Tl-4-methylbenzoate-thiourea	270
Tl-2-hydroxybenzoate-thiourea	267
Tl-4-methoxybenzoate-thiourea	147

Note * denotes single crystal structure obtained

Table 6.1 Enthalpy values for all the complexes.

The enthalpy values were determined from the experimental measurements obtained for thermal events occurring at up to 200°C. This was proven by accurate mass spectroscopy to be associated with the loss of all four thiourea molecules. A standard calibration curve to convert KJ/g to KJ/mole was used.

Table 6.1 above shows that in terms of enthalpy values the complexes fall into two distinct groups, in one group, the four single crystal structures (*) plus the 3-bromo and 2-methyl complexes and in the other group, the remaining complexes. Except for the 2-methyl complex, the higher enthalpy values of the first group can be linked or attributed to the large single endothermic peak at around 200˚C which is indicitive of the four single crystal structures and the 3-bromo complex (see 6.5.1). No clear reason could be ascribed for the relatively high value registered for the 2-methyl complex.

6.5.3 TG

Like the DSC results, the TG results are very similar for all the complexes with a general pattern or trend visible throughout.

By running a thermograph of the 4-amino complex without thiourea it is clear that the endothermic peaks between RT - 200˚C relate to the thiourea mass loss as all the other peaks are identical to the complexes. The single crystal x-ray structure for this compound has been determined (see chapter 2). This result is also substantiated by mass spectroscopy studies in this temperature range, clearly indicating the loss of thiourea.

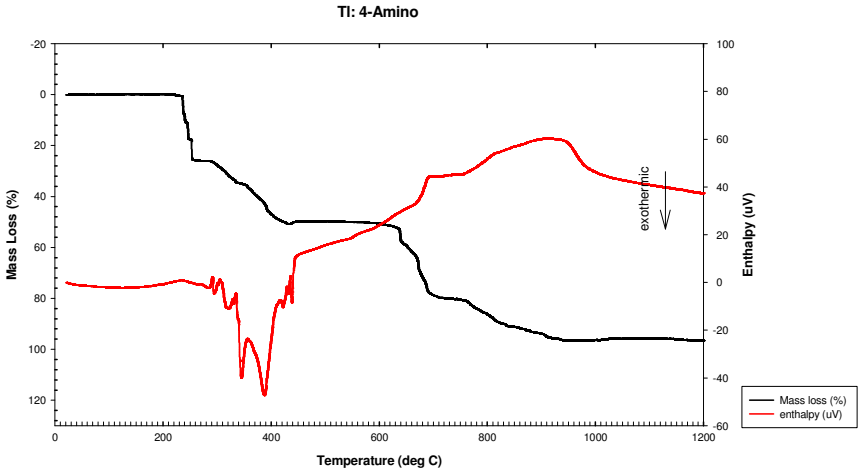

Fig. 6.2 4-amino complex without thiourea

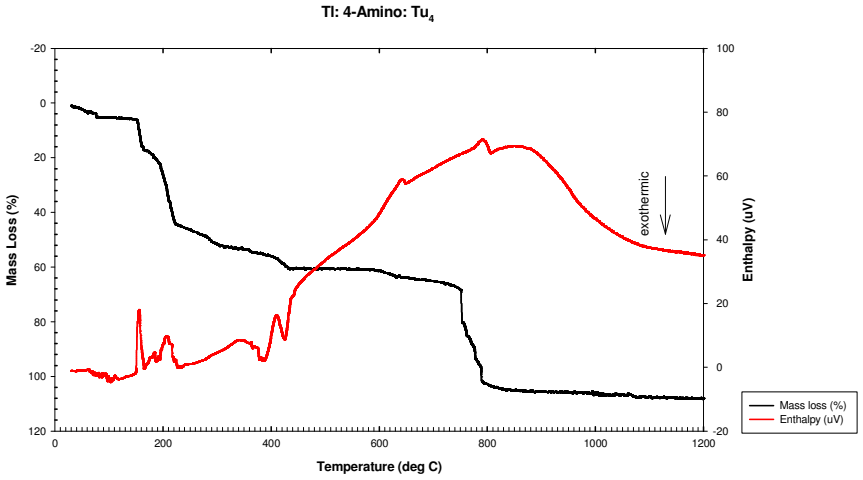

Fig. 6.3 **4-amino complex (with thiourea)**

Further evidence to substantiate that the peaks in the range of RT - 200°C correspond to thiourea is seen in Fig. 6.4 which is a thermogram of pure thiourea.

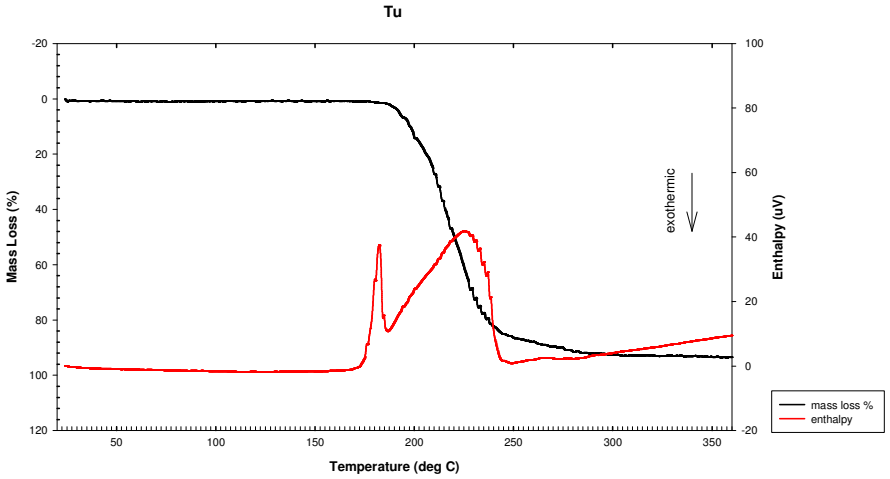

Fig. 6.4 **Pure thiourea**

As with the DSC results, some differences in the TG analysis exist. The TG analysis of 3-amino, 2-fluoro, 3-fluoro benzoates and the unsubstituted benzoate complexes as well as the 3 and 4-bromo complexes appear slightly different to the others. For these six complexes three distinct % mass losses are seen where as the majority of the other complexes have four % mass losses.

The first and largest mass loss coincides with the theoretical mass loss of all four thioureas (~200˚C endothermic peak) and in some cases there also may well be

fragments of the aromatic ring. The second relatively small mass loss of approximately 8 % occurs in the temperature range of between approximately 240˚C and 500˚C and can be correlated to the loss of CO_2 from the complex. Two exceptions are the 2-nitro and 3-nitro complexes which show a mass loss of 19.2 % and 18.6 % respectively. These results can possibly be attributed to the loss of the NO_2 substituent as the combination of the loss of CO_2 and NO_2 fits the two values observed experimentally, however, this could not be proven. Of course one would expect the 4-nitro complex to follow this trend, however the NO_2 must be lost at a different temperature as only the loss of CO_2 is seen. As with the loss of thiourea, this can be shown by means of the mass spectroscopy results.

The final mass loss coincides with the endothermic peak at ~800˚C and relates to the loss of the majority of the thallium as well as some organic residue associated with fragmentation of the substituted aromatic ring, hence the reason why the theoretical mass loss of the thallium is substantially lower than the actual mass loss. It was also proved by mass spectroscopy that some (minor) thallium is already removed at temperatures below 800°C.

Some thermographs suggested that the release of the four thiourea molecules is a two step process (1 + 3 TU), the analysis of the process by mass spectroscopy showed a continuous loss of thiourea from 30°C to 190°C. When the 2-fluoro sample was subjected to analysis with a METTLER TOLEDO TGA/SDTA 851e it was observed that the first step of the loss of one thiourea did not lead to a separate intermediate product containing the remaining three thiourea molecules. But the loss of the remaining 3 thiourea molecules was rather continuous.

The only complexes whose theoretical mass losses of thiourea did not coincide with the actual mass losses were the 2-fluoro, 3-bromo and 4-methoxy complexes. As stated above this was most likely due to the loss of aromatic fragments in this range.

The following shows the actual % mass losses for each complex along with what molecules come off. In brackets are the theoretical % mass losses.

COMPLEX	MASS LOSS %	MOLECULE/FRAGMENT (theoretical mass loss %)		
2-AMINO	12	1 Thiourea (12)		
	34	3 Thiourea (35)		
	8	CO_2 (7)		
	44	Tl + some organic residue		
3-AMINO	51	4 Thiourea (47)		
	12	CO_2 (7)		
	36	Tl + some organic residue		
4-AMINO	12	1 Thiourea (12)		
	37	3 Thiourea (35)		
	10	CO_2 (7)		
	40	Tl + some organic residue		
2-NITRO	11	1 Thiourea (11)		
	36	3 Thiourea (34)		
	19	$CO_2 + NO_2$ (14)		
	52	Tl + some organic residue		
3-NITRO	16	1 Thiourea (11)	51	4 Thiourea (45)
	35	3 Thiourea (34)		
	18	$CO_2 + NO_2$ (14)		
	50	Tl + some organic residue		
4-NITRO	5	1 Thiourea (11)	39	4 Thiourea (45)
	34	3 Thiourea (34)		
	7	CO_2 (7)		
	45	Tl + some organic residue		

2-FLUORO	63	4 Thiourea (47)		
	9	CO_2 (7)		
	40	Tl + some organic residue		
3-FLUORO	52	4 Thiourea (47)		
	13	CO_2 (7)		
	35	Tl + some organic residue		
4-FLUORO	9	1 Thiourea (12)	45	4 Thiourea (47)
	36	3 Thiourea (35)		
	8	CO_2 (7)		
	45	Tl + some organic residue		
2-BROMO	9	1 Thiourea (11)		
	34	3 Thiourea (32)		
	8	CO_2 (6)		
	41	Tl + some organic residue		
3-BROMO	59	4 Thiourea (43)		
	7	CO_2 (6)		
	33	Tl + some organic residue		
4-BROMO	46	4 Thiourea (43)		
	8	CO_2 (6)		
	43	Tl + some organic residue		

2-CHLORO	6	1 Thiourea (12)	44	4 Thiourea (46)
	38	3 Thiourea (34)		
	6	CO_2 (7)		
	43	Tl + some organic residue		
3-CHLORO	6	1 Thiourea (12)	48	4 Thiourea (46)
	42	3 Thiourea (34)		
	7	CO_2 (7)		
	37	Tl + some organic residue		
4-CHLORO	4	1 Thiourea (12)	46	4 Thiourea (46)
	42	3 Thiourea (34)		
	10	CO_2 (7)		
	42	Tl + some organic residue		
2-METHYL	11	1 Thiourea (12)		
	36	3 Thiourea (36)		
	7	CO_2 (7)		
	43	Tl + some organic residue		
3-METHYL	7	1 Thiourea (12)	49	4 Thiourea (47)
	42	3 Thiourea (36)		
	4	CO_2 (7)		
	52	Tl + some organic residue		
4-METHYL	12	1 Thiourea (12)		
	36	3 Thiourea (36)		
	8	CO_2 (7)		
	45	Tl + some organic residue		

2-HYDROXY	5	1 Thiourea (12)		
			47	4 Thiourea (47)
	43	3 Thiourea (36)		
	9	CO_2 (7)		
	43	Tl + some organic residue		
4-METHOXY	5	1 Thiourea (12)		
			35	3 Thiourea (35)
	30	3 Thiourea (35)		
	4	CO_2 (7)		
	59	Tl + some organic residue		
BENZOATE	53	4 Thiourea (48)		
	4	CO_2 (7)		
	33	Tl + some organic residue		

Table 6.2 **Table showing mass losses, molecules and fragments coming off, and theoretical mass losses (%).**

Elemental analysis of the thallium and sulphur content for a selection of ten complexes of which sufficient material were available produced an average ratio of 1:3[6]. The 3-fluoro complex was the only complex with known 1:4 ratio included in these samples and this correct ratio was indeed observed. It must be stated that the physical quality of all the other complexes in general deteriorated upon recrystallisation. Unfortunately it was no longer possible to resynthesise these complexes in sufficient quantity as required for the analysis (5 g of each). Although it is known that some of these complexes do not necessarily have a 1:4 ratio, these results are inconclusive .

6.6 MASS SPECTROMETRY

In order to fully interpret the results obtained from the thermal analysis techniques, some of the complexes were analysed using mass spectrometry obtained over the temperature range corresponding to the observed thermal events. The procedure involved heating the samples to temperatures which coincided with large % mass losses in the TG and at these temperature ranges record the mass spectra to obtain information of the decomposition process.

Due to the fact that all the thermal results were very similar, the 2-fluoro complex was analysed as a representation of the complexes, also with the aim of clarifying the mass loss associated with the loss of thiourea.

As can be seen from the mass spectrum, the thiourea (m/z = 76) is visible at 30˚C, at 150˚C its abundance has decreased substantially and by 190˚C it is completely gone. These results correspond to the TG results which show a mass loss of 63 % in and around the same temperature. It should be noted that the mass loss value of 63 % is higher than the expect value for the loss of four thiourea, 47 %. Due to this large difference, the sample was rerun on the accurate thermal software (see experimental) and a mass loss of 57 % was obtained. This result firstly proves the definite inaccuracies associated with the thermal instrumentation used (as discussed in the experimental) and secondly implies that this mass loss must include aromatic fragments as well as the thiourea.

It is worth noting that the relative masses of both thiourea and C_6H_4 (the aromatic ring) are 76, however, the mass spectroscopy software used was able to give the accurate masses and confirm that the peak at 76 did in fact relate to the thiourea.

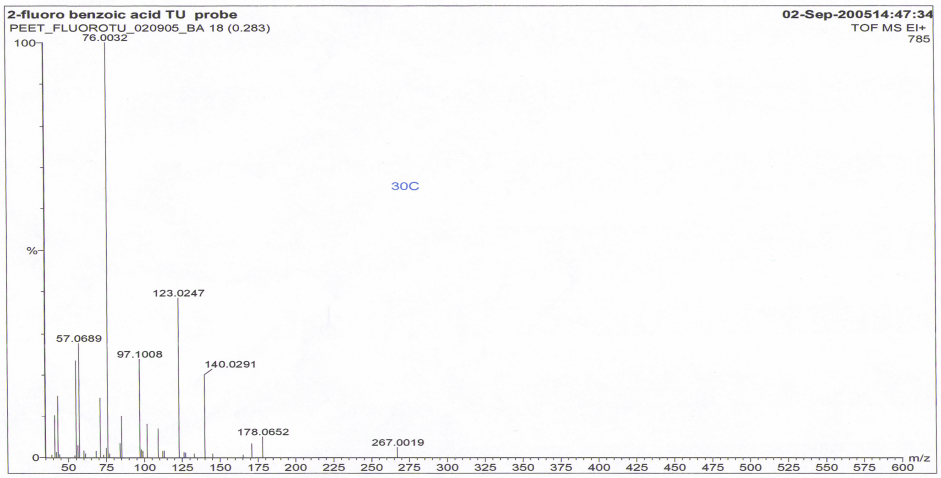

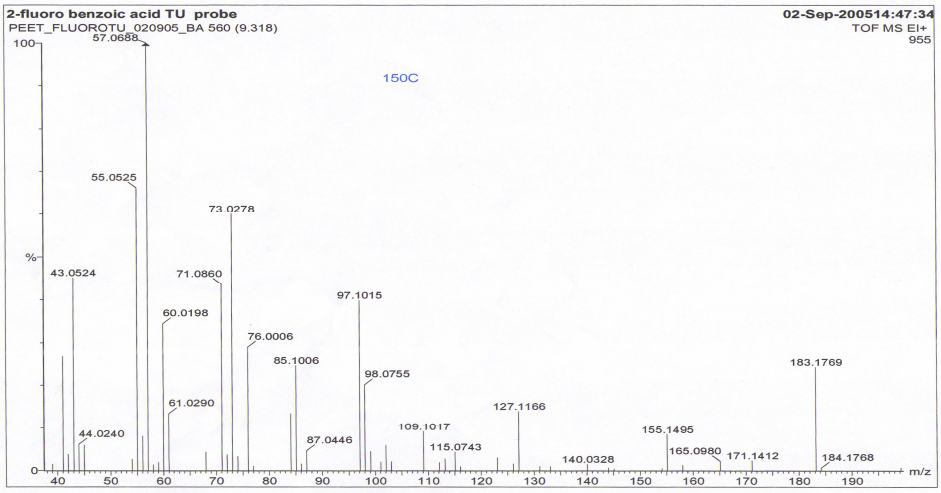

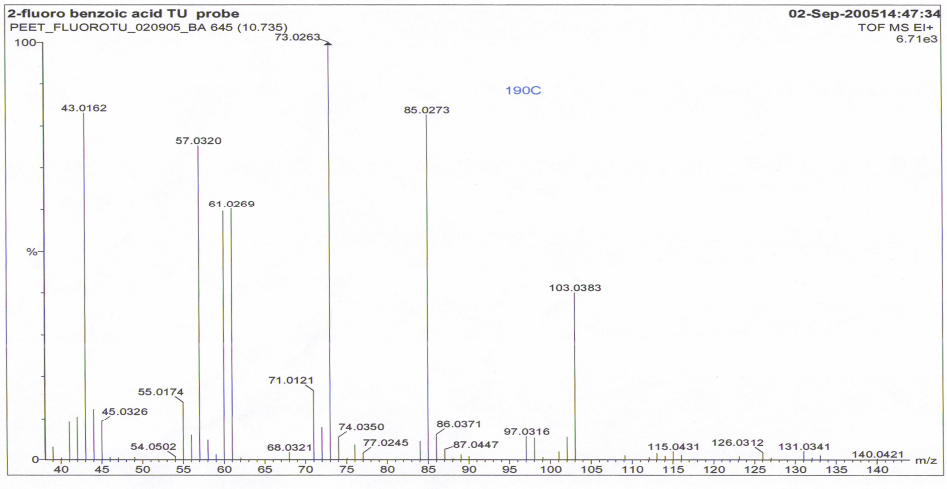

Fig. 6.5 **Mass spectra of 2-fluoro at 30˚C, 150˚C and 190˚C showing the loss of thiourea**

At 350˚C the CO_2 (m/z = 44) is visible (confirmed by the accurate mass given by the software) and corresponds to the second mass loss in the TG results.

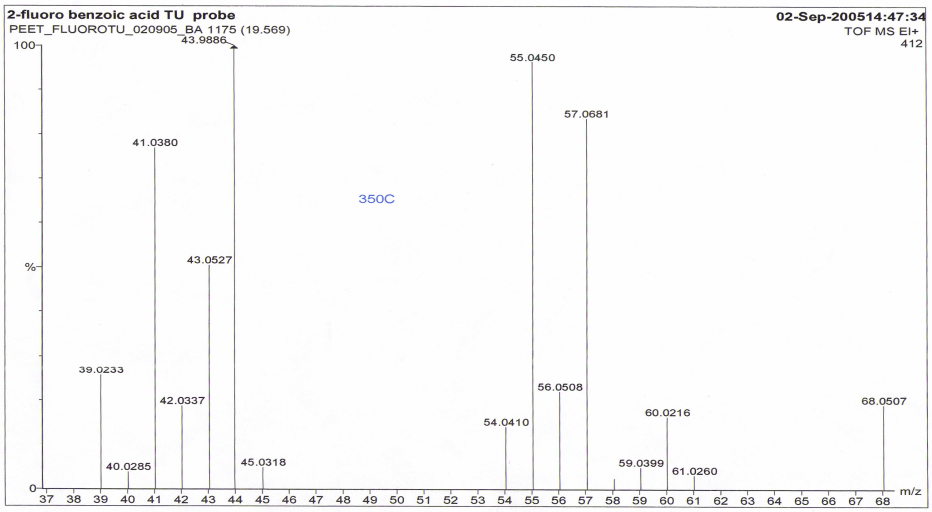

Fig. 6.6 Mass spectrum of 2-fluoro at 350˚C showing the presence of CO_2

Above 550˚C the Thallium (m/z = 205) is visible (confirmed by the accurate mass given by the software) and corresponds to the third mass loss in the TG results.

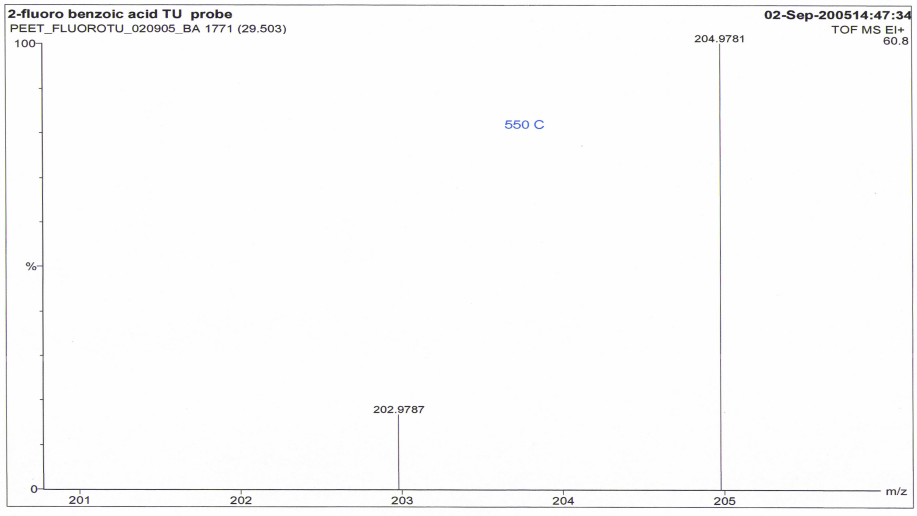

Fig. 6.7 Mass spectrum of 2-fluoro at 550˚C showing the presence of Tl

5.7 MELTING POINTS OF COMPLEXES

It is important to note that the melting points of the complexes were obtained in two ways. Firstly, by the simple method of heating the complex on a hot plate with a thermometer attached and watching for the exact point of melting using a microscope. Secondly, by simply looking at the DSC results and noting the temperature that the first peak appears. As expected the two set of results are not exactly the same due to human and experimental error but they are most certainly in the same approximate range.

MELTING POINTS OBTAINED FROM MELTING POINT INSTRUMENT

COMPLEX	MELTING POINT (˚C)	
Tl-2-aminobenzoate-thiourea	166.7-170.7	
Tl-3-aminobenzoate-thiourea	216.6-219.7	*
Tl-4-aminobenzoate-thiourea	169.7-172.8	
Tl-2-nitrobenzoate-thiourea	163.2-167.5	
Tl-3-nitrobenzoate-thiourea	178.8-183.2	
Tl-4-nitrobenzoate-thiourea	179.8-181.3	
Tl-2-fluorobenzoate-thiourea	208.0-209.8	*
Tl-3-fluorobenzoate-thiourea	205.3-206.1	*
Tl-4-fluorobenzoate-thiourea	185.0-188.3	
Tl-2-bromobenzoate-thiourea	163.0-167.8	
Tl-3-bromobenzoate-thiourea	190.6-192.3	
Tl-4-bromobenzoate-thiourea	188.5-190.0	
Tl-2-chlorobenzoate-thiourea	161.1-164.3	
Tl-3-chlorobenzoate-thiourea	189.5-191.1	
Tl-4-chlorobenzoate-thiourea	182.6-188.9	
Tl-2-methylbenzoate-thiourea	165.2-168.7	
Tl-3-methylbenzoate-thiourea	178.4-180.8	
Tl-4-methylbenzoate-thiourea	175.6-179.4	
Tl-4-methoxybenzoate-thiourea	163.2-167.0	
Tl-2-hydroxybenzoate-thiourea	179.5-184.3	
Tl-benzoatebenzoate-thiourea	211.2-212.5	*

Table 6.3 Melting points of complexes * denotes single crystal structure obtained

Of great importance is to note that the four complexes marked with * in Table 6.3 and Fig. 6.8 yielded very similar single crystal structures and these compounds have have melting points in a distinct temperature range that differs from the rest. No usable single crystals of any of the other complexes could be obtained even after many re-crystallisation experiments.

6.8 MELTING POINTS OF ALL COMPLEXES

The melting point values used in the graph below were obtained from melting point instrument (hotplate, thermometer and microscope) and not from DSC.

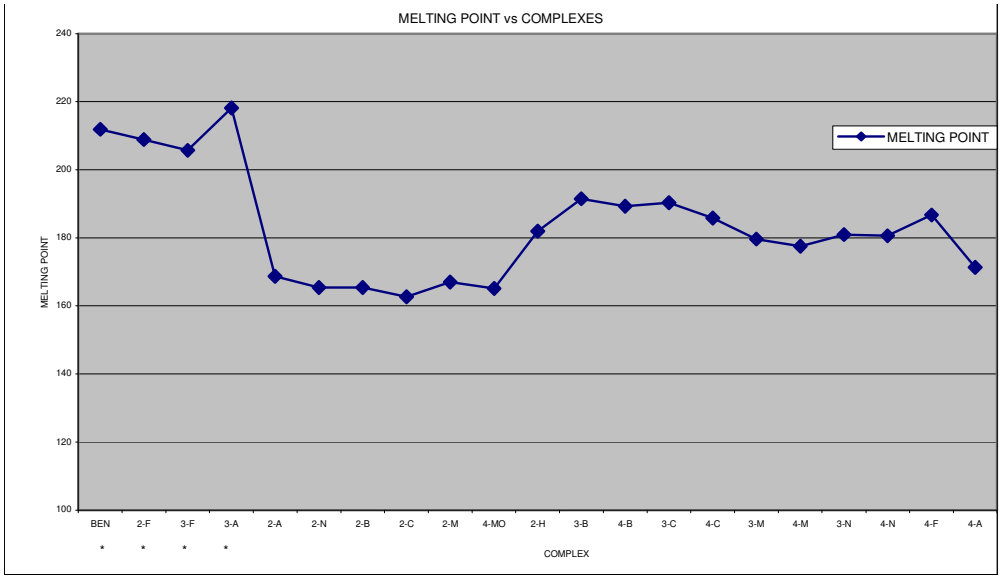

Fig. 6.8 **Graph to show melting point vs molecular weight where the x axis scale relates to the 1st letter of the substituted complexes.**

It can be seen from the graph above that the melting points of all the synthesized complexes can be classified into three categories. Firstly, the 3-amino, 2-fluoro, 3-fluoro, benzoate complexes which produced good single crystals have the highest melting points (218.2°C, 208.9°C, 211.9°C, 205.7˚C respectively).

Of the remaining complexes the ortho substituted complexes, barring the 2-hydroxy complex, have similar melting points in the narrow region of 162.7-168.7°C.

It should be noted that the 2-hydroxy complex is involved in increased hydrogen bonding with in the complex, hence the higher melting point. This can be seen in the IR spectrum where the normally sharp OH band at above 3600 cm^{-1} is not seen but has instead shifted to a lower wavenumber due to hydrogen bonding [7]. However, the band is not seen as it has shifted to the region where the thiourea bands are most prominent and so it is masked. Also included in this category is the 4-methoxy complex with a melting point of 165.1°C. This may be due to the non-planarity of the methoxy substituent relative to the benzene ring.

The third category is the remaining meta and para substituted complexes. Although the overall melting point range of this grouping is rather large, the meta and para positions of the same substituent complexes have very similar melting points, i.e. 3- and 4-nitro, 3- and 4-bromo, etc. The one exception being the 4-fluoro complex.

Of significance is the fact that three of the four complexes that produced diffraction quality single crystals (2-fluoro complex, 3-fluoro complex and benzoate complex) have very narrow melting point ranges which may also be an indication that they are indeed more crystalline than the other complexes. As some of the other complexes were repeatedly re-crystallized it was accepted that the wider range do not necessarily reflect a less pure complex.

6.9 MELTING POINT vs MOLECULAR WEIGHT

Melting points increase with increasing molecular weight as polarisability increases with increasing number of electrons and the number of electrons is in a general way related to the molecular weight. (Polarisability is the ease with which a dipole can be induced in an atom or molecule due to electron charge distortion.) [8]. However, there are both strong ionic and other dipole interactions present in these complexes as well.

The table shows that although the complexes of the same molecular weight have roughly the same melting point, there is no trend which shows melting point increasing with increased molecular weight.

6.10 CONCLUSION

The TG and DSC techniques that were used provided good results which complimented each other in terms of exothermic and endothermic peaks of the DSC occurring in the same regions as the various % mass losses of the TG.
The main conclusions made were as follows:

- The four crystal structures (2-fluoro, 3-fluoro, 3-amino and benzoate complexes) showed comparable enthalpy values associated with the loss of four thiourea molecules. These four values were the highest observed in the group of six highest enthalpy readings. The remaining two complexes were a 2-methyl and a 3-bromo derivative. This also supports the suggestion by the crystallographic results that a more bulky substituent on the 3-position could be accommodated in that existing packing.
- It must be noted that the difference in enthalpy values for the 4-amino and the 4-nitro complexes is very large. The 4-amino complex has a 3 times higher enthalpy value, most likely due to the electron donating character of the amino group resulting in stronger hydrogen bonding when compared with the electron withdrawing effect of the nitro group.
- It is not clear why the 2-amino complex has such a lower enthalpy value than that of the 2-methyl complex. It could be expected that there are small differences in the relative size of these two functional groups, however, the stronger electron donating properties of the amino group does not seem to affect the enthalpy values.
- The 3-bromo and 2-methyl complexes also showed comparable enthalpy values related to the loss of four thiourea molecules. The values were slightly lower than those observed for the four benzoates above, but significantly higher than the rest of the complexes. This may indicate the same type of bonding and or packing strength as for the four benzoates above.
- The remaining complexes differed with no other clear identifiable groupings. However, the group of eight complexes with similar powder diffraction patterns include two of the complexes with the lowest enthalpy values (4-nitro and 4-methoxy).

- It was proven that the four thiourea molecules are released first as confirmed by the mass spectroscopy.

It can also be concluded that varying the substituent on the benzene ring according to different electronic properties does not have any effect on the thermal events that take place in the complexes.

In addition to the two thermal techniques used, the mass spectrometry worked well along side them to give a deeper understanding of the data obtained.

6.11 REFERENCES

CHAPTER 6

1. J. W. Dodds and K. H. Tonge, Thermal Methods, Wiley, 1987, page 1-166
2. www.anasys.co.uk/library/tga1, page 3
3. J. W. Dodds and K. H. Tonge, Thermal Methods, Wiley, 1987, page 5
4. J. W. Robinson, Undergraduate Instrumental Analysis, 1987, pages 483, 492-496
5. S. El-Houte, M. El-Sayed Ali and O. Toft Sorensen, Thermochimica Acta, 1989, **138**, 107-114
6. Professional analysis by Setpoint Holding Company, SPL Report number 5/1976
7. D. Lin-Vien, N. B. Colthup, W. G. Fateley, J. G. Grasselli, The Handbook of Infrared and Raman Characteristic Frequencies of Organic Molecules, Academic Press, Boston, MA, 1991, page 47
8. R. H. Petrucci, General Chemistry, 5th ed., 1989, pages 410-414

6.12 THERMAL DATA OF ALL THE COMPLEXES

COMPLEX	DSC/DTA results T peak (˚C)	TG results T range (˚C)	Mass loss (%)
2-AMINO	145 endo	25-166	12
COMPLEX	170 endo	166-307	34
	193 endo	307-460	8
	360 exo	460-857	44
	407 exo		
	636 endo		
	790 endo		
3-AMINO	210 endo	184-425	51
COMPLEX	389 exo	425-565	12
	473 exo	565-869	36
	638 endo		
	753 endo		
4-AMINO	151 endo	79-176	12
COMPLEX	170 endo	176-368	37
	194 endo	368-703	10
	361 exo	703-655	40
	411 exo		
	632 endo		
	780 endo		

Table 6.4 **Thermal data including DSC/DTA results, TG results and mass loss for the 2/3/4 amino complexes**

COMPLEX	DSC/DTA results T peak (˚C)	TG results T range (˚C)	Mass loss (%)
2-NITRO	151 endo	45-160	11
COMPLEX	170 endo	160-241	36
	200 endo	241-470	19
	355 exo	470-946	52
	405 exo		
	631 endo		
	790 endo		
3-NITRO	150 exo	41-178	16
COMPLEX	173 endo	178-269	35
	198 endo	269-489	19
	367 exo	489-880	50
	435 exo		
	627 endo		
	774 endo		
4-NITRO	154 endo	59-174	5
COMPLEX	173 endo	174-472	34
	197 endo	472-606	7
	379 exo	606-913	45
	480 exo		
	630 endo		
	762 endo		

Table 6.5 **Thermal data including DSC/DTA results, TG results and mass loss for the 2/3/4 nitro complexes**

COMPLEX	DSC/DTA results T peak (˚C)	TG results T range (˚C)	Mass loss (%)
2-FLUORO	204 endo	184-249	63
COMPLEX	356 exo	249-447	9
	406 exo	447-878	40
	645 endo		
	838 endo		
3-FLUORO	195 endo	199-245	52
COMPLEX	360 exo	245-444	13
	420 exo	444-904	35
	472 exo		
	640 endo		
	820 endo		
4-FLUORO	152 endo	62-179	9
COMPLEX	180 endo	179-434	36
	189 endo	434-690	8
	205 endo	690-897	45
	347 exo		
	395 exo		
	638 endo		
	800 endo		

Table 6.6 **Thermal data including DSC/DTA results, TG results and mass loss for the 2/3/4 fluoro complexes**

COMPLEX	DSC/DTA results T peak (˚C)	TG results T range (˚C)	Mass loss (%)
2-CHLORO	150 endo	96-170	6
COMPLEX	183 endo	170-332	38
	203 endo	332-458	6
	367 exo	458-867	43
	402 exo		
	635 endo		
	809 endo		
3-CHLORO	139 exo	55-175	6
COMPLEX	185 endo	175-272	42
	205 endo	272-425	7
	343 exo	425-835	37
	383 exo		
	632 endo		
	777 endo		
4-CHLORO	158 endo	139-173	4
COMPLEX	181 endo	173-272	42
	190 endo	272-451	10
	202 endo	451-860	42
	362 exo		
	400 exo		
	635 endo		
	800 endo		

Table 6.7 **Thermal data including DSC/DTA results, TG results and mass loss for the 2/3/4 chloro complexes**

COMPLEX	DSC/DTA results T peak (˚C)	TG results T range (˚C)	Mass loss (%)
2-BROMO	140 endo	68-171	9
COMPLEX	165 endo	171-338	34
	194 endo	338-434	8
	350 exo	434-917	41
	394 exo		
	634 endo		
	791 endo		
3-BROMO	192 endo	169-244	59
COMPLEX	342 exo	244-660	7
	386 exo	660-1154	33
	630 endo		
	750 endo		
4-BROMO	188 endo	152-267	46
COMPLEX	195 endo	267-453	8
	370 exo	453-862	43
	420 exo		
	640 endo		
	802 endo		

Table 6.8 **Thermal data including DSC/DTA results, TG results and mass loss for the 2/3/4 bromo complexes**

COMPLEX	DSC/DTA results T peak (˚C)	TG results T range (˚C)	Mass loss (%)
2-METHYL	150 endo	126-179	11
COMPLEX	182 endo	179-318	36
	356 exo	318-471	7
	411 exo	471-880	43
	638 endo		
	831 endo		
3-METHYL	141 exo	32-147	7
COMPLEX	175 endo	147-384	42
	201 endo	384-486	4
	354 exo	486-946	52
	400 exo		
	641 endo		
	799 endo		
4-METHYL	158 endo	101-173	12
COMPLEX	173 endo	173-317	36
	192 endo	317-432	8
	398 exo	432-841	45
	621 endo		
	770 endo		

Table 6.9 **Thermal data including DSC/DTA results, TG results and mass loss for the 2/3/4 methyl complexes**

COMPLEX	DSC/DTA results T peak (˚C)	TG results T range (˚C)	Mass loss (%)
4-METHOXY	145 endo	25-173	5
COMPLEX	190 endo	173-313	30
	376 exo	313-568	4
	431 exo	568-1002	59
	640 endo		
	803 endo		
2-HYDROXY	142 exo	106-156	5
COMPLEX	176 endo	156-361	43
	192 endo`	361-490	9
	375 exo	490-919	43
	415 exo		
	626 endo		
	791 endo		
BENZOATE	207 endo	185-238	53
COMPLEX	340 exo	238-418	4
	370 exo	418-878	33
	634 endo		
	730 endo		

Table 6.10 **Thermal data including DSC/DTA results, TG results and mass loss for the 4-methoxy, 2-hydroxy and benzoate complexes**

6.13 TG AND DSC SPECTRA

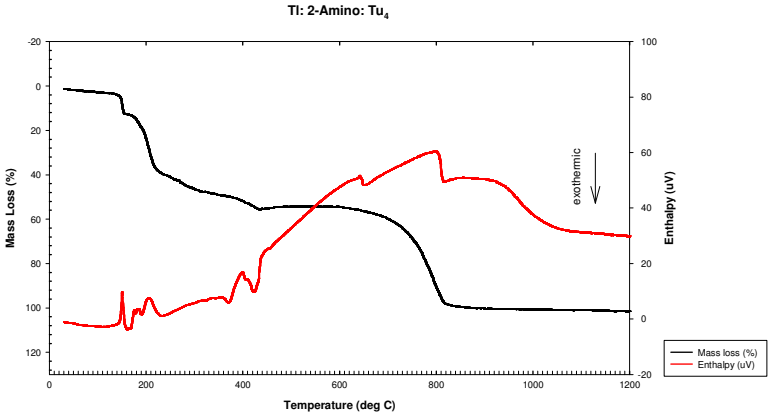

Fig. 6.9 TG and DSC spectrum of the 2-amino complex

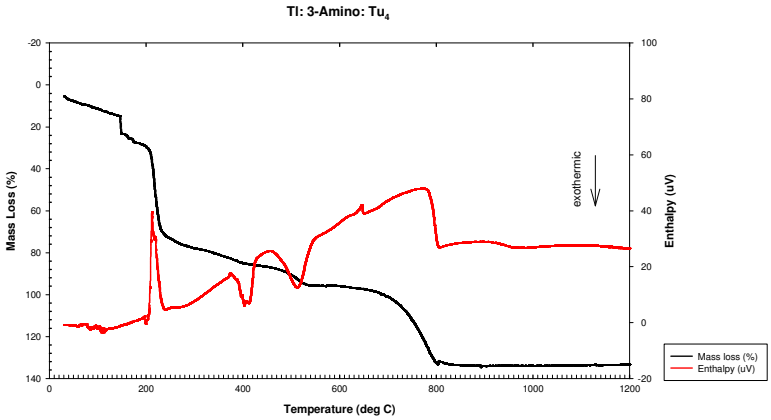

Fig. 6.10 TG and DSC spectrum of the 3-amino complex

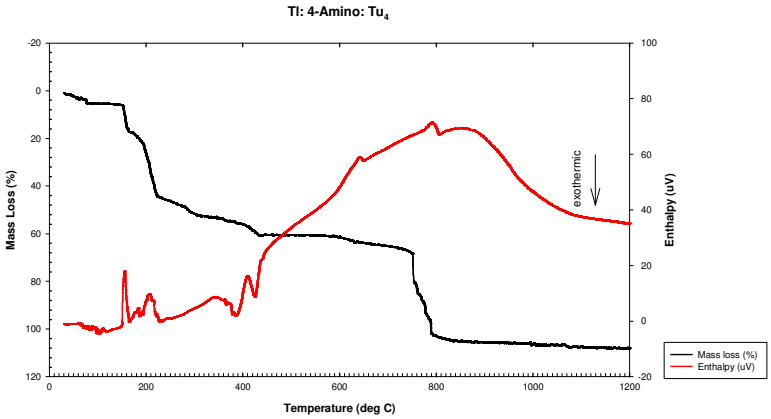

Fig. 6.11 TG and DSC spectrum of the 4-amino complex

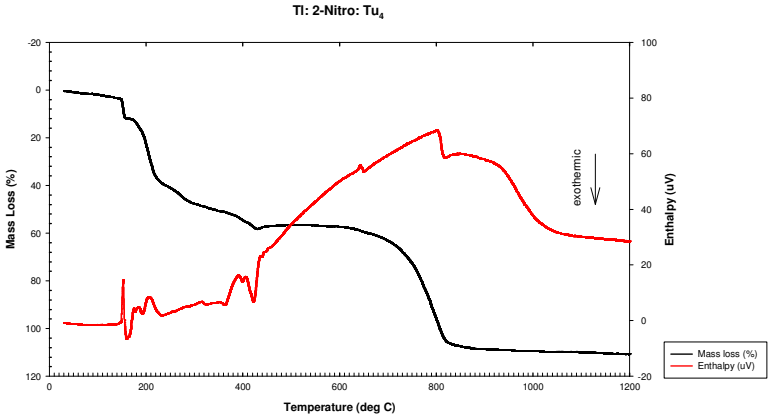

Fig. 6.12 **TG and DSC spectrum of the 2-nitro complex**

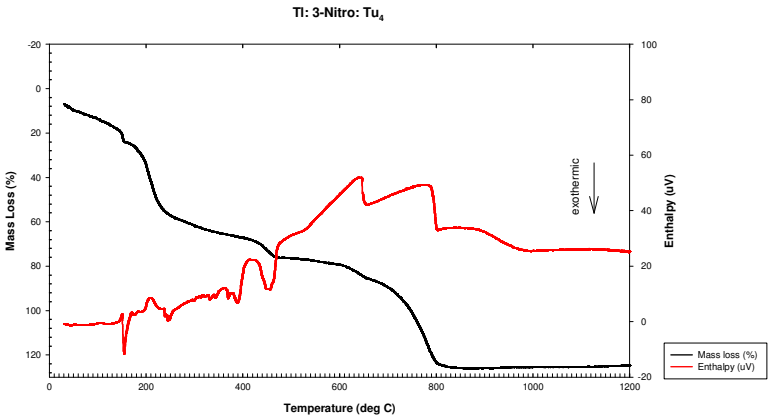

Fig. 6.13 **TG and DSC spectrum of the 3-nitro complex**

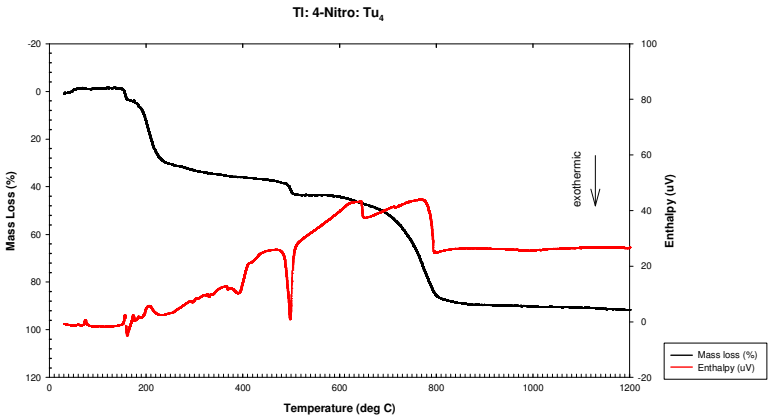

Fig. 6.14 **TG and DSC spectrum of the 4-nitro complex**

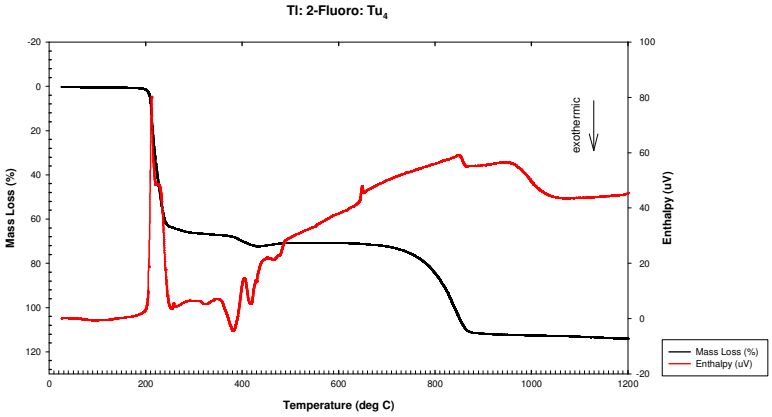

Fig. 6.15 **TG and DSC spectrum of the 2-fluoro complex**

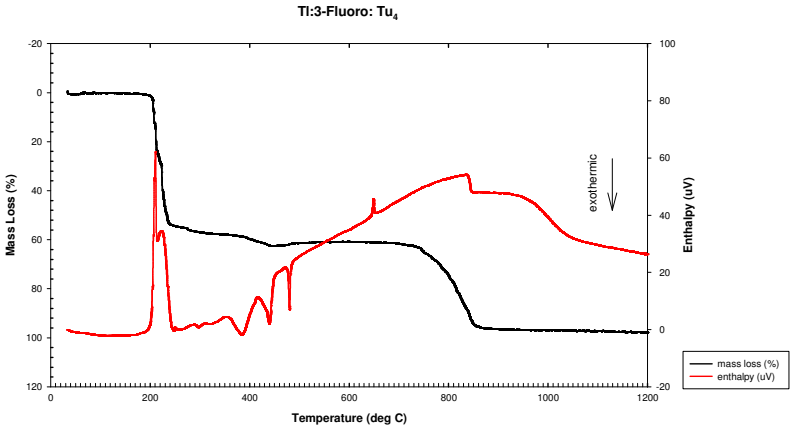

Fig. 6.16 **TG and DSC spectrum of the 3-fluoro complex**

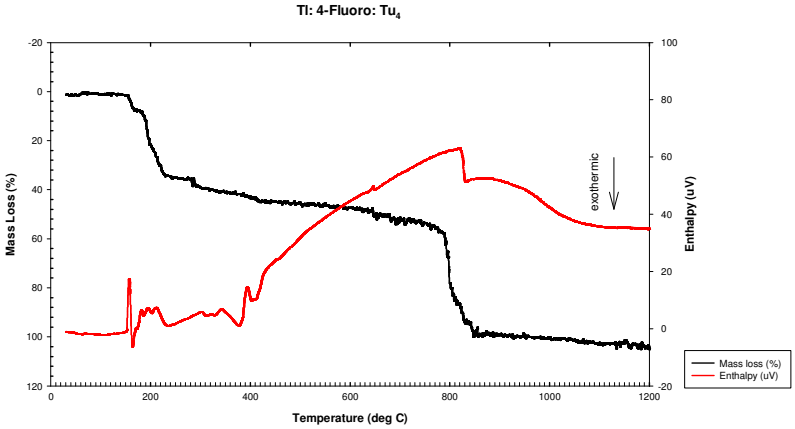

Fig. 6.17 **TG and DSC spectrum of the 4-fluoro complex**

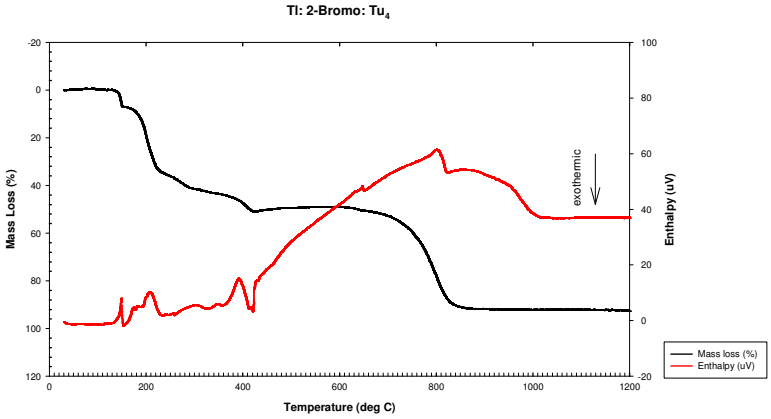

Fig. 6.18 **TG and DSC spectrum of the 2-bromo complex**

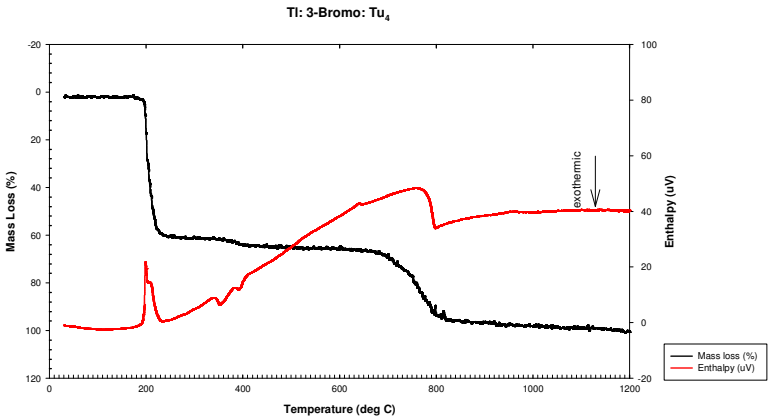

Fig. 6.19 **TG and DSC spectrum of the 3-bromo complex**

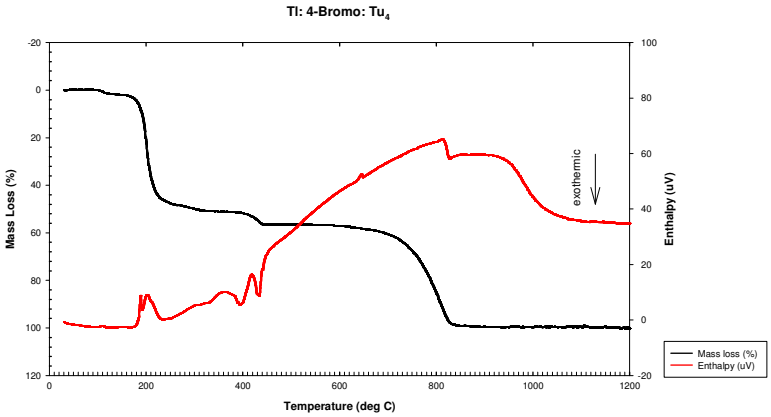

Fig. 6.20 **TG and DSC spectrum of the 4-bromo complex**

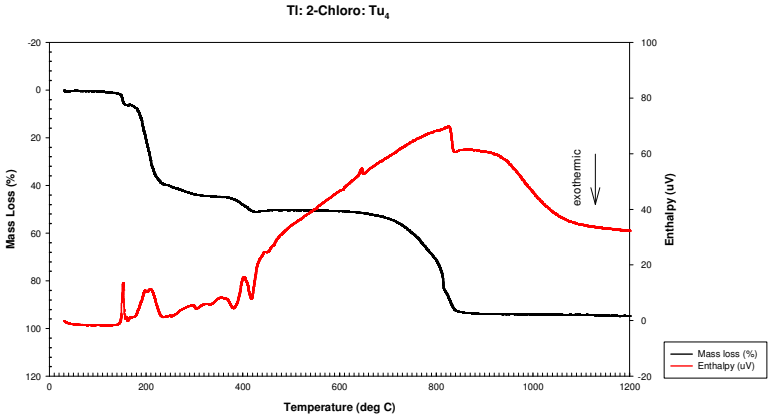

Fig. 6.21 **TG and DSC spectrum of the 2-chloro complex**

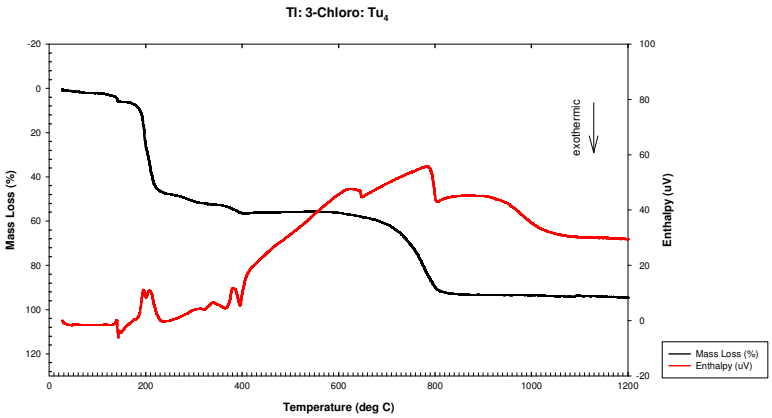

Fig. 6.22 **TG and DSC spectrum of the 3-chloro complex**

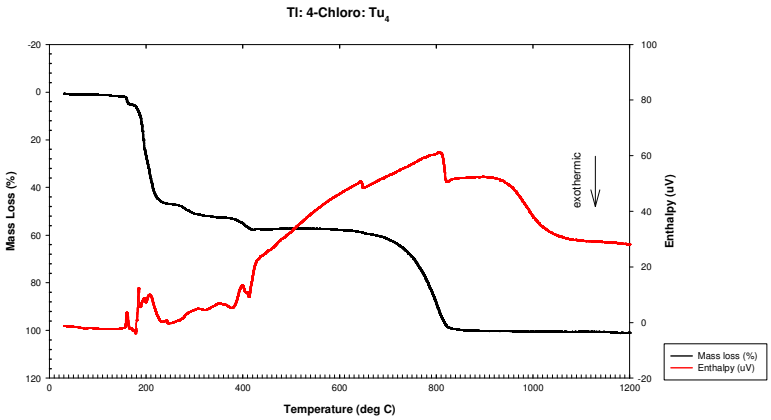

Fig. 6.23 **TG and DSC spectrum of the 4-chloro complex**

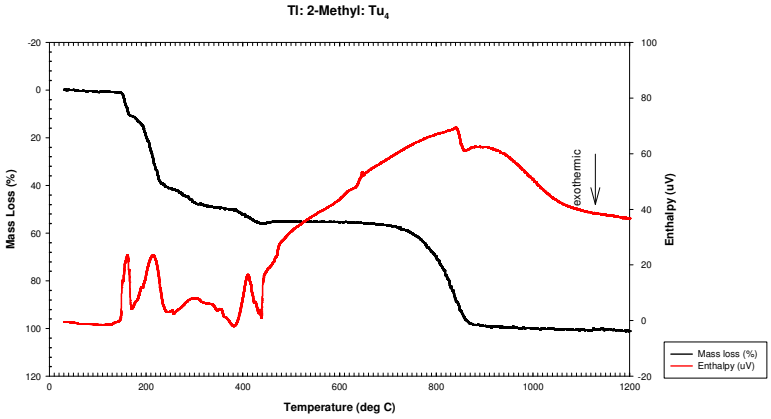

Fig. 6.24 **TG and DSC spectrum of the 2-methyl complex**

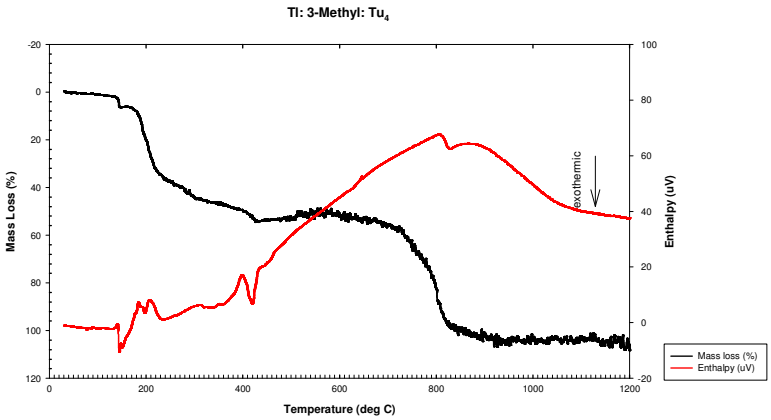

Fig. 6.25 **TG and DSC spectrum of the 3-methyl complex**

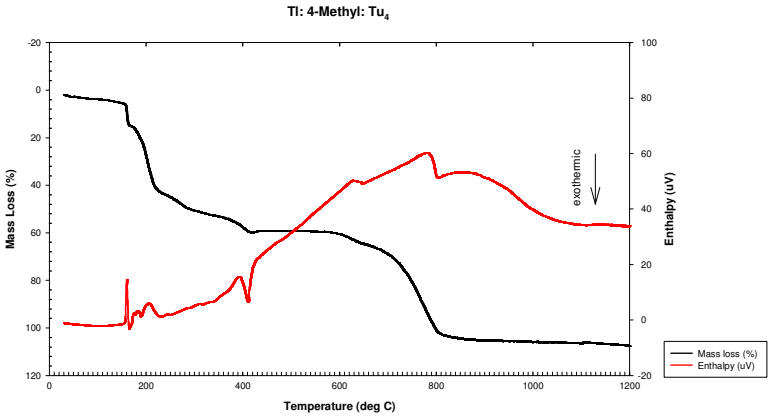

Fig. 6.26 **TG and DSC spectrum of the 4-methyl complex**

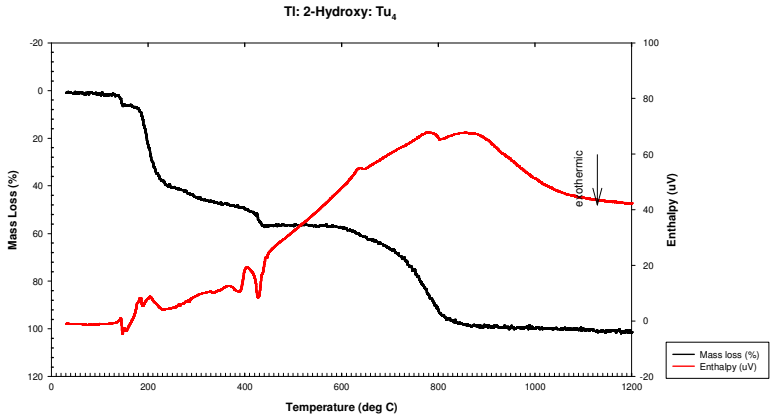

Fig. 6.27 **TG and DSC spectrum of the 2-hydroxy complex**

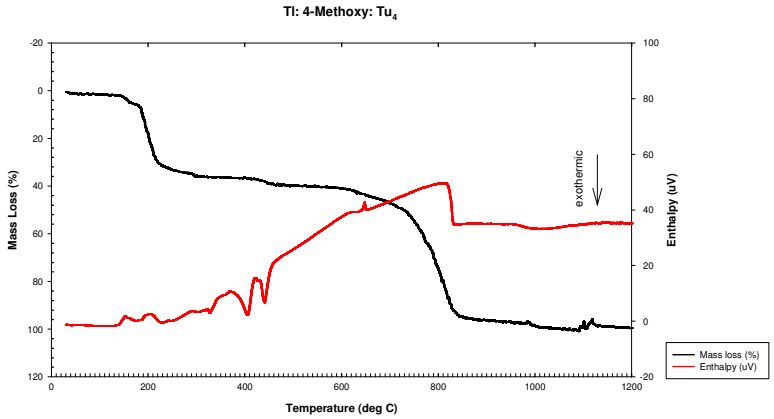

Fig. 6.28 **TG and DSC spectrum of the 4-methoxy complex**

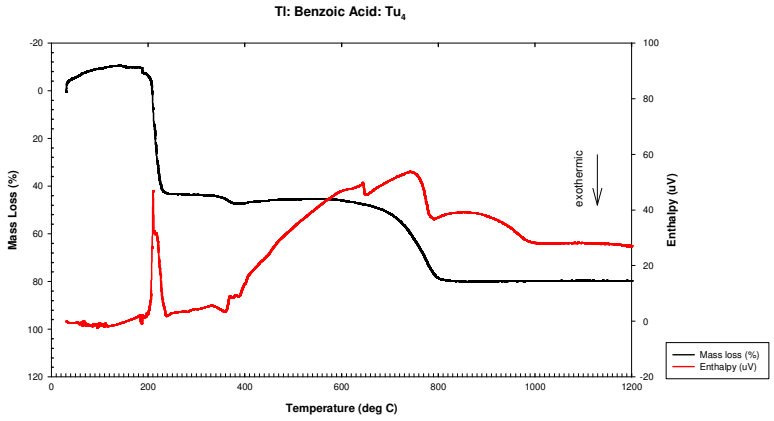

Fig. 6.29 **TG and DSC spectrum of the benzoate complex**